AD-A138 011 MULTIPLE INPUT - MULTIPLE OUTPUT FLIGHT CONTROL DESIGN WITH HIGHLY UNCERT..(U) AIR FORCE INST OF TECH WRIGHT-PATTERSON AFB OH SCHOOL OF ENGI.. R W BETZOLD 1/2

UNCLASSIFIED DEC 83 AFIT/GE/EE/83D-11 F/G 1/2 NL

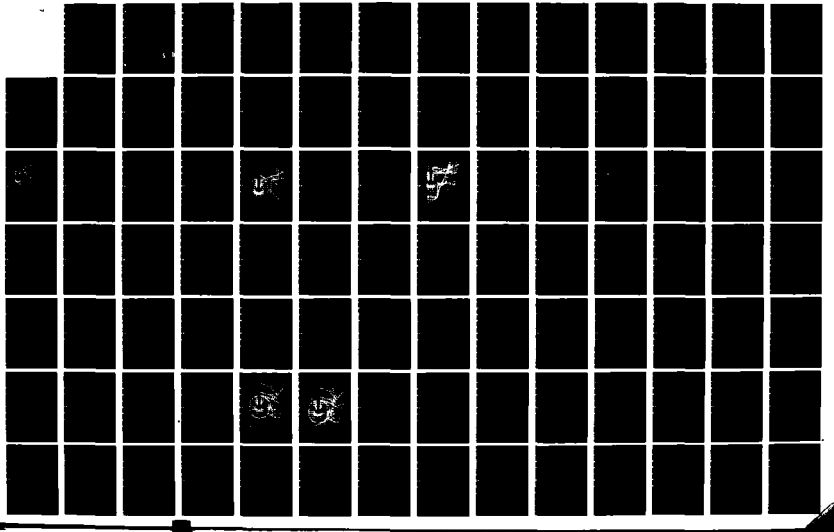

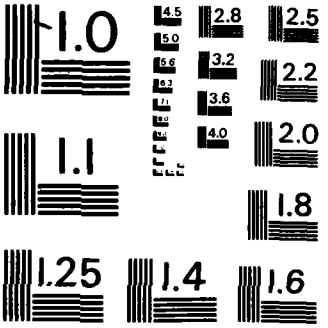

MICROCOPY RESOLUTION TEST CHART
NATIONAL BUREAU OF STANDARDS - 1963 - A

AD A138011

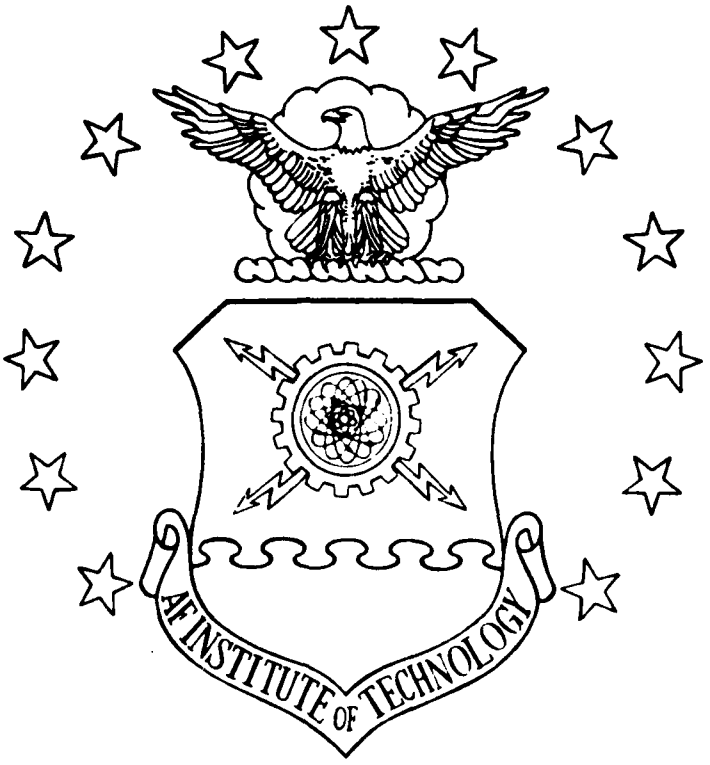

MULTIPLE INPUT - MULTIPLE OUTPUT FLIGHT CONTROL DESIGN WITH HIGHLY UNCERTAIN PARAMETERS; APPLICATION TO THE C-135 AIRCRAFT

THESIS

AFIT/GE/EE/83D-11

Robert W. Betzold
Capt USAF

DTIC FILE COPY

DTIC ELECTE FEB 2 2 1984 S D E

DEPARTMENT OF THE AIR FORCE
AIR UNIVERSITY
AIR FORCE INSTITUTE OF TECHNOLOGY

Wright-Patterson Air Force Base, Ohio

This document has been approved for public release and sale; its distribution is unlimited.

84 02 17 071

AFIT/GE/EE/83D-11

MULTIPLE INPUT - MULTIPLE OUTPUT FLIGHT CONTROL DESIGN WITH HIGHLY UNCERTAIN PARAMETERS; APPLICATION TO THE C-135 AIRCRAFT

THESIS

AFIT/GE/EE/83D-11 Robert W. Betzold
Capt USAF

DTIC
ELECTE
E

Approved for public release; distribution unlimited.

AFIT/GE/EE/83D-11

MULTIPLE INPUT - MULTIPLE OUTPUT FLIGHT CONTROL DESIGN WITH HIGHLY UNCERTAIN PARAMETERS APPLICATION TO THE C-135 AIRCRAFT

THESIS

Presented to the Faculty of the School of Engineering

of the Air Force Institute of Technology

Air University

in Partial Fulfillment of the

Requirements for the Degree of

Master of Science

by

Robert W. Betzold, B.S.E.E.

Capt USAF

Graduate Electrical Engineer

December 1983

Approved for public release; distribution unlimited.

Preface

I chose this thesis topic for two reasons. First, the subject of flight control was my primary area of study in persuing my post-graduate degree. Second, having flown a number of years in transport aircraft, the control of such aircraft interested me.

I would like to thank Mr. Duane P. Rubertus of the Flight Dynamics Laboratory, Wright-Patterson AFB, Ohio for sponsoring this thesis topic and for giving me the freedom I needed to explore the problem.

I want to thank Professor Issac Horowitz for his personal effort and patience in helping me with this thesis. Without his help and understanding this work would never have been completed. I would also like to thank Professor Constantine H. Houpis for serving as co-advisor on this thesis and as my academic advisor. He provided a great deal of help and moral support during this effort and throughout my work at AFIT.

Finally, I must acknowledge my wife, Lita, for her love, patience, and understanding during a very trying eighteen months. To her and to our son, Don, who is still too young to understand, I love you both very much.

Accession For	
NTIS GRA&I	X
DTIC TAB	☐
Unannounced	☐
Justification	
By	
Distribution/	
Availability Codes	
Dist	Avail and/or Special
A-1	

Captain Robert W. Betzold

Contents

Contents

List of Figures

List of Figures

List of Tables

List of Symbols

β - Sideslip Angle

$\underline{\delta}$ - Plant (aircraft) Input Vector

δ_a - Aileron Deflection

δ_r - Rudder Deflection

γ - Ratio of Effective Plant Transfer Functions

θ - Pitch Angle

θ_o - Reference Pitch Angle

ϕ - Roll Angle (bank angle)

ψ - Yaw Angle

ω - Unit of Frequency (rad/sec)

b_{ij} - Modeled Response Bound

d_{ij} - Effective Disturbance

F - Prefilter in Single Loop Design

$\underline{F}$ - Prefilter Matrix

f_{ij} - Element of $\underline{F}$

G - Primary Compensator Element in Single Loop Design

$\underline{G}$ - Compensator matrix

g_i - Element of $\underline{G}$ (matrix is diagonal)

I_{jj} - First Moment of Inertia about j-axis

I_{ij} - Product of Inertia

L - Control Loop Transmission (L = GP)

L_o - Nominal Loop Transmission

L - Rolling Moment

N - Yawing Moment

P - Plant Transfer Function

List of Symbols

P_o - Nominal Plant Transfer Function

$\underline{P}$ - Plant Matrix of System Transfer Functions

p_{ij} - Element of $\underline{P}$

$\underline{P}_o$ - Nominal Plant Matrix

p - Angular Velocity about X-axis (roll)

$\underline{Q}'$ - Inverse of Plant Matrix ($\underline{P}^{-1}$)

q_{ij}' - Element of $\underline{Q}'$

q_{ij} - $1/(q_{ij}')$

q_{ijo} - Nominal q_{ij}

R - Angular Velocity about Z-axis (yaw)

r - Angular Velocity Perturbation about Z-axis

s - Laplace Operator ($s = j\omega$)

T - Compensated System Transfer Function

T_R - Command Response Transfer Function ($FL/[1 + L]$)

T_D - Disturbance Response Transfer Function ($1/[1 + L]$)

U - Velocity in X-direction

U_o - Reference Velocity in X-direction

V - Velocity in Y-direction (sideslip velocity)

v - Velocity Perturbation in Y-direction

X - Force in X-direction

Y - Force in Y-direction

Z - Force in Z-direction

Abstract

This thesis demonstrates the design of a lateral flight controller for the C-135 aircraft using the frequency response approach of Professor Izaac Horowitz, University of Colorado, Boulder, Colorado. A single controller is designed for the entire flight envelope of the aircraft from high speed, high altitude cruise to a low altitude approach condition.

A three degree-of-freedom lateral model is reduced to a two degree-of-freedom model. The equations of motion assume a linearized aircraft model operating around equilibrium flight conditions allowing only small perturbations from equilibruim.

Robustness of the design is guaranteed, since the variation in flight parameters are considered throughout the entire design process. Robustness is demonstrated by simulating the compensated aircraft at the extremes of the flight envelope considered.

This thesis concludes that the approach of Professor Horowitz is useful for the design of flight controllers for the C-135 aircraft. Some software development to aid in the design process is recommended.

MULTIPLE INPUT - MULTIPLE OUTPUT FLIGHT CONTROL DESIGN WITH HIGHLY UNCERTAIN PARAMETERS APPLICATION TO THE C-135 AIRCRAFT

I. Introduction

Dr. Isaac Horowitz of the University of Colorado, Boulder, Colorado has developed a synthesis technique for multiple input - multiple output feedback control systems. He has worked with the U.S. Air Force on a number of projects such as the F-16 CCV. His frequency response approach to controller design has produced successful designs for a number of difficult flight control problems (Ref 9:5-8).

The Air Force is interested in the use of Dr. Horowitz' approach for a variety of aircraft control problems. This thesis deals with the design of a lateral flight controller for the C-135 aircraft using his technique.

This first chapter presents some background, a statement of the problem, the scope, assumptions, approach, and the sequence of presentation for the rest of the thesis.

Background

An aircraft in flight is an uncertain, non-linear, highly coupled multiple input - multiple output (MIMO) control system. The engine(s) and the flight control surfaces, elevator, ailerons, rudder, flaps, spoilers, and often others provide the inputs to the system. The outputs are the velocity vector, the angles and the angular rates of the aircraft body with respect to some predetermined axis system. In

general, each input exists to primarily affect only one or two of the outputs. But in practice, an input usually affects a number of outputs in addition to those it was designed to control. For instance, the ailerons control roll rate and thereby control bank angle. But in addition to a roll rate, an aileron input produces a yaw rate and a pitch angle change due to asymmetric drag and a change in the lift vector respectively. Thus the inputs and outputs are interrelated or coupled. These relationships of inputs to outputs are not linear and are seldom known with a high degree of certainty (Ref 9:1).

Classically, engineers assumed their mathematical models of these input/output relationships to be linear and invariant in small regions around equillibrium points (Ref 4:154). The MIMO problem was then uncoupled to achieve a set of single input - single output (SISO) problems (Ref 3:162). The designs resulting from this approach were often successful but usually involved a great deal of trial and error (Ref 9:1).

More recently, control designs consisting of feedback gains have been derived from the state space representation of the aircraft model using the digital computer to perform the complex matrix operations required. These techniques are often grouped under the heading of Modern or Optimal Control. (Ref 3:523-62). The robustness in these designs tends to break down when required state information is unavailable or has to be estimated. Another approach, based upon the state-variable approach is the method of Professor Brian Porter. This method has demonstrated ability to achieve robustness, but can't predict the range of uncertainty over which the design will be valid in advance.

The essence of Dr. Horowitz' method is the consideration of

the performance specifications and the uncertainty in the plant quantitatively from the very beginning of the design process. The uncertain MIMO plant model can be derived directly from the linear differential equations or from the state space representation of the MIMO system. By the use of elementary matrix operations the MIMO system is separated into SISO systems. The designer derives a controller for each of the resulting SISO loops based on the design specifications and any loop design(s) already completed. If each individual SISO design meets its requirements, then the combination of them is guaranteed to meet the overall design specifications (Ref 11:977).

Problem

The purpose of this thesis is to apply the method of Dr. Horowitz to a lateral control design for a large transport aircraft, specifically the C-135. The primary objective is that an engineer with a reasonable backgound in control theory and in the frequency response method of analysis should be able to follow the design steps and be able to apply this technique to similar problems.

Subordinate objectives are as follows:

1. Achievement of competence and insight in feedback theory, i.e., the means and cost of attaining desired performance despite uncertainty.

2. Analysis of design in achieving robustness, or the range of flight conditions over which the design is valid.

3. Qualitative comparison of the design resulting from this thesis to the design resulting from a concurrent C-135 thesis using the method of Professor Brian Porter.

Scope

This thesis is limited to a lateral flight control design for the C-135 aircraft using the Horowitz method. Comparisons are made between these results and those of a Porter method design for the same aircraft, but the comparisons are qualitative only.

The analysis of design robustness is limited by the availability of valid data representing the flight characteristics of the aircraft under varying conditions.

Assumptions

The following assumptions are made:

1. Flat, non-rotating Earth inertial reference frame.
2. Quasi-steady airflow (Ref 2:22).
3. Rigid body aircraft.
4. Constant aircraft mass.

In addition, it is assumed that computer simulations in the computer aided design program, TOTAL, provide realistic representations of aircraft motion in flight.

Approach

The first step in the approach to this problem is to reduce the aircraft data into a matrix representation of the plant model at each flight condition. The result is a plant matrix, $\underline{P}$, such that $\underline{y} = \underline{P}\underline{\delta}$, where $\underline{y}$ is the output vector and $\underline{\delta}$ is the input vector. Inverting the $\underline{P}$ matrix produces the effective SISO plant transfer functions used during each loop design.

The second step is to derive a frequency domain representation of

the desired specifications. This is admittedly the weakest part of this thesis. Military specifications for transport aircraft are not very demanding. Therefore, in this thesis, much stricter demands are imposed on the aircraft response. These demands are somewhat arbitrary and may be unrealistic.

The third step is to apply the Horowitz method to the design itself. The primary objective of this thesis is the presentation of this application of this method. The method also promises to provide insight into the costs and trade-offs involved in a design problem. As these become apparent, they are identified.

When the design is complete, the fourth step is to simulate the compensated system. This is done using the program, TOTAL. Aircraft response and control surface movements to a step command for a 30-degree bank turn are presented.

The fifth and final step is to compare, qualitatively, this design with the design resulting from a concurrent C-135 thesis using the Porter method. The ease of application, success in meeting specifications, and the resulting robustness of the two design methods are the primary comparisons made.

Presentation

This thesis consists of seven chapters. Chapter II presents the single input - single output (SISO) design theory of Professor Horowitz. The design of multiple input - multiple output (MIMO) systems is covered in Chapter III. Chapters II and III are co-written by Lt. Brian Pawlowski, GE-83D, author of another thesis using Professor Horowitz' technique and this author. Chapter IV contains the C-135 aircraft model

used in this thesis. Two designs are presented in Chapter V. The first design is presented in detail, the second is simply shown for comparison. The results of simulations for both designs are found in Chapter VI. Finally, Chapter VII consists of conclusions, recommendations, and a comparison of the results of this thesis to the results of a concurrent C-135 thesis using Porter's method.

II. Single Input - Single Output Theory

Introduction

Chapters II and III present an overview of the Quantitative Feedback Synthesis Technique used in the design of multiple input - multiple output flight control systems for this thesis. Examples are presented to aid in the understanding of the material. The technique is valid for the general n-by-n case. However, for simplicity, the examples below are either single loop or two-by-two systems. For a discussion of the three-by-three case and extrapolation to the more general case, see Reference 8 in the bibliography.

The flight control problem involves a multiple input - multiple output (MIMO) plant requiring regulation and control due to parameter uncertainty and disturbances. The mathematical equations describing the motion of an aircraft are highly non-linear. For design purposes, these equations are linearized about a point in the flight envelope, or flight condition. Uncertainty arises as the linearized coefficients vary with airspeed and altitude (see Chapter IV).

The Quantitative Feedback Synthesis Technique developed by Dr. Isaac Horowitz uses feedback to achieve closed-loop system response within performance tolerances despite plant uncertainty. The range of plant uncertainty and the output performance specifications are quantitative parameters in the design process (Ref 8:81). The fundamentals of the design method are presented in the discussion of the single input - single output design problem of Chapter II. The multiple input - multiple output design procedure is described in Chapter III, using the fundamentals developed in Chapter II.

Problem Definition

The general single input - single output (SISO) problem involves a plant transfer function, P, with uncertain parameters (gain, poles, and zeros) known only to be members of finite sets. The design specifications dictate the desired response of the plant to inputs and/or disturbances. The problem is to obtain a controller forcing the plant output to satisfy performance tolerances over the range of plant uncertainty.

The basic SISO control loop structure is shown in Fig II-1.

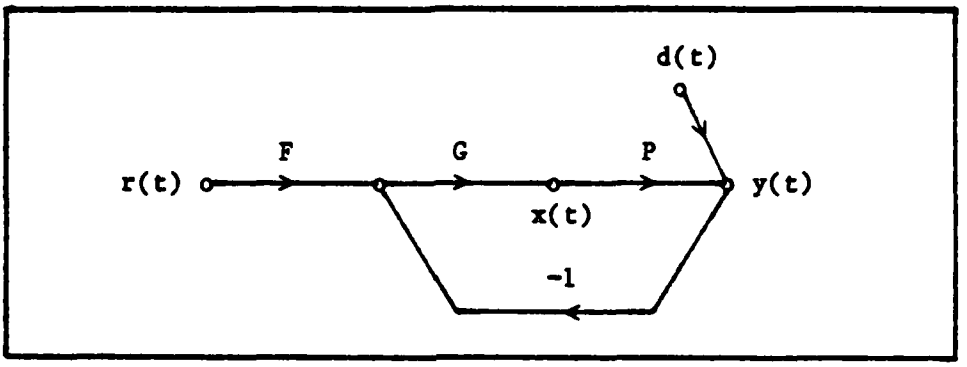

Fig II-1 Two Degree-of-Freedom Control Loop

In this figure, r(t) is the command input to the system and d(t) is a disturbance input to be attenuated. P is the plant transfer function, the characteristics of which are not precisely known. The compensator, G, and the prefilter, F, are to be designed to force the system output, y(t), to be an element of a set of acceptable responses, despite the uncertainty in P and the disturbance input, d(t). The plant input signal, x(t), is identified since it is generally of interest because of physical or practical constraints. The signals, r(t) and y(t) are assumed measurable quantities and the latter is available for feedback. Access to both signals allows the use of the two degree-of-freedom structure of Fig II-1 and provides the designer with two independent

compensator elements, F and G (Ref 9:13). It is also assumed that r(t), y(t), and (for now) P, such that y(t) = Px(t), are all Laplace transformable functions (Ref 9:8).

There are four transfer functions of interest in Fig II-1, where the loop transmission, L, is defined as; L = G P. The system output due to the command and disturbance inputs, respectively, are;

$$T_R = Y(s)/R(s) = \frac{F\,G\,P}{(1 + G\,P)} = \frac{F\,L}{(1 + L)} \qquad \text{(II-1)}$$

$$T_D = Y(s)/D(s) = \frac{1}{(1 + G\,P)} = \frac{1}{(1 + L)} \qquad \text{(II-2)}$$

and the plant input due to the command and disturbance inputs, respectively, are:

$$I_R = X(s)/R(s) = \frac{F\,G}{(1 + G\,P)} = \frac{F\,G}{(1 + L)} \qquad \text{(II-3)}$$

$$I_D = X(s)/D(s) = \frac{-G}{(1 + G\,P)} = \frac{-G}{(1 + L)} \qquad \text{(II-4)}$$

The design specifications may impose constraints on any or all of these transfer functions, but for the purpose of this example, only the first two are considered.

Design Specifications

The design specifications, or closed-loop system response tolerances, describe the upper and lower limits for acceptable output response to a desired input or disturbance. Any output response between the two bounds is assumed acceptable. The response specifications must

be determined prior to applying the design method. Typically, response specifications are given in the time domain, such as the figures of merit M_p, t_s, t_p, and K_m based upon a step forcing function, (Ref 3:346) or as a bounded region as shown in Fig II-2. Response to a step input is a good initial test of system response. Bounds (T_L) and (T_U) of the figure are the acceptable lower and upper limits of a system's tracking performance to a step input. Desired system response to a step disturbance generally requires maintaining the output below a given value, thus only an upper bound is necessary as shown by curve (T_D) in Fig II-2. Additional similar bounds are needed if other inputs are to be considered.

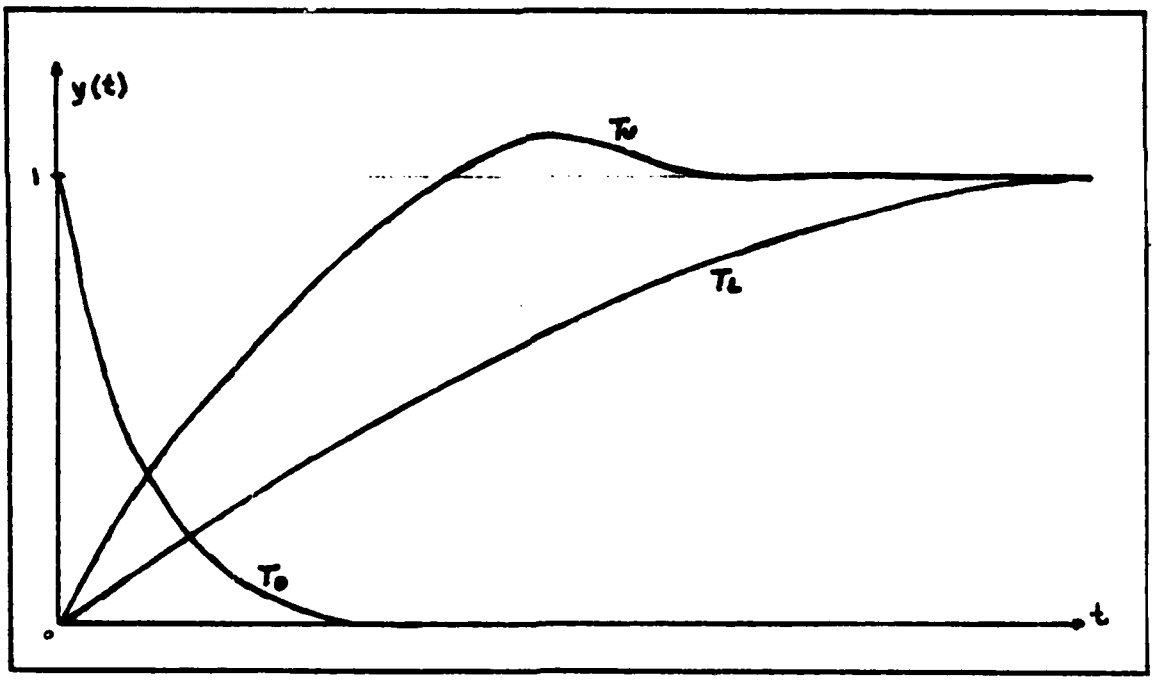

Fig II-2 Time Domain Step Response Specifications

The design technique is a frequency domain approach, therefore the time domain specifications must be translated to bounds in the frequency

domain. Desired control ratios, $T_{MR} = [Y/R]_{MR}$ and $T_{MD} = [Y/D]_{MD}$, are modeled to satisfy the performance specifications using the pole-zero placement method as described in Section 12-2 of Ref 3. For response to a step input, a third order model with one zero is suggested.

$$T_M = \frac{A\,(s + z_1)}{(s^2 + 2\zeta\omega_n s + \omega_n{}^2)(s + p_3)} \qquad \text{(II-5)}$$

The pole-zero pattern of Equation II-5 is shown in Fig II-3. The locations of the roots are adjusted until the step response of the modeled control ratio matches the bound.

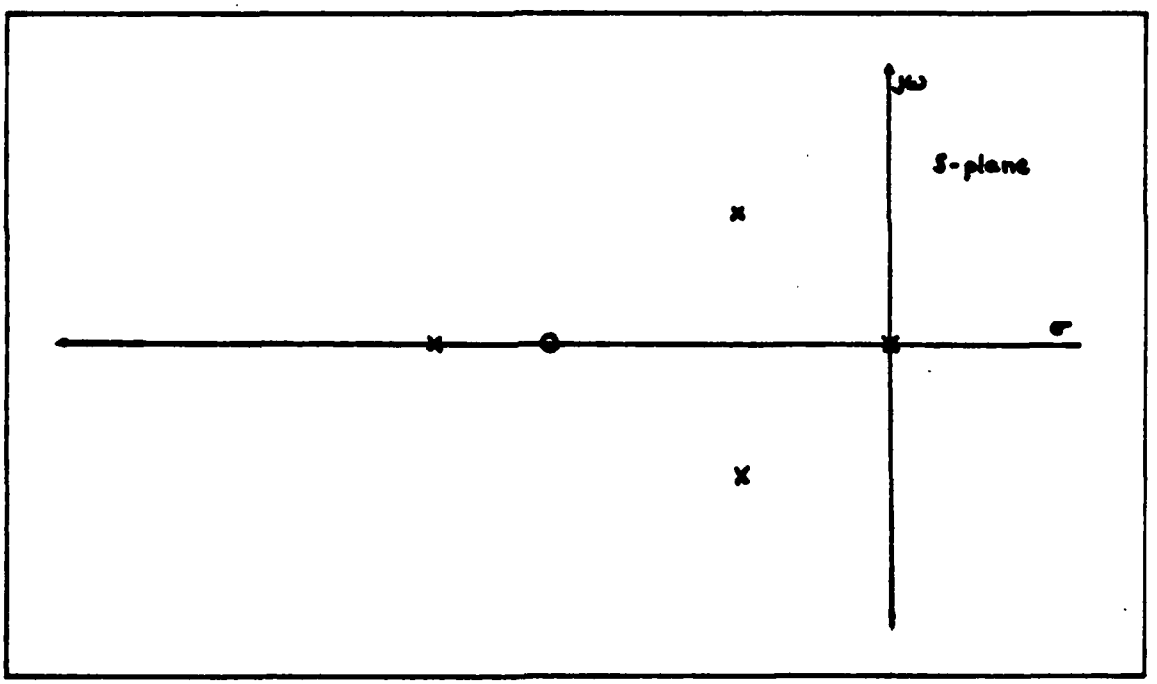

Fig II-3 Third-Order Control Ratio Pole-Zero Pattern

The frequency domain characteristics are considered during the response modeling. It is desireable to keep the magnitude difference (as a function of frequency) between the upper and lower bound models of

$|\underline{T}_{MR}(j\omega)|$ as large as possible at all frequencies. Choosing a lower bound model with a greater pole to zero ratio than the upper one ensures that the magnitude difference approaches infinity in the limit as ω approaches infinity.

Errors made during this modeling process manifest themselves in one of two ways. First, if the worst acceptable response model is not really acceptable, the system may not meet the specifications over the assumed range of uncertainty in P. And second, if the entire range of allowable outputs is not considered, the bandwidth of the compensation will be higher than necessary, increasing the cost of the compensator (Ref 9:5).

Once control ratios are obtained for each time response bound, a magnitude plot of the frequency response (Bode plot) for each $\underline{T}_M(j\omega)$ is made on the same graph as shown in Fig II-4. These plots are the frequency domain representation of the design specifications on T_R and T_D. These derived frequency domain specifications are used to obtain the bounds on the loop transmission, $\underline{L}(j\omega)$, as described later.

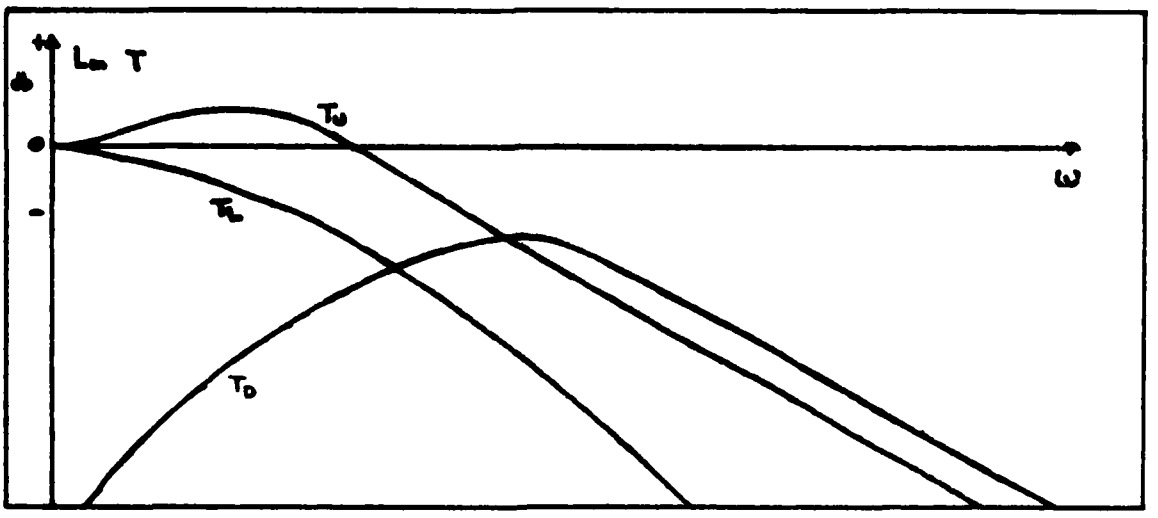

Fig II-4 Frequency Domain Specifications

Nichols Chart

The primary tool used in the design of the compensator elements, G and F is the Nichols chart, shown in Fig II-5. If the open loop transmission of a unity feedback system (L = GP, assuming F = 1 for now, in Fig II-1) is plotted using the horizontal and vertical scales on the chart, then at any given frequency, the magnitude and phase angle of T_R = L/(1+L) can be read directly from the curved scales. Conversely, any point corresponding to the magnitude and angle of T_R on the curved scales provides a point corresponding to the magnitude and angle of L on the horizontal and vertical scales (Ref 3:332-334). This correspondence between L and T_R on the Nichols chart is very important.

Likewise, the Nichols chart can be used for the disturbance response. Recall that $T_D = 1/(1 + L)$. By way of Sidi's transformation, L = 1/m (Ref 1:152-155) the system control ratio due to the disturbance becomes $T_D = m/(1 + m)$, which is of the same form as $T_R = L/(1 + L)$. One could design the inverse of the loop transmission, m, directly on the Nichols chart, but it is much easier to realize that by turning the Nichols chart upside down, reflecting the vertical angle of L lines about the -180 degree line (i.e. -190 becomes -170, -210 becomes -150, etc.), and reversing the signs on all magnitude lines, the chart can be used directly to design L itself. The horizontal and vertical lines still correspond to the magnitude and angle of L, and the curved magnitude lines correspond to the magnitude of (1 + L) (Ref 1:155). For design purposes, only the magnitude of (1 + L) is required. Therefore the curved angle lines on the chart can be ignored. In practice Sidi's transformation is merely implied by turning the Nichols chart upside down and modifying the scales as described above. The dummy variable,

m, need not be considered further.

Plant Templates

A plant template is a plot on the Nichols chart of the range of uncertainty in the plant P at a given frequency (Ref 7:290). Consider the example $P(s) = K/s(s+a)$ where the gain K is described by: $2 < K < 8$, and the location of the second pole is given by: $0.5 < a < 2.0$. An infinite number of possible P's exist due to the variation in parameters, K and a; however each parameter is a member of a set with finite boundaries. Likewise, the magnitude and phase angle of all possible P's lie within finite boundaries when plotted at a given frequency. The plant template is obtained by plotting $Lm[\underline{P}(j\omega)]$ vs. $Ang[\underline{P}(j\omega)]$ for all possible $\underline{P}(j\omega)$'s at a given frequency on the Nichols chart. Note, only the outer edges of the template need be calculated. The plant transfer functions at the boundaries are found by holding one parameter constant at a boundary value, i.e. set $K = 2$, and vary a in increments from 0.5 to 2.0. The frequency response at $\omega = 1$ for the P's obtained above provide a set of points from A, (K=2, a=0.5), to D, (K=2, a=2), on the Nichols chart as shown in Fig II-5. The process is continued until the complete template is formed. For example, for $a = 0.5$, vary K from 2 to 8 to obtain the line from A, (a=0.5, K=2), to B, (a=0.5, K=8). Templates are needed for a number of frequencies taken at regular intervals, such as every octave. A set of templates is shown in the figure to demonstrate the change in size and location of the range of uncertainty in P for different frequencies.

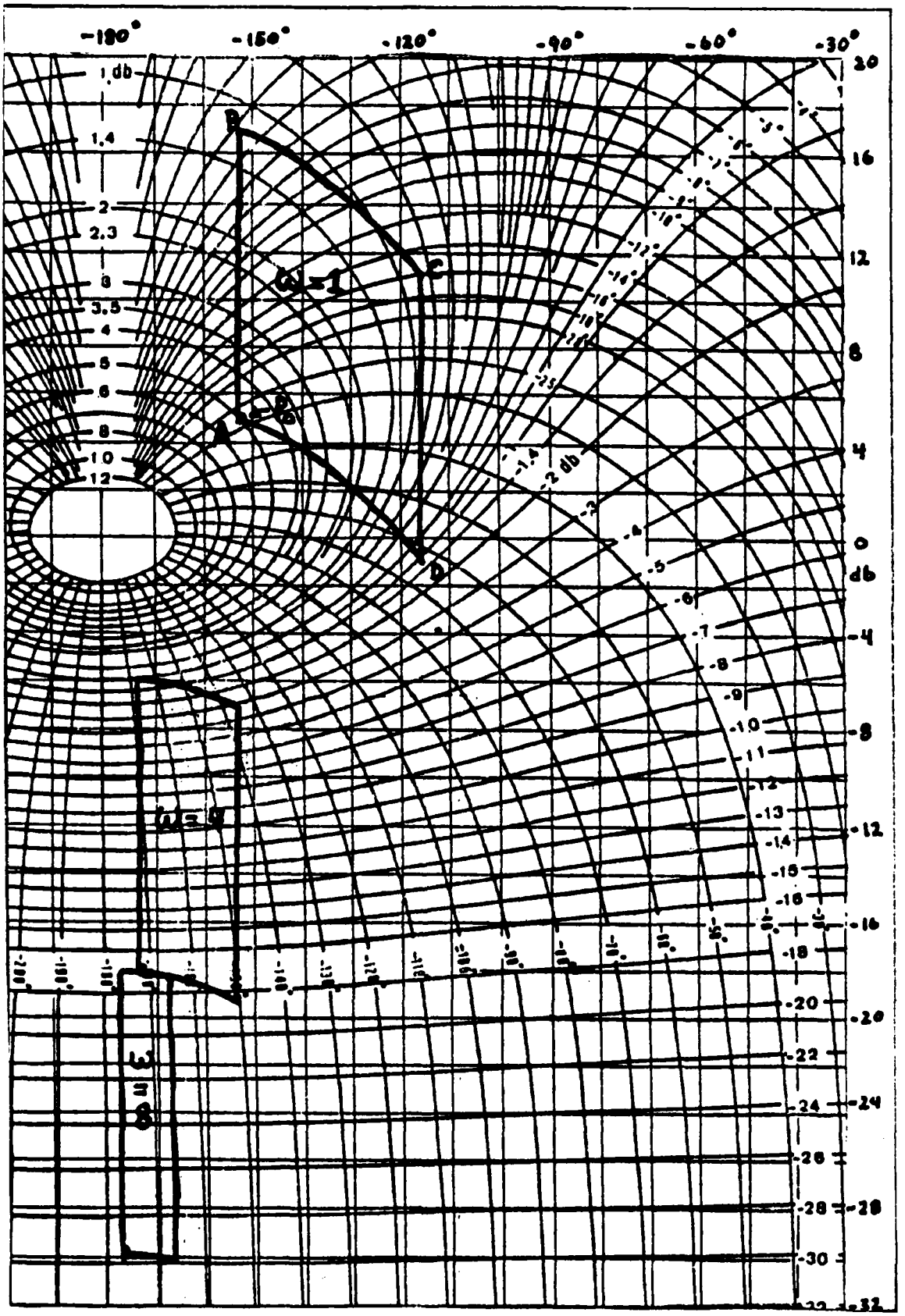

Fig II-5 Nichols Chart with Plant Templates

Nominal Plant

To facilitate the shaping of the loop transmission, the designer needs a reference or nominal plant transfer function. This nominal plant, P_o, chosen by the designer is nothing more than a reference plant to be used in the definition and shaping of the nominal loop transmission, $L_o = GP_o$. There are no rules or constraints on the selection of P_o. It doesn't even have to be from the set of possible P's, but it is usually convenient to choose P_o such that it lies at a recognizable point on the templates. It is convenient, as is the case with the example, to select P_o such that it lies at the lower, left corner of the templates which helps keep the bounds on L_o, to be described next, as near the center of the Nichols chart as possible. Once selected, the P_o point should be marked on each template, as in Fig II-5. For the example, the plant described by $P_o = 2/(s + 0.5)$ is chosen as the nominal plant.

Derivation of Bounds on L

The system step response y(t) is uniquely determined by the transfer function T(s). Likewise, T(s), for a stable, minimum phase system (no right-half-plane poles or zeros), is completely specified by the magnitude of the frequency response $|\underline{T}(j\omega)|$ as described in References 7 and 9. From the design specifications, the frequency response of the output $|\underline{Y}(j\omega)|$ can vary from the value of the bound (T_U) to the value on the bound (T_L) at a given frequency (see Fig II-4). For the given example, at the frequency, $\omega = 1$, assume that $|\underline{Y}(j1)|$ can vary from 0.7 db to -0.8 db. The relative variation in $|\underline{Y}(j1)|$ is (0.7) db - (-0.8) db or 1.5 db. In general, the allowable relative change in $\underline{Y}(j\omega)$ at a

given frequency is expressed as:

$$\Delta Lm\ [\underline{Y}(j\omega_i)] = Lm\ [\underline{T}_U(j\omega_i)] - Lm\ [\underline{T}_L(j\omega_i)] \qquad \text{(II-6)}$$

where $\underline{T}_U(j\omega)$ and $\underline{T}_L(j\omega)$ are the frequency domain bounds on $\underline{Y}(j\omega)$.

The relative change in the output is related to the control ratio as follows. From Fig II-1 and Equation II-1, $\Delta LmY = \Delta LmT = \Delta Lm[FL/(1+L)]$ where $L = GP$ and it is assumed that no uncertainty exists in G and F. Then,

$$\Delta Lm\ [\underline{Y}(j\omega_i)] = \Delta Lm\ [\underline{T}(j\omega_i)] = \Delta Lm\ \frac{\underline{L}(j\omega_i)}{[1 + \underline{L}(j\omega_i)]} \qquad \text{(II-7)}$$

Likewise, the relative change in $\underline{L}(j\omega)$ is equal to the relative change in the plant.

$$\Delta Lm\ [\underline{L}(j\omega_i)] = \Delta Lm\ [\underline{P}(j\omega_i)] \qquad \text{(II-8)}$$

The variation in P arises due to parameter uncertainty, thus the problem is to find an L such that the relative change requirements on the closed-loop response are satisfied for the entire uncertainty range of P. The design specifications state the requirements on the closed-loop response $\underline{Y}(j\omega)$ and thus $\underline{T}(j\omega)$ as given by Equation II-7. Constraints on the loop transmission $\underline{L}(j\omega)$ are desired (Ref 7:291, 9:18).

$\underline{L}(j\omega)$ Bounds on the Nichols Chart

The relative uncertainty in L is shown to be equal to the range of uncertainty in P by Equation II-8. As described earlier, the plant template is a plot on the Nichols chart of the range of uncertainty in P at a given frequency. Because Lm (L) = Lm (P) + Lm (G) and also

Ang(L) = Ang(P) + Ang(G), a template may be translated (but not rotated) horizontally or vertically on the Nichols chart, where horizontal and vertical translations correspond to the angle and magnitude requirements on $\underline{G}(j\omega)$ respectively at a given frequency (Ref 7:290). Drawing a line on each of the templates parallel to the horizontal or vertical grid lines (see Fig II-5) of the Nichols chart is suggested to maintain correct template orientation.

With the template corresponding to $\omega = 1$ of Fig II-5, translate it to position 1 shown in Fig II-6. Since the template is the range of uncertainty in P and L = GP, where G is to be precisely determined, it follows that the area now covered by the template corresponds to the variation in L and in T due to the uncertainty of P. Recall the correspondence between L and T on the Nichols chart. Using the curved magnitude contours, i.e. contours of constant $Lm[\underline{T}(j\omega)]$, read the maximum and minimum values of T covered by the template. If the difference between the maximum and minimum values is greater than the allowable variation in T at the frequency $\omega = 1$, ($\Delta Lm\ [\underline{T}(j1)]$ as given by Eq II-7 and determined from Fig II-4), shift the template vertically, as shown in Fig II-6, until the difference is equal to $\Delta Lm\ [\underline{T}(j1)]$ (to position 2). Conversely, if the difference is less than that allowed, move the template vertically downward until the equality is obtained. When the position of the template achieves the equality (position 2 of the example), mark the nominal point P_o of the template on the Nichols chart. The point marked corresponds to a bound on the magnitude and phase angle values of $\underline{L}_o(j1)$ read from the horizontal and vertical scales of the Nichols chart, where the nominal loop transmission, $\underline{L}_o(j\omega_i)$, is given by:

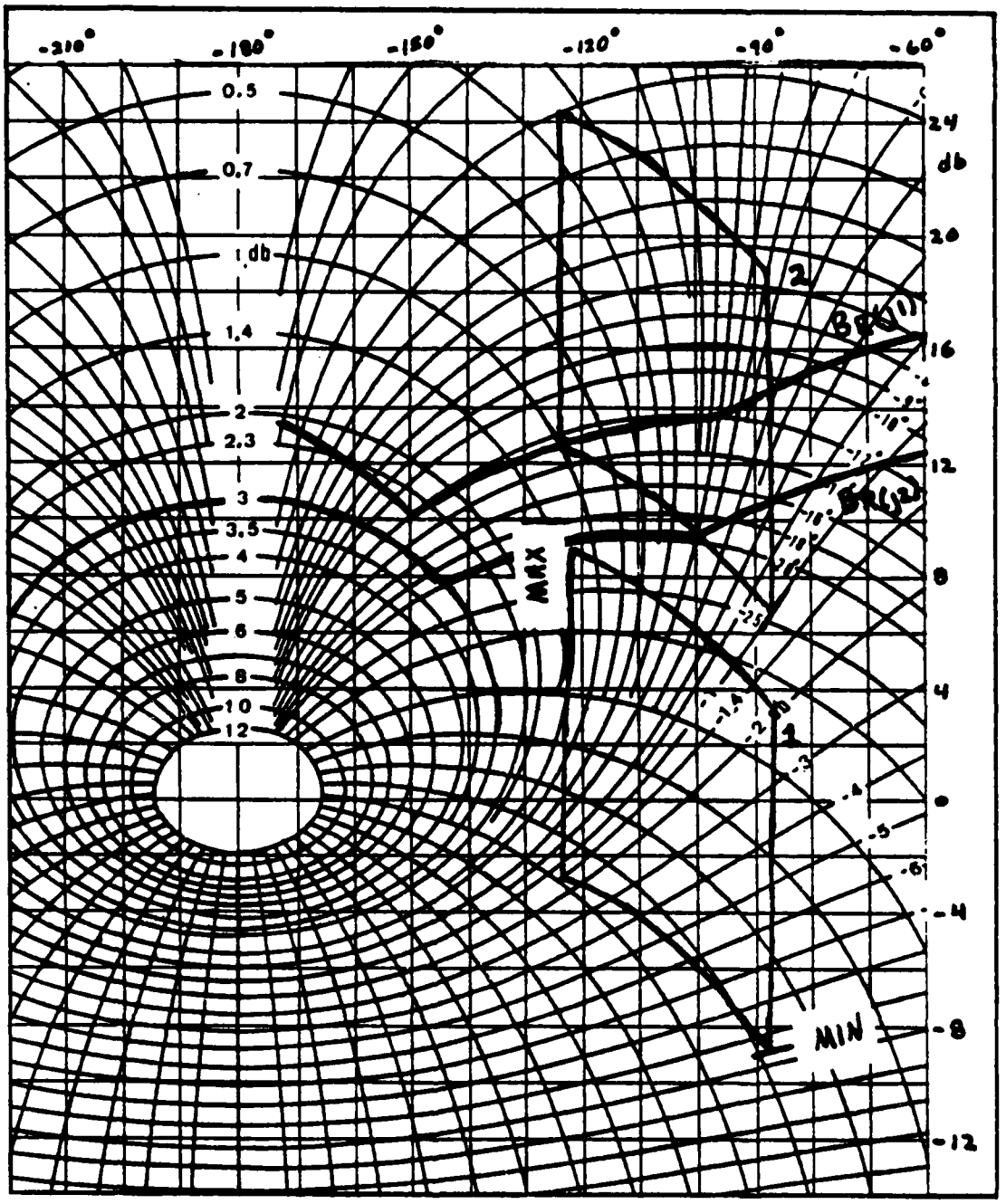

Fig II-6 $\underline{L}_o(j\omega_i)$ Bounds on the Nichols Chart

$$\underline{L}_o(j\omega_i) = \underline{G}(j\omega_i)\underline{P}_o(j\omega_i) \qquad \text{(II-9)}$$

Repeat the process horizontally across the chart at different values of Ang(L_o). The points marked on the chart form a curve, $\underline{B}_R(j\omega_i)$, representing the boundary of $\underline{L}_o(j\omega_i)$ at the given frequency of the template. As long as $\underline{L}_o(j\omega_i)$ lies outside or above the boundary, $\underline{B}_R(j\omega_i)$, corresponding to $\omega = \omega_i$ at the frequency $\omega = \omega_i$, the variation in T due to the uncertainty in P is less than or equal to the relative change in T allowed by the design specifications at that frequency. Repeat this boundary, $\underline{B}_R(j\omega_i)$, derivation for various frequencies, ω_i using the corresponding plant templates to obtain a series of bounds on $\underline{L}_o(j\omega_i)$ (Ref 7:291-292).

Likewise, the step disturbance response specification (line T_D on Fig II-4), is converted to bounds on $\underline{L}_o(j\omega)$. In order to effectively reject the disturbance the following inequality must be satisfied;

$$\frac{1}{|1 + \underline{L}(j\omega)|} \leq |\underline{C}(j\omega)| \qquad \text{(II-10)}$$

where $|\underline{C}(j\omega)|$ is the magnitude of the boundary, (T_D), on Fig II-4. Converting the magnitudes to decibels and rearanging terms, the inequality can be expressed as:

$$\text{Lm } [1 + \underline{L}(j\omega)] \geq - \text{Lm } [\underline{C}(j\omega)] \qquad \text{(II-11)}$$

Now a template is placed on the inverted Nichols chart such that its lowest point rests directly on the contour of constant Lm $[1 + \underline{L}(j\omega)]$ equal to -Lm $[\underline{C}(j\omega)]$ at the frequency, ω_i, for which the template is drawn. The point, P_o, is marked and the template slid along the same contour forming a bound, $\underline{B}_D(j\omega_i)$ for L_o. Bounds are formed for each

frequency, in this manner using each template. Using the rectangular (Lm L) grid, transcribe the bounds, $\underline{B}_D(j\omega_i)$, on L_o onto the upright Nichols chart which already contains the command response bounds, $\underline{B}_R(j\omega)$, on L_o as shown in Fig II-7. For each frequency of interest, erase the lower of the two L_o bounds, where the remaining bound is labeled, $\underline{B}_o(j\omega)$. The point here is that the worse bound must be used in the shaping of L_o.

Universal Frequency Bound

The universal frequency (UF) bound ensures the loop transmission, L, has positive phase and gain margins, whose values depend on the oval of constant magnitude chosen (see Fig II-7). As the frequency, ω, increases, the plant templates become narrower and can be considered vertical lines as ω approaches infinity. The allowable variation in T increases with frequency also. The result is the bounds of $\underline{L}_o(j\omega_i)$ tend to become a very narrow region around the 0 db, -180 degree point (origin) of the Nichols chart at high frequency. To avoid placing closed-loop poles near the $j\omega$ axis resulting in oscillatory disturbance response, a UF bound is needed on the Nichols chart. With increasing ω, the bounds on L_o approximately follow the ovals encircling the origin. Choose one of the ovals near the origin. In Fig II-7, the contour of constant magnitude equal to 5 db is used in this example. From the templates corresponding to high frequency, find the template with the greatest vertical displacement, Δv, in db. Δv may be accurately determined by finding the maximum change in $Lm[\underline{P}(j\omega)]$ in the limit as ω goes to infinity. Translate the lower half of the 5 db oval down the length of the template, i.e. Δv db, as shown, thus obtaining the UF bound (see

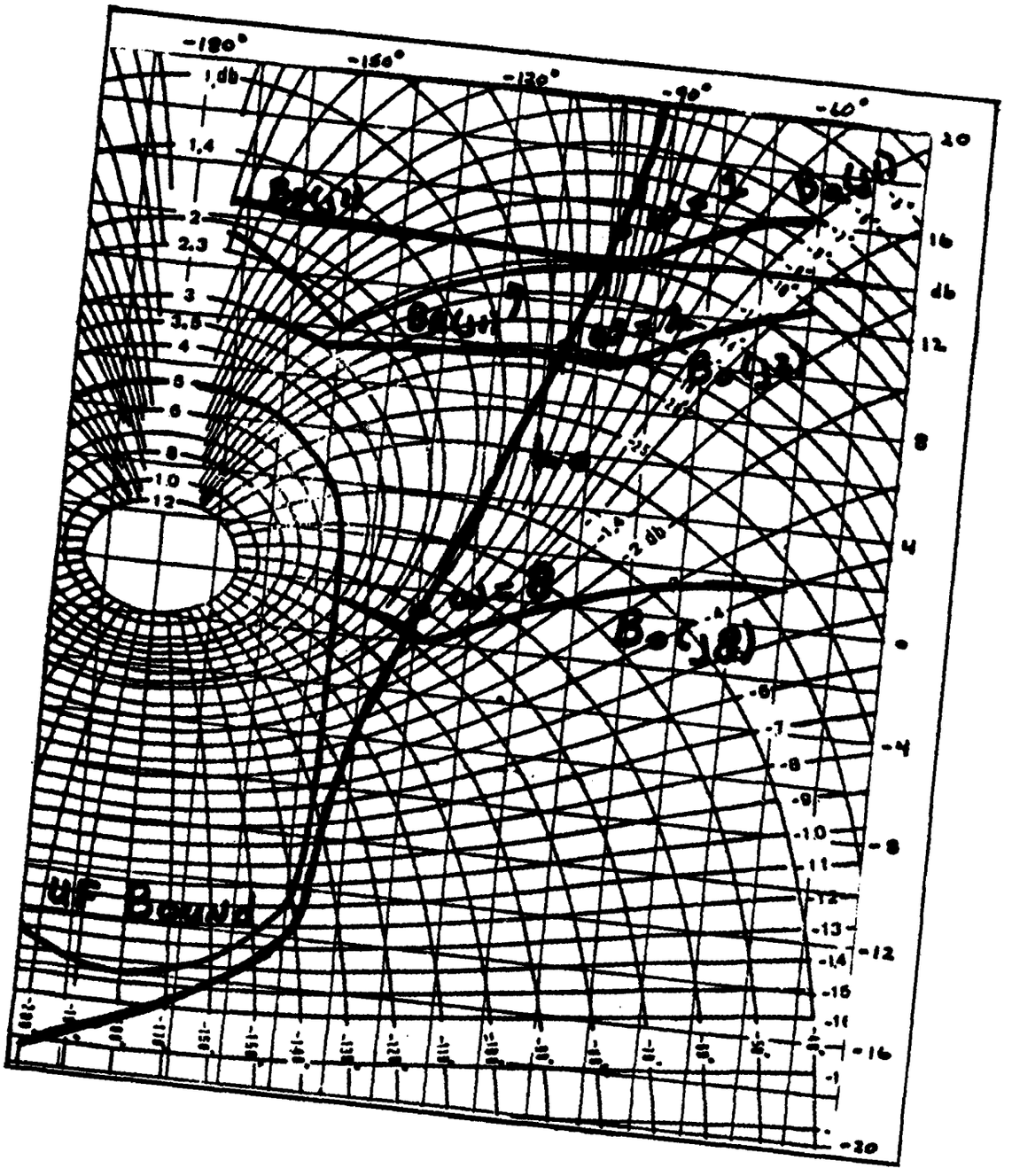

Fig II-7 Nominal $L_o(j\omega_1)$

Fig II-7) (Note: Professor Horowitz refers to this bound as the Universal High Frequency (UHF) Bound) (Ref 9:20-22).

Shaping of the Nominal Loop Transmission

The shaping of a nominal loop transmission conforming to the boundaries of L_o is a most crucial step in the design process. A minimum bandwidth design has the value of L_o on its corresponding bound at each frequency. In practical designs, the goal is to have the value of L_o occurring above the corresponding bound, but as close as possible to keep the bandwidth to a minimum. Fig II-7 shows a practical design for L_o. Note, any right-half-plane (rhp) poles and/or zeros of P_o must be included in L_o to avoid any attempt to cancel them with zeros and/or poles of G. Although not required, using the poles and zeros of P_o as a starting point in the design of L_o is suggested, to avoid any implicit cancellation of roots in determining G. For a discussion of loop transmission shaping, with examples, see Appendix A.

Solving for G

The compensator, G, is obtained from the relation: $G = L_o/P_o$. If the L_o found above does not contain the roots of P_o, then the compensator G must cancel them. Note, cancellation occurs only for purposes of design using the nominal plant transfer function. In actual implementation, exact cancellation does not result (nor is it necessary) since P can vary over the entire uncertainty range.

Provided the nominal loop transmission, L_o, is shaped properly, i.e. meets the requirement of being on or above the bound, $\underline{B}_o(j\omega_i)$, at

each corresponding frequency, the variation in T resulting from the uncertainty in P is guaranteed to be less than or equal to the allowable relative change in T allowed by the design specifications (Ref 7:291). The design of the prefilter, F, is the final step in the design process.

Design of F

Design of a proper L_o only guarantees the variation in $|\underline{T}(j\omega)|$ is less than or equal to that allowed. The purpose of the prefilter is to position $Lm[\underline{T}(j\omega)]$ within the frequency domain specifications. For the example given above, the magnitude of the frequency response must lie within the bounds shown in Fig II-4 which are redrawn in Fig II-8. One method for determining the bounds on the prefilter, F, is as follows. Place the nominal point of the $\omega = 1$ template on the Nichols chart where the $\underline{L}_o(j1)$ point occurs. Record the maximum and minimum values of Lm(T), 1.2 and 1.0 in the example, obtained from the curved magnitude contours. Compare the values found above to the maximum and minimum values allowed by the frequency domain specifications of Fig II-4 at $\omega = 1$, (0.7 db and -0.8 db). Determine the range, in db, Lm(T) must be raised or lowered to fit within the bounds of the specifications. For example, at $\omega = 1$, the actual Lm(T) must be within $[Lm(T_U) = 0.7 \text{ db}] > Lm[\underline{T}(j1)] > [Lm(T_L) = -0.8 \text{ db}]$. But, from the plot of L_o, the actual range of Lm(T) is: 1.2 db > $Lm[\underline{T}(j1)]$ > 1.0 db. To lower $Lm[\underline{T}(j1)]$ from the actual range to the desired range, the prefilter, Lm(F) required is: (0.7 - 1.2 db) > $Lm[\underline{F}(j1)]$ > (-0.8 - 1.0 db), or -0.5 db > $Lm[\underline{F}(j1)]$ > -1.8 db (See Fig II-8). The process is repeated for each frequency corresponding to the templates used in the design of L_o. Therefore in Fig II-9 the difference between the T_U and T_{max} curves and the difference

between the T_L and T_{min} curves indicate the requirements for F as a function of frequency.

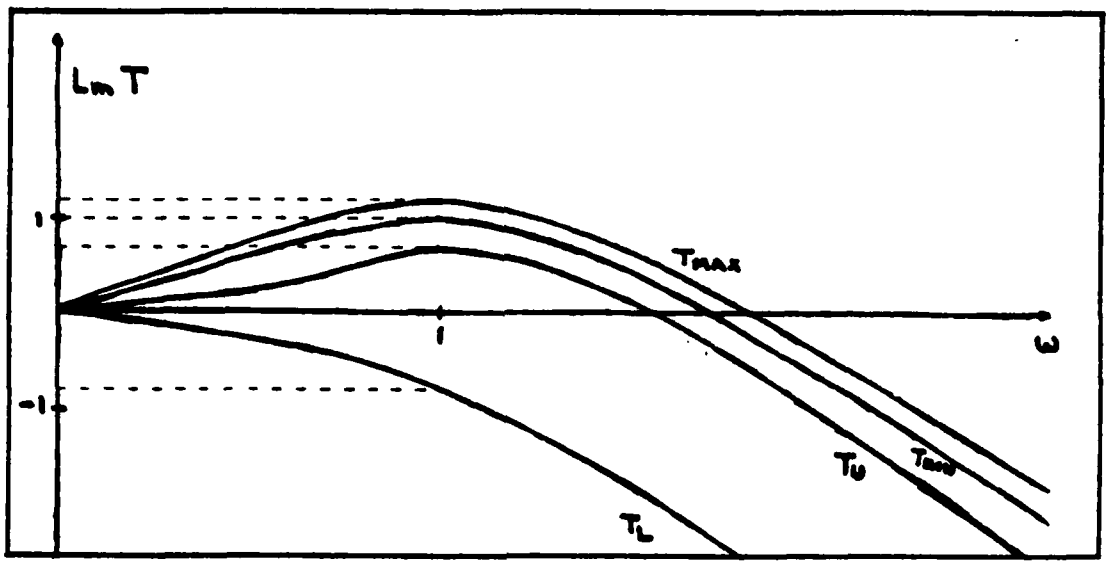

Fig II-8 Requirements on F

Bounds on F, $[Lm(T_U) - Lm(T_{max})] > Lm(F) > [Lm(T_L) - Lm(T_{min})]$, are plotted as a function of frequency as shown in Fig II-9. By use of the straight line approximation, determine a transfer function, F, such that its magnitude lies within these bounds. The transfer function obtained in this manner is the prefilter, F (Ref 7:301).

The single loop design is complete with the design of F. The system response is guaranteed to remain within the bounds of the design specifications, provided the uncertainty in P stays within the range assumed at the beginning of the design process (Ref 7:288).

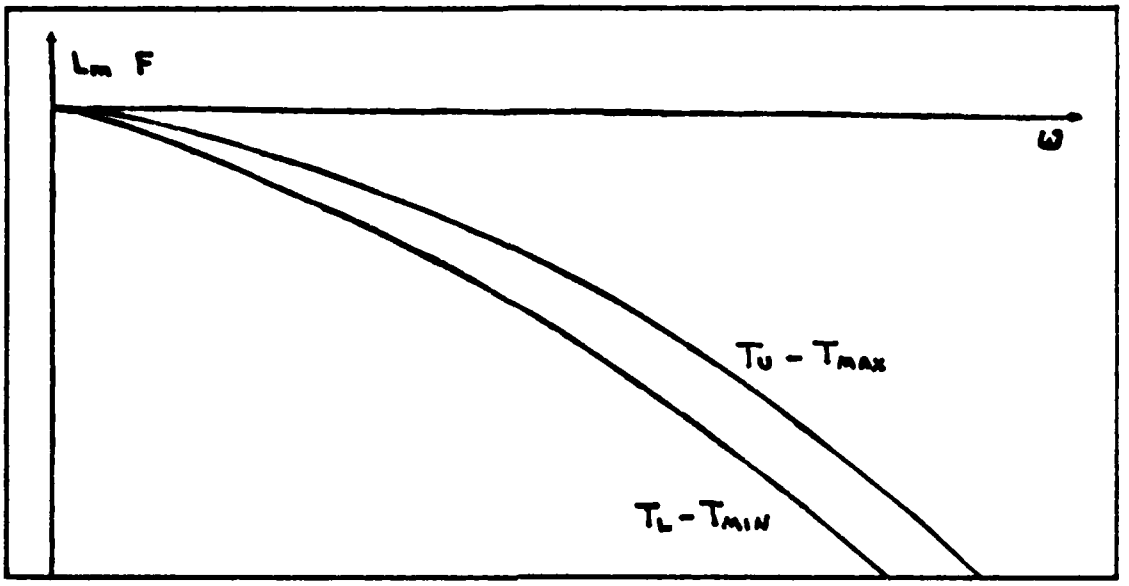

Fig. II-9 Frequency Bounds on the Prefilter, F

Summary

This chapter presents an overview of the SISO design technique of Profesor Horowitz for single loop systems with uncertain plants. The technique is entirely based in the frequency domain, and makes considerable use of the Nichols and Bode plots. Much of the designing can be done by graphical methods.

Design specifications are translated into the frequency domain and constitute limits or boundaries on the frequency response of the system control ratio and the loop transmission. Two compensator elements, G and F, are synthesized to control the system response to inputs and disturbances.

III. Multiple Input - Multiple Output Theory

Introduction

The design approach for each loop of the MIMO system is identical to that for the SISO system described in Chapter II. But first the MIMO system must be seperated into SISO loops which are equivalent to the actual MIMO model.

In general, an n-by-n MIMO system can be represented in matrix notation as $\underline{y} = \underline{P}\underline{u}$, where $\underline{y}$ is the vector of plant outputs, $\underline{u}$ is the vector of plant inputs, and $\underline{P}$ is the plant matrix of transfer functions relating $\underline{u}$ to $\underline{y}$. This $\underline{P}$ matrix is formed from either the linear differential equations describing the system or directly from the system state space representation.

Professor Horowitz has shown, by the use of fixed point theory, that the inverse of the $\underline{P}$ matrix, referred to as $\underline{Q}'$, contains elements which are the inverses of n^2 single loop transfer functions equivalent to the original MIMO plant. The MIMO problem is then broken up into n loop designs and n^2 prefilter/disturbance problems, which are each handled as described in Chapter II (Ref 10:677).

The MIMO Plant

Consider the multiple input - multiple output plant of Fig III-1. The n x 1 input vector, $\underline{u}$, produces an n x 1 output vector, $\underline{y}$. The relationship between $\underline{y}$ and $\underline{u}$ is described by the n x n plant matrix, $\underline{P}$, which is known only to be an element of a set of possible $\underline{P}'$s. It is assumed that the range of uncertainty in $\underline{P}$ can be determined, probably in the form of empirical data relating $\underline{u}$ to $\underline{y}$.

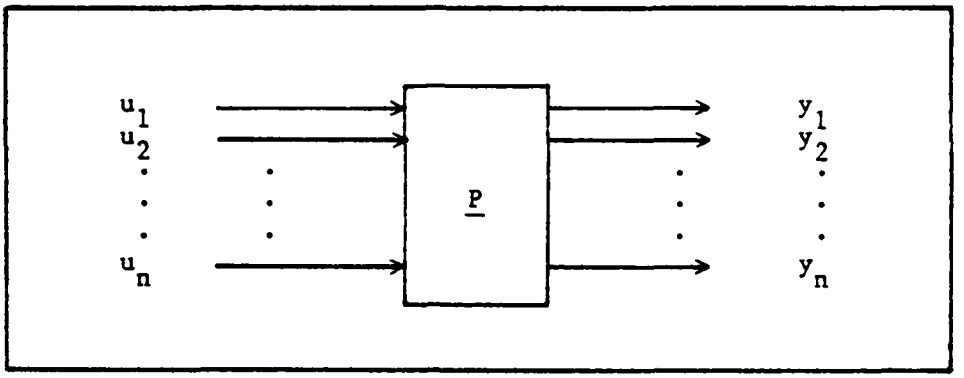

Fig III-1 MIMO Plant

Note that the input and output vectors are assumed to be of the same dimension. Although this may appear to be a restrictive assumption, it can be shown that with n inputs, at most n outputs can be independently controlled (Ref 6:530-536). Thus if the existing model defines an unequal number of inputs and outputs, the first step is to modify the model such that the dimensions of the input and output vectors are equal. An example of such a modification is presented in Chapter V.

The plant matrix, $\underline{P}$, can be derived directly from the set of coupled, linear, time-invariant differential equations describing the behavior of the plant in response to its inputs. Consider a general plant model of the form:

$$(a)y_1 + (bs^2 + cs)y_2 = (f)u_1 + (g)u_2$$
$$(ds)y_1 + (e)y_2 = (h)u_1 + (i)u_2 \qquad \text{(III-1)}$$

where a through i are the constant coefficients, the y's are the outputs, and the u's are the inputs to the plant. The system of Equation III-1 can be represented in matrix notation as;

$$\begin{bmatrix} a & bs^2 + cs \\ ds & e \end{bmatrix} \underline{y} = \begin{bmatrix} f & g \\ h & i \end{bmatrix} \underline{u} \qquad \text{(III-2)}$$

Define the matrix multiplying the output vector as $\underline{M}$ and the matrix multiplying the input vector as $\underline{N}$. The system is now described by;

$$\underline{My} = \underline{Nu} \qquad \text{(III-3)}$$

The plant matrix needed is defined by;

$$\underline{y} = \underline{Pu} \qquad \text{(III-4)}$$

Thus the plant matrix, $\underline{P}$ is simply;

$$\underline{P} = \underline{M}^{-1}\underline{N} \qquad \text{(III-5)}$$

The standard state space representation for a system is described by the equations (Ref 3:93);

$$\begin{aligned} \dot{\underline{x}} &= \underline{Ax} + \underline{Bu} \\ \underline{y} &= \underline{Cx} \end{aligned} \qquad \text{(III-6)}$$

The block diagram for this system is shown in Fig III-2.

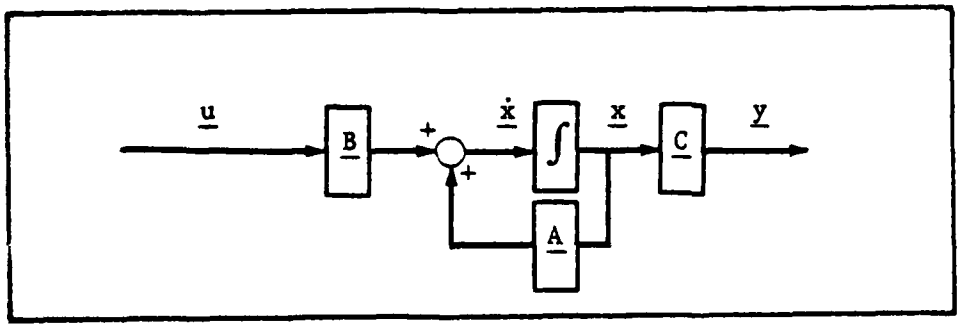

Fig III-2 Standard State Space Diagram

Although, any number of states may be represented, it is again assumed that the input and output vectors, $\underline{u}$ and $\underline{y}$ respectively, are of the same dimension. Assuming the system is linearized and the $\underline{A}$, $\underline{B}$, and $\underline{C}$ matrices are time invariant, the plant matrix is;

$$\underline{P} = \underline{C}[s\underline{I} - \underline{A}]^{-1}\underline{B} \qquad \text{(III-7)}$$

This plant matrix is actually a representative member of a set of possible plant matrices due to the uncertainty in the plant parameters. In practice, a finite set of $\underline{P}$ matrices are formed representing the plant under varying conditions.

MIMO Compensation

The compensation scheme for the MIMO system is similar to that of the SISO system of Chapter II. The basic MIMO control structure is shown in Fig II-3 where $\underline{P}$ is the uncertain plant matrix, $\underline{G}$ is a diagonal compensator matrix, and $\underline{F}$ is a prefilter matrix. Designs involving a non-diagonal $\underline{G}$ matrix are not considered in this thesis (Ref 12:14).

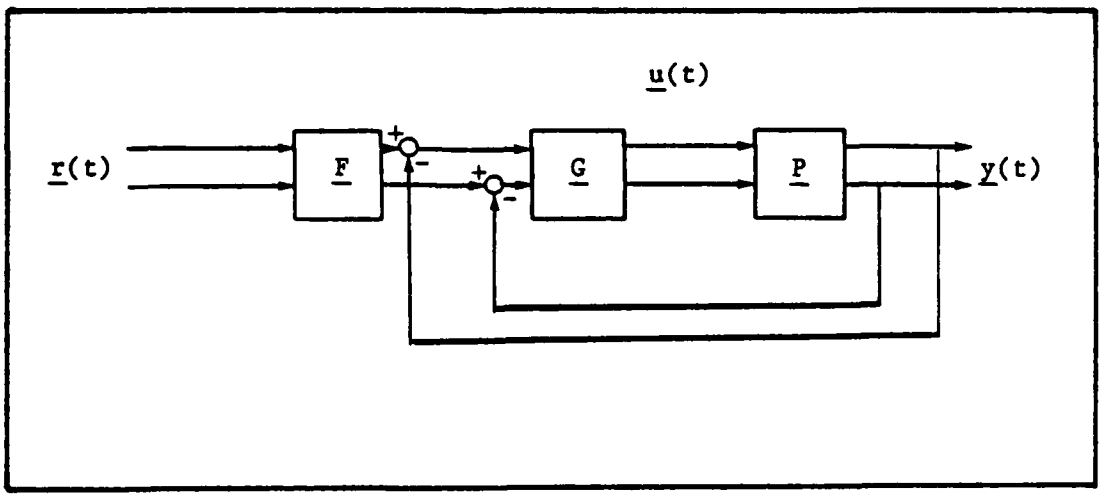

Fig III-3 MIMO Control Structure

The functions of $\underline{G}$ and $\underline{F}$ are identical to those of G and F of the SISO system of Chapter II. Fig III-4 shows a more detailed breakdown of a two-by-two MIMO system where:

$$\underline{G} = \begin{bmatrix} g_1 & 0 \\ 0 & g_2 \end{bmatrix} \qquad \underline{F} = \begin{bmatrix} f_{11} & f_{12} \\ f_{21} & f_{22} \end{bmatrix} \qquad \underline{P} = \begin{bmatrix} p_{11} & p_{12} \\ p_{21} & p_{22} \end{bmatrix}$$

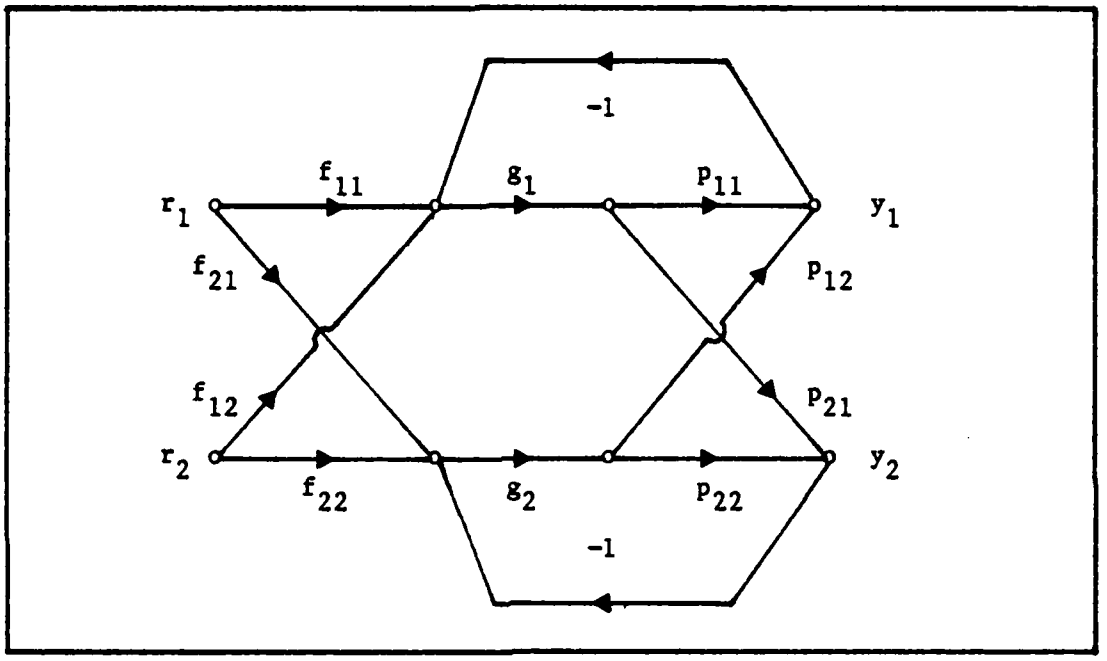

Fig III-4 Two-by-Two MIMO System

Constraints on the Plant Matrix

The set of $\underline{P}$ matrices must be tested to ensure that two critical conditions are met (Ref 8:86-90):

1. $\underline{P}$ must not be singular for any possible combination of plant parameters. i.e. $\underline{P}^{-1}$ must exist.

2. As $s \to \infty$, $|p_{11}p_{22}| > |p_{12}p_{21}|$ for all possible plants. This is the requirement for a two-by two plant. For explanation of the constraint inequality for the three-by-three or higher cases see Ref 8.

The first condition is absolutely necessary to ensure controllability of the plant. The inverse of $\underline{P}$ produces the effective transfer

functions used in the design. If condition 2 is not satisfied, it may be possible to change the ordering of the input or output vector which changes the ordering of the $\underline{P}$ matrix elements.

Effective SISO Loops

Now define a matrix $\underline{Q}' = \underline{P}^{-1}$ which has elements, q_{ij}'. The n^2 effective transfer functions needed are; $q_{ij} = 1/q_{ij}'$. Ref 8 contains the derivation and proof of this equivalence. The n x n MIMO system is now treated as n^2 SISO problems. Fig III-5 shows the four effective SISO loops resulting from the two-by-two MIMO system (Ref 10:682).

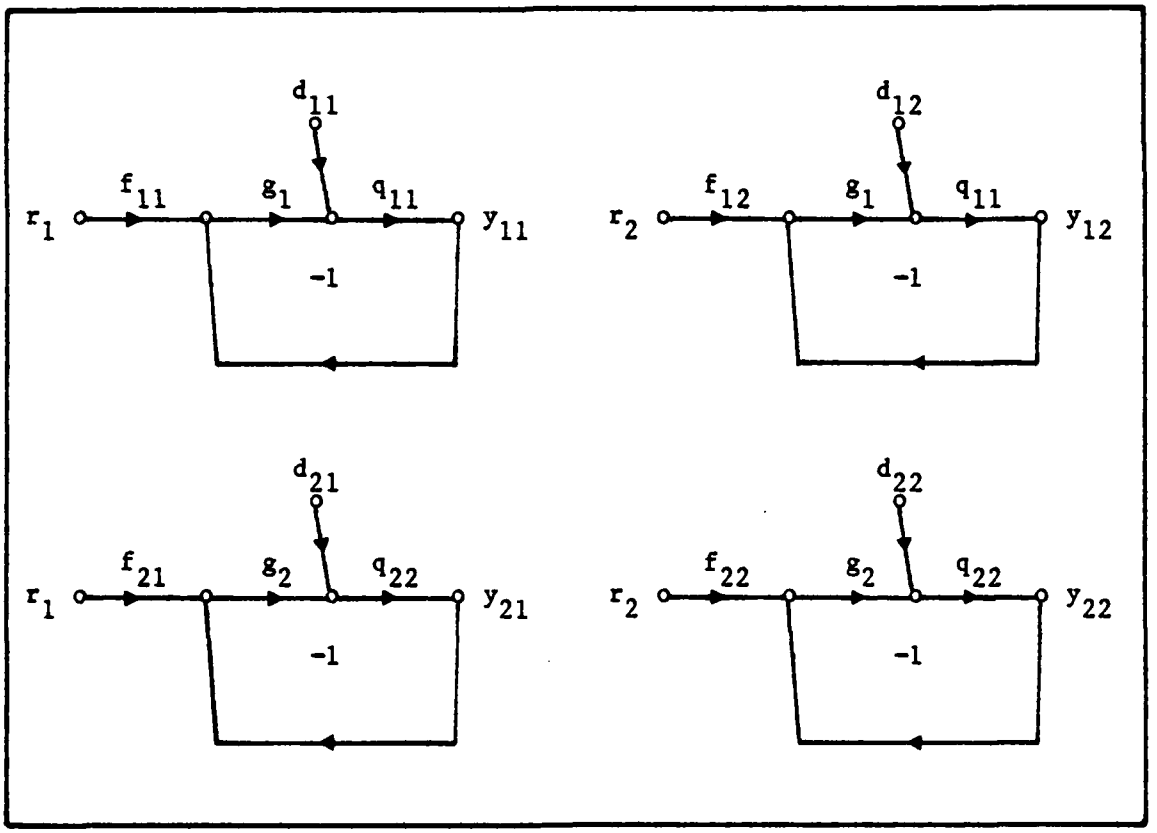

Fig III-5 Effective SISO Loops

Each loop in Fig III-5 is handled as an individual SISO design problem in accordance with the procedures presented in Chapter II. The f's and g's are the compensator elements F and G described previously. The disturbances, d_{ij} represent the interaction between the loops.

$$-d_{ij} = \sum_{k} \frac{b_{kj}}{q_{ik}} \quad , k \neq i \tag{III-8}$$

The b_{kj} in the above equation is the upper response bound, (T_U or T_D in Fig II-4), for the respective input/output relationship. These are obtained from the design specifications (Ref 10:681-684). Note that the first digit of the subscript of b_{kj} refers to the output and the second digit to the input. Thus b_{kj} is a function of the response requirements on the output, y_k, due to the input, r_j.

A recent improvement in the design technique involves modification of the q's on the second and subsequent loops based on the g's already designed. This reduces the overdesign inherent in the early part of the design process. During the design of the final loop the exact equation, representing the loop and the interactions of the other loops, is used (Ref 11:977). The use of this improvement is demonstrated in the actual design, Chapter V.

Basically Non-interacting (BNIC) Loops

When the response of an output, y_k, due to an input, r_j, is ideally zero, the y_{kj} loop is called a basically non-interacting (BNIC) loop (Ref 10:679). Due to loop interaction and plant uncertainty, this ideal response is not achievable. Therefore, the performance specifications describe maximum responses and the loop is handled exclusively as

a disturbance rejection problem.

Summary

This chapter describes the multiple input - multiple output plant and the plant matrix which describes it. Guidelines are presented for finding the $\underline{P}$ matrix, which relates the input vector to the output vector.

The division of the MIMO system into separate SISO loops is presented via inverse of the $\underline{P}$ matrix. After the equivalent SISO loops are determined, each is designed in accordance with the SISO design theory, presented in Chapter II.

IV. Aircraft

Introduction

This thesis concerns a lateral controller for the C-135 aircraft. A linear three degree-of-freedom lateral model is generated for each of three flight conditions. The linear, time invariant (LTI) differential equations represent the motion of the aircraft operating near equilibrium at each flight condition. The three flight conditions chosen are representative of most of the aircraft flight envelope, i.e., they represent, as closely as possible, the domain of plant parameter uncertainty. The changes in the aircraft flying characteristics from one flight condition to the next constitute the parameter uncertainties considered in this problem. The goal, then, is to design a controller capable of producing desirable flight characteristics throughout the entire flight range of the aircraft without the use of gain scheduling.

The three flight conditions chosen are a high speed, high altitude cruise of MACH 0.75 at 42,000 feet, a moderate speed, medium altitude cruise of MACH 0.65 at 25,000 feet, and a low speed, low altitude approach configuration of 275 ft/sec at sea level (Ref 5:13).

Lateral Equations of Motion

Below are the three lateral equations of motion used in this thesis. For a complete development of these equations and the applicable assumptions see Ref 5. These equations are linearized about a straight, level, and unaccelerating, equilibrium flight condition. perturbations from equilibrium are assumed to be small.

Forces in Y direction

$$\dot{v} + U_o r - g\psi \sin\theta_o - g\phi\cos\theta_o = Y_r r + Y_v v + Y_{\dot{v}}\dot{v} + Y_p p + Y_{\delta_a}\delta a + Y_{\delta_r}\delta r \qquad \text{(IV-1)}$$

Rolling Moments

$$\dot{p} - [I_{xz}/I_{xx}]\dot{r} = L_r r + L_v v + L_{\dot{v}}\dot{v} + L_p p + L_{\delta_a}\delta a + L_{\delta_r}\delta r \qquad \text{(IV-2)}$$

Yawing Moments

$$\dot{r} - [I_{xz}/I_{zz}]\dot{p} = N_r r + N_v v + N_{\dot{v}}\dot{v} + N_p p + N_{\delta_a}\delta a + N_{\delta_r}\delta r \qquad \text{(IV-3)}$$

Since perturbations are assumed small, the following simplifying assumptions are made. First, the roll rate, $\dot{\phi}$, is assumed to be equal to the angular velocity about the X-axis, p. Second, the yaw rate, $\dot{\psi}$, is assumed equal to the angular velocity about the Z-axis, r. The actual relationship between the sideslip angle, β, and the sideslip velocity, v, is;

$$\tan\beta = v/U_o \qquad \text{(IV-4)}$$

The small angle approximation, $\tan\beta = \sin\beta = \beta$ is assumed valid since β is small.

These assumptions are summarized below:

$$\dot{\phi} = p \qquad \text{(IV-5)}$$

$$\dot{\psi} = r \qquad \text{(IV-6)}$$

$$\beta = v/U_o \qquad \text{(IV-7)}$$

Substituting the results of these assumptions into the differential equations and taking the Laplace transforms of the resulting equations gives:

Forces in Y direction

$$[(1 - Y_{\dot{v}})s - Y_v]\beta - [(Y_p s + g \cos \theta_o)/U_o]\phi + [(1 - Y_r/U_o)s - (g \sin \theta_o)/U_o]\psi = (Y_{\delta_a}/U_o)\delta a + (Y_{\delta_r}/U_o)\delta r \quad \text{(IV-8)}$$

Rolling Moments

$$-(L_{\dot{\beta}} s + L_\beta)\beta + (s^2 - L_p s)\phi - [(I_{xz}/I_{xx})s^2 + L_r s]\psi = L_{\delta_a}\delta a + L_{\delta_r}\delta r \quad \text{(IV-9)}$$

Yawing Moments

$$-(N_{\dot{\beta}} s + N_\beta)\beta - [(I_{xz}/I_{zz})s^2 + N_p s]\phi + (s^2 - N_r s)\psi = N_{\delta_a}\delta a + N_{\delta_r}\delta r \quad \text{(IV-10)}$$

Flight Conditions

The three flight conditions chosen and all the related data are obtained from Ref 5. Table IV-I summarizes the flight conditions.

Table IV-1

C-135 Flight Conditions

Flight Condition	Altitude (ft)	Mach No. M	Gross Wt. (lbs)	Velocity U_o (ft/sec)
Cruise 1	42,000	.75	190,000	726
Cruise 2	25,000	.65	250,000	660
Power Approach	Sea Level	---	165,000	275

All angles and angular rates considered in this thesis and imbedded in the data are measured in degrees (Ref 5:13).

Table IV-2, on following page, contains the C-135 stability derivatives for the three flight conditions considered.

Table IV-2

C-135 Stability Derivatives

Parameter	Cruise 1	Cruise 2	Power Approach
Y_v	-5.74×10^{-2}	-9.46×10^{-2}	-1.279×10^{-1}
$Y_{\dot{v}}$	0	0	0
Y_p	-1.337	-1.583	-2.294
Y_r	2.621	3.204	4.277
Y_{δ_a}	0	0	0
Y_{δ_r}	16.68	18.73	10.55
L_β	-2.384	-3.109	-1.631
$L_{\dot{\beta}}$	0	0	0
L_p	-4.695×10^{-1}	-6.381×10^{-1}	-9.074×10^{-1}
L_r	2.341×10^{-1}	3.248×10^{-1}	5.943×10^{-1}
L_{δ_a}	7.227×10^{-1}	7.114×10^{-1}	1.433
L_{δ_r}	2.235×10^{-1}	3.162×10^{-1}	1.223×10^{-1}
N_β	5.089×10^{-1}	7.745×10^{-1}	2.345×10^{-1}
$N_{\dot{\beta}}$	1.10×10^{-2}	0	1.62×10^{-2}
N_p	-5.87×10^{-2}	-9.21×10^{-2}	-1.293×10^{-1}
N_r	-9.27×10^{-2}	-1.506×10^{-1}	-1.503×10^{-1}
N_{δ_a}	3.63×10^{-2}	6.00×10^{-2}	4.03×10^{-2}
N_{δ_r}	-4.965×10^{-1}	-8.278×10^{-1}	-3.305×10^{-1}
I_{xx}	3.602×10^{6}	4.013×10^{6}	2.813×10^{6}
I_{zz}	8.648×10^{6}	8.737×10^{6}	7.687×10^{6}
I_{xz}	-7.235×10^{5}	-2.483×10^{5}	-2.561×10^{5}
θ_o	0	0	-3.0

The reference axis system used in this model is a conventional stability axis system with the X-axis pointing forward, the Y-axis pointing to the right, and the Z-axis pointing down.

As is mentioned in the previous chapter, this model has three outputs, β, θ, and ψ, and only two inputs, δa and δr. In order to produce a square plant matrix, one of the outputs must be eliminated. Since the sideslip angle, β, and the yaw angle, ψ, are closely related (in fact equal with opposite signs in the steady state), the yaw angle output is mathematically eliminated from the model. This is actually done individually for each flight condition in the next chapter.

Summary

This chapter presents the differential equations and data that make up the C-135 aircraft model used in this thesis. A number of simplifications based on the small perturbation assumption are incorporated into the model.

The flight conditions chosen represent a large portion of the C-135 flight envelope from a low altitude approach to a high altitude cruise.

V. Design

Introduction

This chapter follows the design of the C-135 lateral flight controller from start to finish. It begins with the manipulation of the three degree-of-freedom model to obtain the two-by-two P and Q matrices used in the remainder of the design process. Next, the desired system output is modeled to obtain a frequency domain representation of the design specifications. This is followed by the determination of the bounds for the first loop. This leads to the shaping of the first loop transmission from which the first element of the compensator matrix, G is obtained. Since there is no sideslip command to follow, there are only two loops to consider and only two elements of G to be determined.

The recent improvement in the MIMO design technique, mentioned in Chapter III, is used during the design of the second loop. This involves using the exact equation for the system during the design of the last loop, based on all the previously designed elements of G.

Finally, this chapter presents comments about the completed design and possible ways to improve it. In order to reduce the large bandwidth of this design, a second design is presented without derivation. Simulation results for both designs are included in Chapter VI.

The Plant Matrices

The first step in finding the P matrix is the elimination of the yaw angle output in the model for each flight condition. Using the values of the parameters for Cruise 1 in the equations for the model yields:

$$(s + 0.0574)\beta + (0.00184s - 0.0443)\phi + (0.996s)\psi$$
$$= (0)\delta a + (0.023)\delta r \qquad \text{(V-1)}$$

$$(2.384)\beta + (s^2 + 0.4695s)\phi + (0.201s^2 - 0.2341s)\psi$$
$$= (0.7227)\delta a + (0.2235)\delta r \qquad \text{(V-2)}$$

$$-(0.011s + 0.5089)\beta + (0.0837s^2 + 0.0587s)\phi$$
$$+ (s^2 + 0.0927s)\psi = (0.0363)\delta a - (0.4965)\delta r \qquad \text{(V-3)}$$

Solving for ψ in the first equation gives:

$$\psi = [0.023/s]\delta r - [(1.004s + 0.058)/s]\beta$$
$$- [(0.002s - 0.044)/s]\phi \qquad \text{(V-4)}$$

Substituting this into the other two equations results in:

$$(-0.2016s^2 + 0.2234s + 2.398)\beta$$
$$+ (0.9996s^2 + 0.4789s - 0.0104)\phi$$
$$= (0.7227)\delta a + (-0.0046s + 0.2289)\delta r \qquad \text{(V-5)}$$

$$(-1.004s^2 - 0.1616s - 0.5142)\beta$$
$$+ (0.0818s^2 + 0.103s + 0.0041)\phi$$
$$= (0.0363)\delta a + (-0.0231s - 0.4986)\delta r \qquad \text{(V-6)}$$

These two equations no longer explicitly represent the aircraft rolling and yawing moments because elements of the sideforces are now included in each. But the validity of the mathematical representation of the aircraft in flight is retained.

To obtain the matrix representation of the system, define an input vector, $\underline{\delta}$, and an output vector, $\underline{y}$.

$$\underline{\delta} = \begin{bmatrix} \delta_a \\ \delta_r \end{bmatrix} \qquad (V\text{-}7) \;, \qquad \underline{y} = \begin{bmatrix} \phi \\ \beta \end{bmatrix} \qquad (V\text{-}8)$$

Thus the matrix model for the aircraft at this flight condition is:

$$\begin{bmatrix} 0.996s^2 + 0.4789s - 0.0104 & -0.2016s^2 + 0.2234s + 2.398 \\ 0.0818s^2 + 0.103s + 0.0041 & -1.004s^2 - 0.1616s - 0.5142 \end{bmatrix} \underline{y}$$

$$= \begin{bmatrix} 0.7727 & -0.0046s + 0.2289 \\ 0.0363 & -0.023s - 0.4986 \end{bmatrix} \underline{\delta} \qquad (V\text{-}9)$$

For clarity, temporarily name the two-by-two matrices above $\underline{M}$ and $\underline{N}$ respectively. The goal of this exercise is to find the plant matrix which relates the input vector to the output vector by $\underline{y} = \underline{P}\,\underline{\delta}$ and the $\underline{Q}'$ matrix which is $\underline{P}^{-1}$.

Since $\underline{My} = \underline{N\delta}$, then $\underline{y} = \underline{M}^{-1}\underline{N\delta}$ yielding, $\underline{P} = \underline{M}^{-1}\underline{N}$ and $\underline{Q}' = \underline{P}^{-1} = \underline{N}^{-1}\underline{M}$.

In general, actual computation of $\underline{P}$ is recommended for use in ensuring the constraints on it are met. But, in the two-by-two case, the constraints can be checked easily using $\underline{Q}'$. It should be obvious that if $\underline{N}$ is singular, then $\underline{P}$ is singular and $\underline{Q}'$ doesn't exist. Likewise the converse is true if $\underline{M}$ is singular. The first constraint on $\underline{P}$ is that its inverse must exist. Since neither $\underline{M}$ nor $\underline{N}$ is singular, both $\underline{P}$ and $\underline{Q}'$ exist and the first constraint is met.

Using a computer program, $\underline{Q}'$ is computed directly from $\underline{M}$ and $\underline{N}$ as described above. The result is:

$$\underline{Q}' = \begin{matrix} \dfrac{(s + 22.77)(s + 0.5238)(s - 0.0157)}{0.7278\ (s + 22.3459)} & \dfrac{(s + 1.631)(s - 2.038)}{-0.051\ (s + 22.3459)} \\ \dfrac{(s + 2.438)(s + 0.0603)}{-0.7224\ (s + 22.3459)} & \dfrac{(s + 0.087 \pm j0.7945)}{0.023\ (s + 22.3459)} \end{matrix} \qquad \text{(V-10)}$$

Notice that in the elements of $\underline{Q}'$, q_{ij}', the constant gain terms are displayed in the denominators and that the root(s) of the denominators are identical. As seen in Chapter III, the effective SISO transfer functions used in the loop designs are the inverses of the elements of $\underline{Q}'$. So, q_{ij} represents the inverse of the element in the ith row and jth column of the $\underline{Q}'$ matrix ($q_{ij} = 1/[q_{ij}']$). For this flight condition;

$$q_{11} = \frac{0.7278\ (s + 22.3459)}{(s + 22.77)(s + 0.5238)(s - 0.0157)} \qquad \text{(V-11)}$$

$$q_{12} = \frac{-0.0509\ (s + 22.3459)}{(s + 1.631)(s - 2.038)} \qquad \text{(V-12)}$$

$$q_{21} = \frac{-0.7224\ (s + 22.3459)}{(s + 2.438)(s + 0.0603)} \qquad \text{(V-13)}$$

$$q_{22} = \frac{0.023\ \ (s + 22.3459)}{(s + 0.087 \pm j0.7945)} \qquad \text{(V-14)}$$

The second constraint on $\underline{P}$ is that as ω becomes large;

$$|p_{11}p_{22}| > |p_{12}p_{21}| \qquad \text{(V-15)}$$

It's easy to show that if the elements, q_{ij}', of $\underline{Q}'$ (not q_{ij}) meet this constraint, so do the elements of $\underline{P}$. In this case as ω becomes large the elements of $\underline{Q}'$ in the above constraint equation become;

$$s^3 > s^2 \qquad \text{(V-16)}$$

which is, of course, true.

The $\underline{Q}'$s and the resulting q_{ij} terms for the other two flight condi-

tions are found in exactly the same manner. The results are:

Cruise 2

$$q_{11} = \frac{0.7088\ (s + 30.297)}{(s + 29.46)(s + 0.7228)(s - 0.032)} \qquad \text{(V-17)}$$

$$q_{12} = \frac{-0.055\ (s + 30.297)}{(s + 2.178)(s - 2.93)} \qquad \text{(V-18)}$$

$$q_{21} = \frac{0.486\ (s + 30.297)}{(s + 0.095)(s - 1.58)} \qquad \text{(V-19)}$$

$$q_{22} = \frac{0.028\ (s + 30.297)}{(s + 0.137 \pm j1.017)} \qquad \text{(V-20)}$$

Power Approach

$$q_{11} = \frac{1.434\ (s + 4.12)(s + 0.006)}{s(s + 3.79)(s + 1.26)(s - 0.04)} \qquad \text{(V-21)}$$

$$q_{12} = \frac{-0.403\ (s + 4.12)}{(s + 0.932)(s - 1.78)} \qquad \text{(V-22)}$$

$$q_{21} = \frac{11.95\ (s + 4.12)(s + 0.006)}{s(s + 0.093)(s - 67.97)} \qquad \text{(V-23)}$$

$$q_{22} = \frac{0.038\ (s + 4.12)}{(s + 0.153 \pm j0.5226)} \qquad \text{(V-24)}$$

These two sets of q's meet the two constraints just as the first set did. For the remainder of the design these q's are used as the effective transfer functions for single loop designs. Before proceeding, notice the following about the q's for each flight condition.

The most obvious thing to note about the q's is that some of them are unstable, or have poles in the right half plane (rhp). This is not a problem. But if any of the q's have zeros in the rhp, then there is a problem. The solution for systems with rhp zeros in the q's is not addressed in this thesis.

Response Modeling

In general, the design specifications describe for the designer the range of acceptable responses. To determine these specifications and/or to relate them to the range of acceptable responses requires some engineering insight and experience. It is crucial to know the range of time responses acceptable for the system if Horowitz' quantitative method is to be used.

For this thesis, the design specifications are left entirely up to the author. The decision is made to command a bank angle of thirty degrees and try to keep the sideslip angle as small as possible throughout the maneuver.

For the bank angle output, a first-order step response model with a settling time of about four seconds is considered optimum and a first-order step response model with a settling time of about ten seconds is considered the worst acceptable response. For the sideslip angle output, a maximum value of 2.0 degrees which settles to zero in about ten seconds is considered the worst acceptable response.

Using the computer-aided-design program, TOTAL, and following the procedure described in Chapter II, transfer functions are found whose time domain responses conform to the response descriptions above. The only consideration given to the actual plant (aircraft) model during this process is an attempt to model reasonable responses.

Appendix B contains the TOTAL output produced during the modeling of the responses. Included are printer plots of the time and frequency responses for each transfer function.

Fig V-1 is the plot of Lm vs. ω for the bank angle response models. Note that at low frequency, there is very little difference between the

two curves. But as ω becomes larger, the difference between them increases. Had the specifications allowed for some overshoot in the optimum response the difference between the two curves would become larger at low frequency.

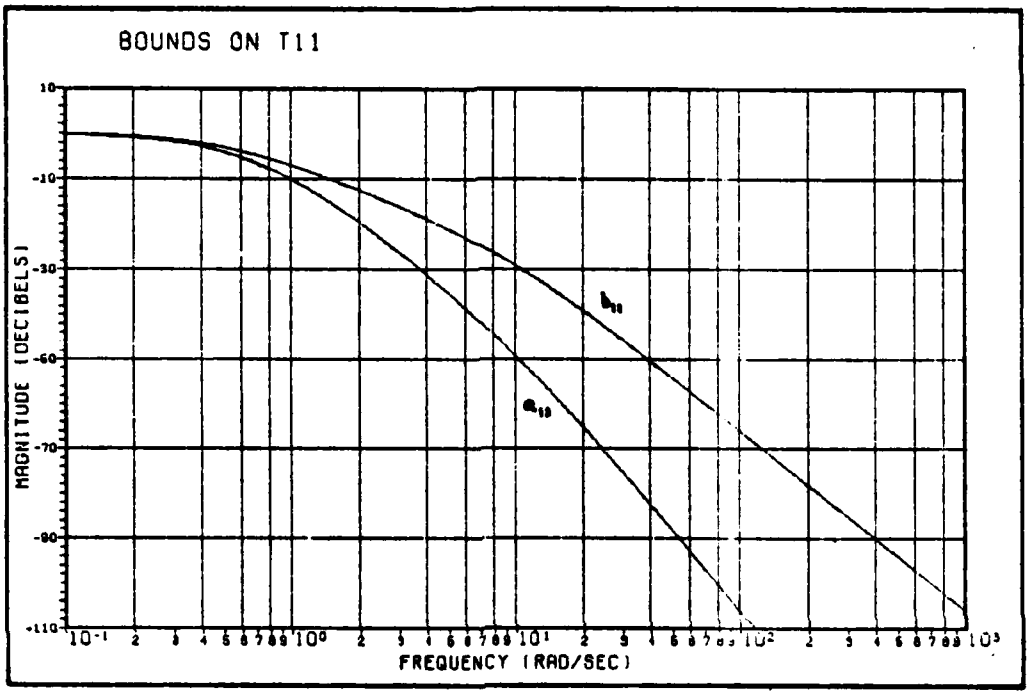

Fig V-1 Bounds on Bank Angle Response

In this figure, the b_{11} and a_{11} curves correspond directly to the T_U and T_L curves of Fig II-4 respectively. The subscripts indicate that they are bounds on the first output response due to the first command input.

Fig V-2 is the plot of Lm vs. ω for the sideslip angle response model. Note that its magnitude never gets above zero. This is typical of a basically noninteracting (BNIC) loop in a MIMO control system. The b_{21} of Fig V-2 corresponds to the T_D curve of Fig II-4. The subscript indicates that this is the bound on the second output response due to the first command input.

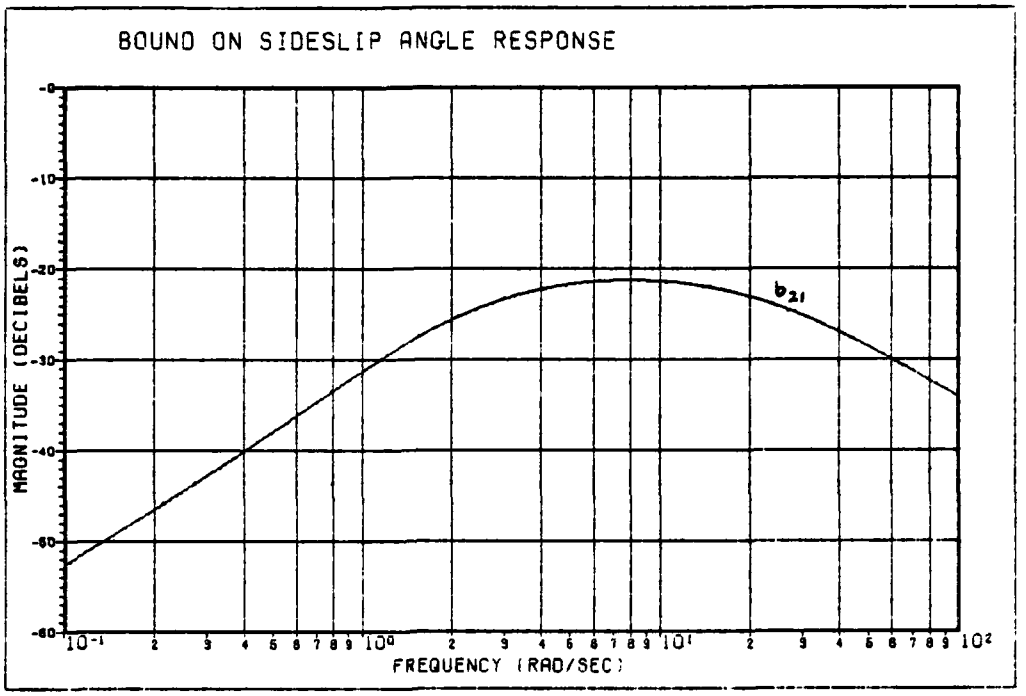

Fig V-2 Bound on Sideslip Angle Response

These plots of response model magnitudes vs. frequency, based on the design specifications are all the information needed to insure the final system responses are acceptable. These plots are used to form the boundaries for the transfer functions of the effective SISO control loops during the design.

Selection of the First Loop to Design

In this problem there is no sideslip command, r_2, therefore, only two of the four SISO loops of Fig III-5, resulting from the two-by-two MIMO system need to be considered. These are the bank angle output due to a bank command, y_{11}, and the sideslip angle output due to a bank command, y_{21}. Fig V-3 is Fig III-5 redrawn. Recall that d_{12} and d_{22}

are functions of the response requirements due to the effects of r_2. Since r_2 is zero, the y_{12} and the y_{22} loops can be ignored.

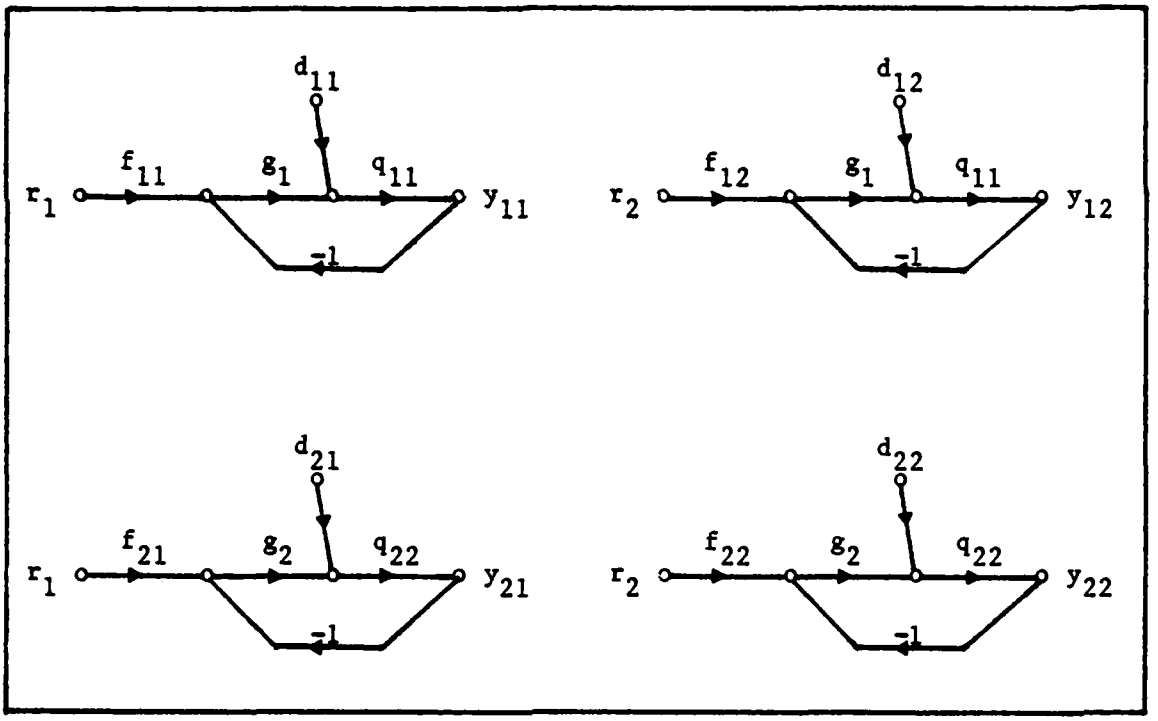

Fig V-3 Effective SISO Loops

Of the two remaining loops, one must be selected for consideration first. There is no hard and fast rule as to which loop to design first but in general BNIC loops are easier since there is no command to consider. Notice that in the y_{21} loop of Fig V-3 the effects of input, r_1, can follow either of two paths to the output, y_{21}. It enters as part of the disturbance, d_{21}, and directly through f_{21}. Since it is desireable for y_{21} to be zero, the less effect r_1 has on the loop, the better. Nothing can be done to eliminate the disturbance, but f_{21} is to be designed and can be made zero, leaving only the disturbance to consider. The second loop, the sideslip output due to a bank command is a BNIC loop and is, therefore, designed first. Thus, one is left with a

simple disturbance rejection problem. Fig V-4 shows the y_{21} loop as it is dealt with for this problem.

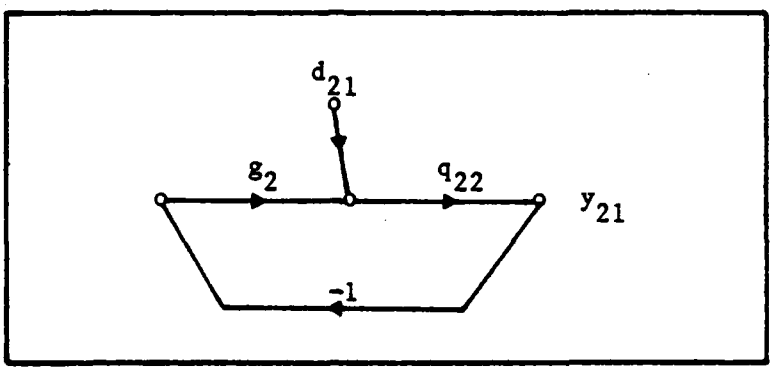

Fig V-4 Diagram of y_{21} Loop

Bounds on BNIC Loop Transmission

Recall that the disturbance term, d_{21}, is $|b_{11}|/|q_{21}|$ where the b_{11} term is the upper of the two bank response curves. This provides a worst case approximation for the disturbance.

In order to ensure rejection of the disturbance, the following inequality must be satisfied:

$$|y_{21}| = \frac{|b_{11}||q_{22}|}{|q_{21}||1 + g_2q_{22}|} \leq |b_{21}| \qquad \text{(V-25)}$$

Now, define $l_2 = g_2q_{22}$ and rearrange the equation to obtain;

$$|1 + l_2| \geq \frac{|b_{11}||q_{22}|}{|b_{21}||q_{21}|} \qquad \text{(V-26)}$$

This is the inequality used to design l_{2o}, where the nominal loop transmission, $l_{2o} = g_2q_{22o}$.

The first step in the design is to derive bounds on l_{2o} based on

the above inequality. At any given frequency, the right side of the inequality reduces simply to a number greater than zero. It is helpful to have Bode plots of each of the terms on the right side. With these, one can simply add and subtract the magnitudes at each frequency to obtain a minimum for Lm $(1 + l_2)$ in db. For clarity, define a new variable, $E(\omega)$, such that;

$$E(\omega) = \frac{b_{11}(\omega)\ |q_{22}(j\omega)|}{b_{21}(\omega)\ |q_{21}(j\omega)|} \qquad \text{(V-27)}$$

thus;

$$\text{Lm}\ (E) = \text{Lm}\ (b_{11}) + \text{Lm}\ (q_{22}) - \text{Lm}\ (b_{21}) - \text{Lm}\ (q_{21}) \qquad \text{(V-28)}$$

By way of the transformation, $m = 1/l_2$, turn the Nichols chart upside down, as described in Chapter II. Lm $(1 + l_2) > -3$ db is chosen as the UF bound, based on phase margin considerations [remember to reverse the signs on the Lm $(1 + l_2)$ curves] (see Eqs II-10 and 11). At this point, there are a number of ways to obtain the bounds on l_{2o}. If q_{22o} is chosen such that it lies at the lowest point of the templates at all frequencies, then the bounds on Lm $(1 + l_2)$ which are greater than 0 db can be used directly. Simply select the flight condition which produces the largest Lm $[E(\omega_i)]$ and draw in the $\omega = \omega_i$ bound along the curved Lm $(1 + l_2)$ line corresponding to the value of Lm $[E(\omega_i)]$, realizing that any possible q_{22} other that q_{22o} puts Lm (l_2) and the resulting Lm $(1 + l_2)$ above the boundary at $\omega = \omega_i$.

When the minimum value for Lm $(1 + l_2)$ is less than the UF bound, the process becomes a little more complicated. And, since the magnitudes for the three q_{22}'s vs. frequency for this problem cross each

other (i.e. no lowest q_{22o} can be chosen), another scheme must be found.

Consider the following:

$$l_{2o} = g_2 q_{22o} = \frac{g_2 q_{22} q_{22o}}{q_{22}} = \frac{l_2 q_{22o}}{q_{22}} \qquad \text{(V-29)}$$

Using the Nichols chart, the minimum for Lm $(1 + l_2)$ at each flight condition is converted into a minimum for Lm (l_2) at regular phase angle intervals. When the Lm $[E(\omega_1)]$ is less than -3 db (UF bound), then -3 db becomes the bound. Since the values are in db, the multiplication and division indicated in Equation V-29 become addition and subtraction. When the magnitude and angle differences between q_{22o} and q_{22} at a particular flight condition and frequency are added to the minimum for l_2, the result is a minimum for the magnitude and angle of l_{2o} at that flight condition and frequency. This is done for each of the three flight conditions and the worst case boundary of the three is chosen as the boundary for l_{2o}. Below are two examples of this process.

Example 1 The q_{22o} chosen for this problem is;

$$q_{22o} = \frac{0.03(s + 30)}{(s + 0.15 + j1)} \qquad \text{(V-30)}$$

Notice that this is not one of the actual q_{22}'s as listed in Equations (V-14), (V-20), or (V-24). There is no requirement for q_{22o} to be an actual q of the system. Because no convenient q_{22o} exists for this problem, a simplified form of q_{22} for the flight condition, Cruise 2, is chosen as q_{22o}.

Table V - 1 contains the relevent information for the point, where ω = 0.1 rad/sec. The information is obtained from the Bode plots of the

responses and of the q's.

Table V-1

	Cruise 1	Cruise 2	Pow. App.
$\|b_{11}\|$	----->	-0.17 db	<-----
$\|b_{21}\|$	----->	-52.6 db	<-----
q_{22o}	---->	-1.0 db -1.5°	<----
q_{21}	35.1 db -241°	36.6 db -223°	14.5 db -229°
q_{22}	-1.8 db -1.3°	-1.7 db -1.3°	-6.1 db -4.1°

In order to satisfy Equation V-26, Lm $(1 + l_2)$ for all three flight conditions at $\omega = 0.1$ rad/sec must be greater than Lm (E). This works out to 15.5 db for Cruise 1, 14.1 db for Cruise 2, and 31.8 db for the Powered Approach. The Powered Approach condition produces the largest bound and therefore dominates at this frequency. On the inverted Nichols chart, note that the Lm $(1 + 1) = 32$ db curve is nearly a horizontal line, which deviates from the Lm $(1) = 32$ db line very little. This makes sense, since $1 \gg 1$, Lm $(1 + 1)$ = Lm (1) is a good approximation. The idea here is not to make the approximation, but to point out the relationship between Lm (1) and Lm $(1 + 1)$ on the Nichols chart more clearly.

For the Powered Approach condition, the difference between q_{22o} and q_{22} is 5.1 db and 2.6°. Adding these values to the bound of Lm $(1 + l_2)$ = 31.8 db results in a curve that has the same shape as Lm $(1 + 1)$ = 31.8 but shifted 5.1 db up and 2.6° to the right. This curve is now the bound on $|1 + l_{2o}|$ and on l_{2o} for this flight condition.

This is repeated for the other two flight conditions but at $\omega = 0.1$

rad/sec the other two flight conditions produce boundaries that are below the Powered Approach bound. Therefore the Powered Approach bound dominates at $\omega = 0.1$ rad/sec and is the one used during the design of 1_{2o}.

Example 2 At $\omega = 2$ rad/sec the process is repeated to demonstrate how to deal with the UF boundary. Table V-2 contains the relevent information for $\omega = 2$ rad/sec.

Table V-2

	Cruise 1	Cruise 2	Pow. App.
$\|b_{11}\|$	----->	-12.5 db	<-----
$\|b_{21}\|$	----->	-25.6 db	<-----
q_{22o}	---->	-10.5 db -165^{o}	<----
q_{21}	8.2 db -303^{o}	9.2 db -212^{o}	-7.9 db -240^{o}
q_{22}	-16.3 db -169^{o}	-10.8 db -166^{o}	-26.5 db -145^{o}

Again the value of Lm (E) is the maximum for Lm $(1 + 1_2)$. This is -11.4 db for Cruise 1, -6.9 db for Cruise 2, and -5.5 db for the Powered Approach condition. All three of these values are less than -3 db. Therefore the UF boundary value of -3 db prevails at this frequency and (as it works out) all frequencies higher than 2 rad/sec.

So, for all three flight conditions the boundary for Lm $(1 + 1_2)$ is the oval corresponding to -3 db on the inverted Nichols chart. To get the bounds on Lm $(1 + 1_{2o})$, repeat the steps taken for $\omega = 0.1$ rad/sec. For example, for Cruise 1, the difference between q_{22o} and q_{22} is 5.8 db and 4^{o}. The bound for Cruise 1 is the exact shape of the -3 db oval shifted 5.8 db up and 4^{o} to the right. If this is repeated for the

other two flight conditions, each shifts the oval a different amount. The overall boundary on $|1 + l_{2o}|$ and thus on l_{2o} is the outer boundary of the shape formed by this shifting of the -3 db oval for the three flight contidions.

Bounds, $B_D(j\omega_i)$, are found in this manner at frequency intervals of about every octave between $\omega = 0.1$ and $\omega = 500$ rad/sec. Fig V-5 shows the bounds for l_{2o}.

Shaping of BNIC Loop Transmission

Once the bounds on l_{2o} are determined, the loop transmission is shaped as described in Chapter II. In this case the dominate bound is at $\omega = 1$ rad/sec. In other words, if Lm (l_{2o}) is at or greater than about 36 db at $\omega = 1$, all the bounds at lower frequencies are also met (assuming a relatively constant slope of -6 db/decade due to a pole at $\omega = 0$ rad/sec). Therefore, $Lm(l_{2o})$ equals 36 db at $\omega = 1$ rad/sec is used as a starting point in the shaping of l_{2o}.

At and beyond $\omega = 2$ rad/sec the only consideration is ensuring the loop transmission does not enter the UF bounds which are represented by the ovate shapes on the Nichols chart. Fig V-6 shows the Nichols chart with the boundaries, $B_D(j\omega)$, and the shaped l_{2o}.

The final mathematical description of the l_{2o} chosen is:

$$\frac{58.2\ (1 + s)^2(1 + \frac{s}{5})(1 + \frac{s}{30})}{s(1 + \frac{s}{2})(1 + \frac{s}{20})[1 + \frac{0.3s}{(1.01)}2 + \left(\frac{s}{1.01}\right)^2][1 + \frac{228s}{(190)}2 + \left(\frac{s}{190}\right)^2]^2} \qquad \text{(V-31)}$$

Dividing through by q_{22o} to get g_2 yields;

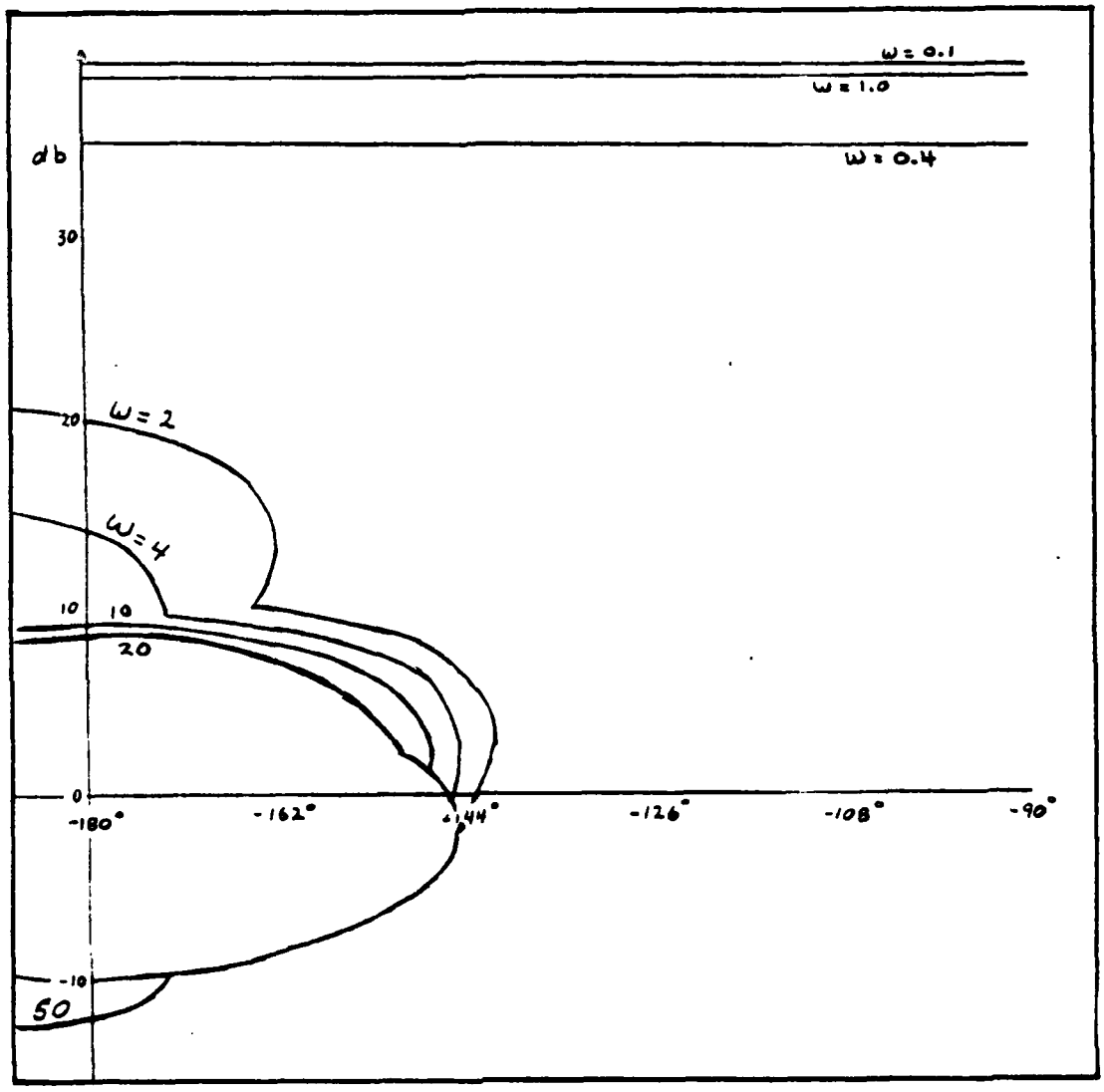

Fig V-5 Bounds, $B_D(j\omega)$, on l_{2o}

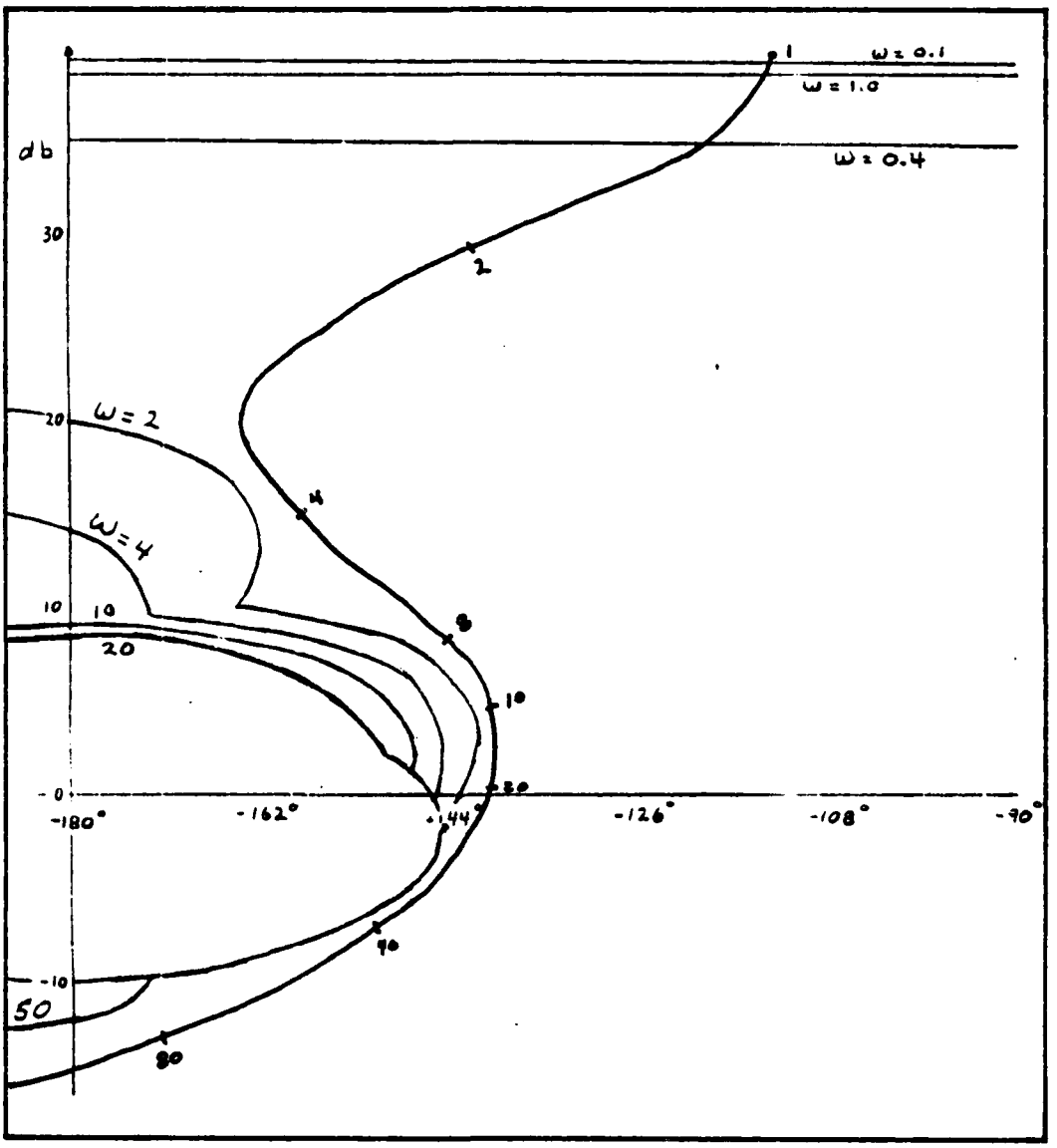

Fig V-6 Nominal Loop Transmission (l_{2o})

$$g_2 = \frac{66.1\ (1+s)^2(1+\frac{s}{5})}{s(1+\frac{s}{2})(1+\frac{s}{20})([1+\frac{228s}{(190)^2}+\left(\frac{s}{190}\right)^2]^2} \qquad \text{(V-32)}$$

This loop is driven entirely by the effective disturbance. Therefore, there is no command and no $\underline{F}$ matrix element for this loop. With this element of $\underline{G}$ designed it's time to turn to the other loop.

Effective Plant for Second Loop

The entire compensated system can be represented by a signal flow diagram as shown in Fig V-7. The p_{ij}'s are the elements of the plant matrix, $\underline{P}$.

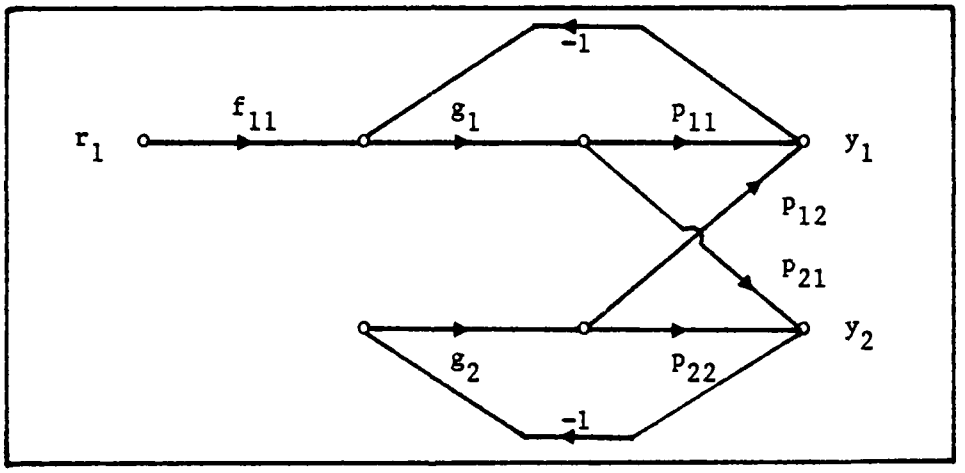

Fig V-7 Compensated System

Note that Fig V-7 is a simplification of Fig III-4. By use of Mason's Gain Formula (Ref 3:162-164) the transfer function, $t_{11} = y_1/r_1$, can be obtained. The following substitutions are used to obtain t_{11} in terms of the q_{ij}'s instead of the p_{ij}'s:

$$\Delta = \det(\underline{P}) = p_{11}p_{22} - p_{12}p_{21} \qquad \text{(V-33)}$$

$$p_{11} = \Delta/q_{22} \qquad \text{(V-34)}$$

$$p_{22} = \Delta/q_{11} \tag{V-35}$$

$$p_{ij} = -\Delta/q_{ij} \qquad i \neq j \tag{V-36}$$

$$l_{ii} = g_i q_{ii} \tag{V-37}$$

$$\gamma = \frac{q_{11}q_{22}}{q_{12}q_{21}} \tag{V-38}$$

$$1/\Delta = \frac{1}{q_{11}q_{22}} - \frac{1}{q_{12}q_{12}} \tag{V-39}$$

From Fig V-7 t_{11} is:

$$t_{11} = \frac{f_{11}\, g_1\, p_{11}\, (1 + g_2\, p_{22}) - f_1\, g_1\, p_{21}\, g_2\, p_{12}}{1 + g_1\, p_{11} + g_2\, p_{22} - g_1\, p_{21}\, g_2\, p_{12} + g_1\, p_{11}\, g_2\, p_{22}} \tag{V-40}$$

Rearanging terms and substituting for the p_{ij}'s yields:

$$t_{11} = \frac{f_{11}\, g_1\, [(\Delta/q_{22}) + g_2\, \Delta\,]}{1 + (g_1\, \Delta)/q_{22} + (g_2\, \Delta)/q_{11} + g_1\, g_2 \Delta} \tag{V-41}$$

Dividing through by Δ and substituting Equation V-39 for $1/\Delta$ yields:

$$t_{11} = \frac{f_{11}\, g_1\, (1/q_{22} + g_2)}{1/(q_{11}\, q_{22}) - 1/(q_{12}\, q_{21}) + g_1/q_{22} + g_2/q_{11} + g_1\, g_2} \tag{V-42}$$

Now multiply through by $q_{11}q_{22}$ and substitute Equation V-38 into the denominator to get:

$$t_{11} = \frac{f_{11}\, g_1\, (q_{11} + g_2\, q_{11}\, q_{22})}{1 - \gamma + g_1\, q_{11} + g_1\, q_{11}\, g_2\, q_{22} + g_2\, q_{22}} \tag{V-43}$$

Combining terms and using Equation V-37, the resulting actual equation for t_{11} is;

$$t_{11} = \frac{f_{11} l_1 (1 + l_2)}{(1 + l_1)(1 + l_2) - \gamma} \qquad \text{(V-44)}$$

Now if a new loop transmission, l_1^* is defined as;

$$l_1^* = \frac{l_1}{1 - \frac{\gamma}{1 + l_2}} \qquad \text{(V-45)}$$

then t_{11} can be manipulated into (Ref 12:102);

$$t_{11} = \frac{f_{11}\, l_1^*}{1 + l_1^*} \qquad \text{(V-46)}$$

Now $l_1^* = g_1 q_{11}^*$ where q_{11}^* is;

$$q_{11}^* = \frac{q_{11}}{1 - \frac{\gamma}{1 + l_2}} \qquad \text{(V-47)}$$

Since g_2 has already been designed, l_2 is known and q_{11}^* can be determined. Using TOTAL, q_{11}^* is found for each flight condition. The resulting transfer functions can be found in Appendix C. Fig V-8 shows the Bode plots of q_{11}^* for all three flight conditions.

The design of l_{1o}^* can now be accomplished as a simple single loop problem where q_{11o}^* is the nominal plant transfer function. The q_{11}^* for flight condition, Cruise 2, is chosen as q_{11o}^* since it has the smallest magnitude for all frequencies. Bounds on l_{11o}^* are found based on the allowable variation in t_{11} from the response plots, Fig V-1. Fig V-9 is the Nichols chart with templates of q_{11}^* and bounds on l_{1o}^*.

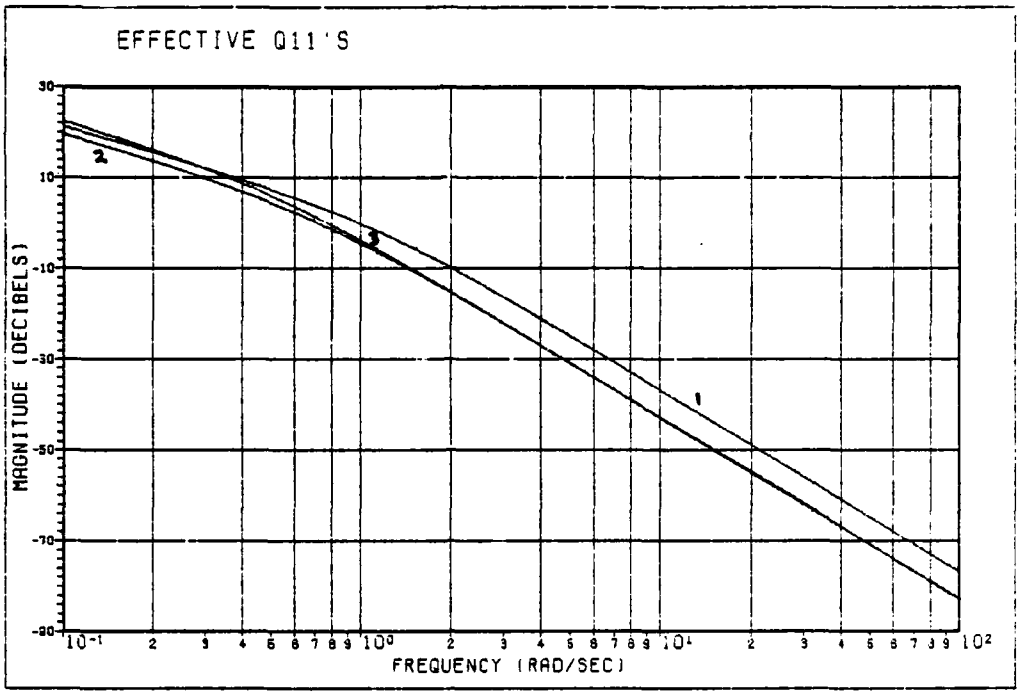

Fig V-8 Plots of q_{11}^*

Shaping of the Bank Response Loop

With the bounds on l_{1o}^* defined, the loop transmission is shaped exactly as described in Chapter II. Although it is not as obvious as in the last loop, the dominant bound occurs at $\omega = 0.4$ rad/sec. Fig V-10 is the Nichols plot of the resulting l_{1o}^* which is:

$$l_{1o}^* = \frac{-43.4\ (1 + \frac{s}{0.87})(1 + s)}{(1 - \frac{s}{0.03})[1 + \frac{1.6s}{(0.78)^2} + \left(\frac{s}{0.78}\right)^2][1 + \frac{9.6s}{(8)^2} + \left(\frac{s}{8}\right)^2]^2} \qquad \text{(V-48)}$$

Notice the unstable pole of l_{1o}^*. This pole is part of q_{11o}^* and it is very important that any unstable poles of the nominal q_{11}^* be included in l_{11o}^*. If the loop is shaped without including an unstable pole, solving for g_1 results in a rhp zero cancelling it. Since one

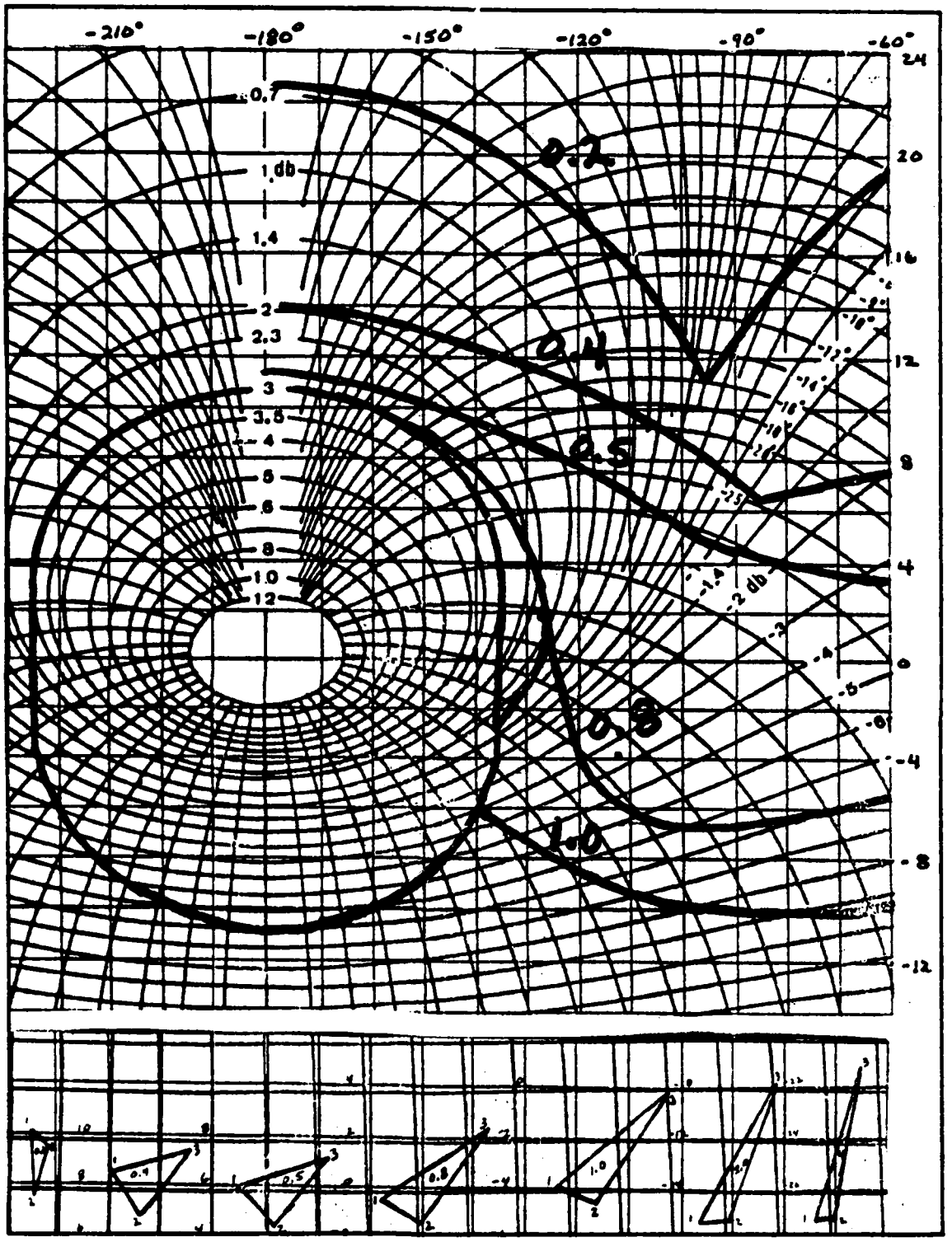

Fig V-9 Bounds on l_{lo}^{*}

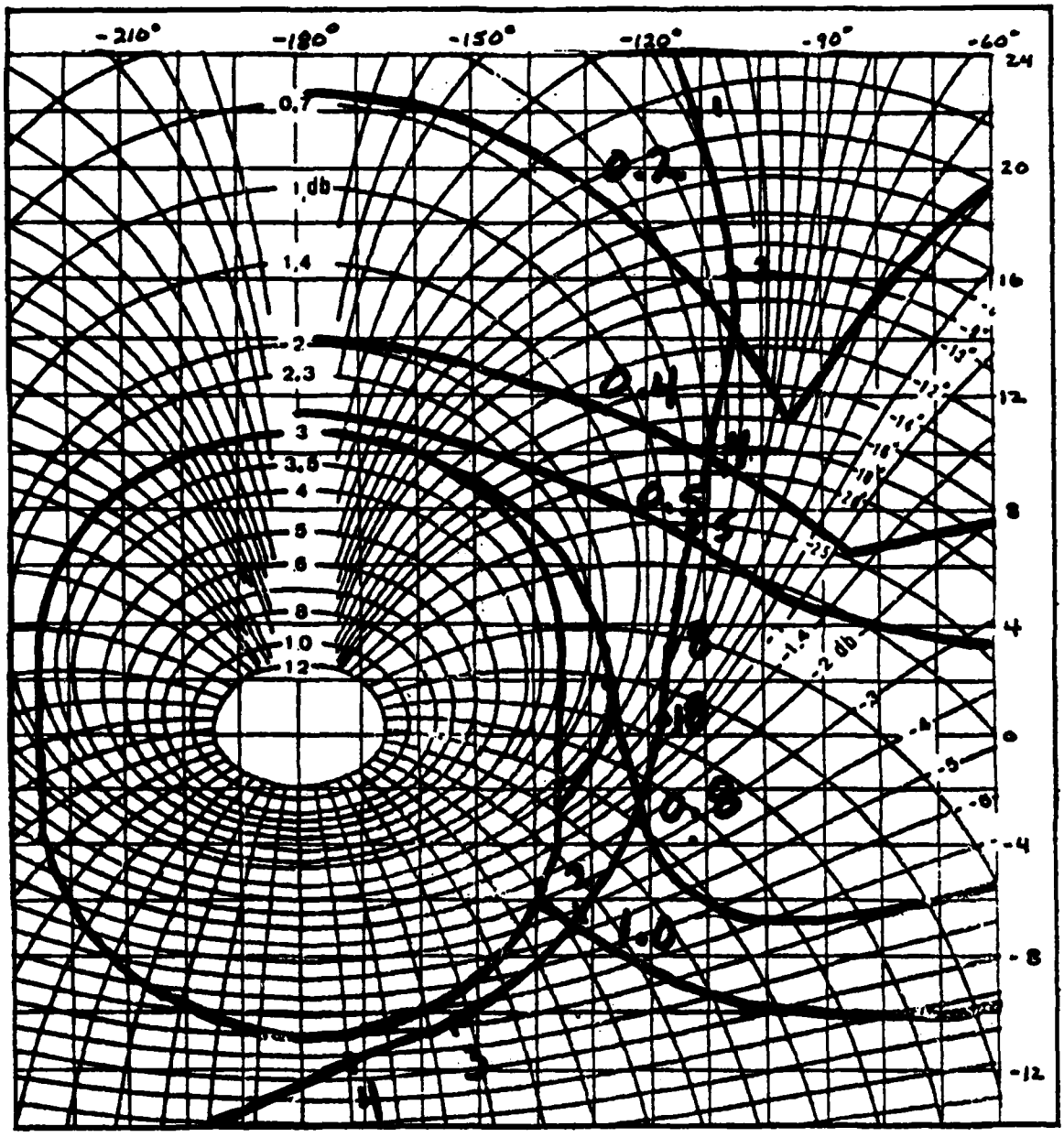

Fig V-10 Magnitude and Phase of 1_{lo}^{*}

cannot rely on exact cancellation, then an unstable system mey result. If the rhp poles are included, the loop can be shaped to ensure adequate stability and phase margins, as is the case here. The resulting g_1 is;

$$g_1 = \frac{1.29\ (\ 1 + s)}{[1 + \frac{9.6s}{(8)^2} + \left(\frac{s}{8}\right)^2]^2} \qquad \text{(V-49)}$$

Prefilter Design

There is only one prefilter element to be designed for this problem. That element is f_{11}. As explained in Chapter II, g_1 ensures that the variation in the magnitude of t_{11}, as a function of frequency, remains within limits specified by the difference between the magnitudes of the allowable responses. The prefilter element f_{11} is to ensure that the actual magnitude of t_{11} remains between those bounds.

Fig V-11 is the Bode plot of the three t_{11}'s resulting from the three flight conditions superimposed on the t_{11} response bounds. This plot indicates the form the frequency response of f_{11} must take.

The prefilter element chosen is of the simplest form possible. Note that this f_{11} only ensures the proper t_{11} in the low frequency region. A more complicated f_{11} may ensure a proper t_{11} for a larger frequency range but a more complicated f_{11} is not necessary to meet the specifications. The f_{11} chosen is;

$$f_{11} = \frac{0.7}{(s + 0.7)} = \frac{1}{(1 + \frac{s}{0.7})} \qquad \text{(V-50)}$$

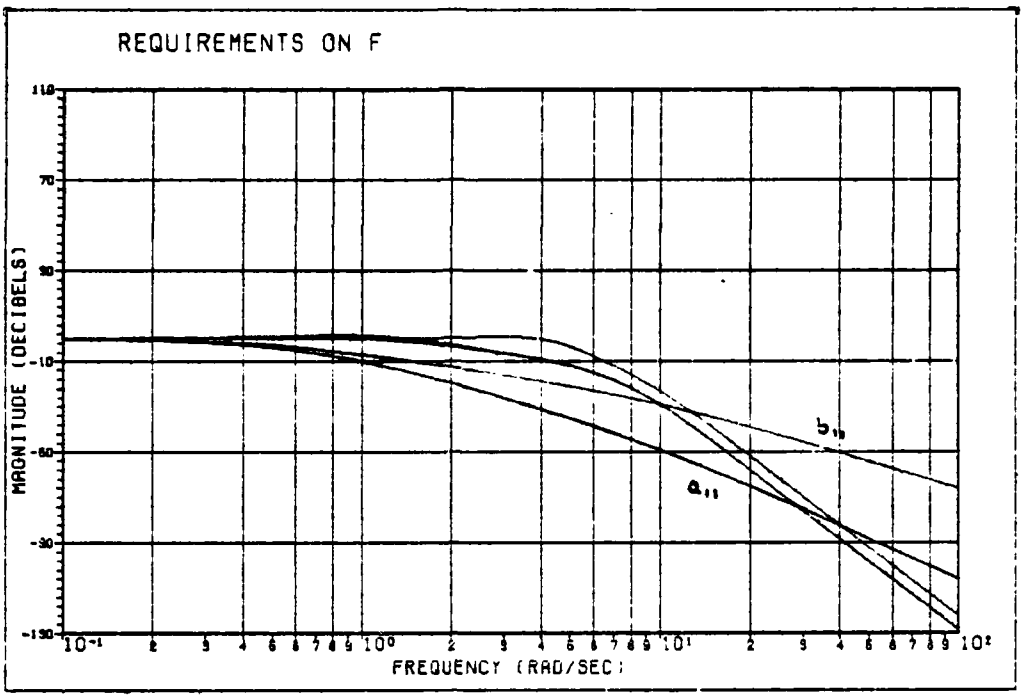

Fig V-11 Bounds and Resulting t_{11}'s

This completes the design of the compensator and, as shown in the next chapter, it meets the specifications easily. The bandwidth of the g_2 element is quite large and may be unreasonable in terms of susceptibility to sensor noise and/or implementation of the element transfer function.

Alternative Design

In an effort to reduce the bandwidth of g_2 a second design is offered. Remember that the dominate bound on 1_{2o} occurs at $\omega = 1$ rad/sec and is nearly constant at 36 db. The difference between the straight line approximation of the magnitude of 1_{2o} and the exact value at $\omega = 1$ rad/sec is about 15 db. This is due to the very small damping

factor of the q_{22o} pole pair at $\omega = 1$. Notice that each q_{22} has a similar, underdamped pole pair. In order to take advantage of this, another 1_{2o} is shaped ignoring the bound at $\omega = 1$.

The compensator element g_2 for the second design is;

$$g_2 = \frac{14.4\ (1 + \frac{0.24s}{(0.8)}2 + \left(\frac{s}{0.8}\right)^2)(1 + \frac{s}{4})}{s(1 + s)(1 + \frac{s}{15})[1 + \frac{s}{(85)}2 + \left(\frac{s}{85}\right)^2]^2} \qquad \text{(V-51)}$$

Since g_2 is different, the effective plant, q_{11}^* is different also. Therefore the entire design process for g_1 is reaccomplished beginning with the computation of q_{11}^* for each flight condition. In this case, by coincidence, the frequency characteristics of the new q_{11}^*'s change very little as a result of changing g_2. The g_1 and the f_{11} of the first design also meet the respective requirements for the second design and are left unchanged.

It will be seen in Chapter VI that the results for the second design are not acceptable. It is presented here for comparison and to demonstrate the consequences of ignoring a boundary.

Summary

This chapter follows the design of the three required controller elements, g_2, g_1, and f_{11}, from the elimination of the yaw angle output from the model, through the actual formulation of the compensator transfer functions. Because of the large bandwidth of the g_2 element of the first design, a second design is also presented.

The results of computer simulations for both designs are presented

in Chapter VI. A discussion of these results is presented in Chapter VII.

VI. Simulation Results

Introduction

This chapter presents the results of simulations for both designs presented in Chapter V. All the simulations are products of the computer-aided-design program, TOTAL. The input for each simulation is a step command input demanding thirty degrees of bank.

The first design meets the specifications set forth in Chapter V easily. The second, which is the result of ingnoring the dominant bound on the second loop, does not meet the specifications. It is presented here as an example of the consequences of ignoring a boundary. Transfer functions for all simulations are in Appendix C.

Design One

Figs VI-1 through VI-4 are the results of simulations for the high altitude, high airspeed condition, Cruise 1. Fig VI-1 is the bank angle response to a thirty degree step bank angle command. The desired first-order response is achieved with about a four second settling time. Fig VI-2 is the deflection of the control wheel during the maneuver. Fig VI-3 is the sideslip response. Note that the peak value of sideslip is less than 0.02 degrees throughout the maneuver. Fig VI-4 is the deflection of the rudder during the maneuver. As expected, the aircraft response at this flight condition is excellent.

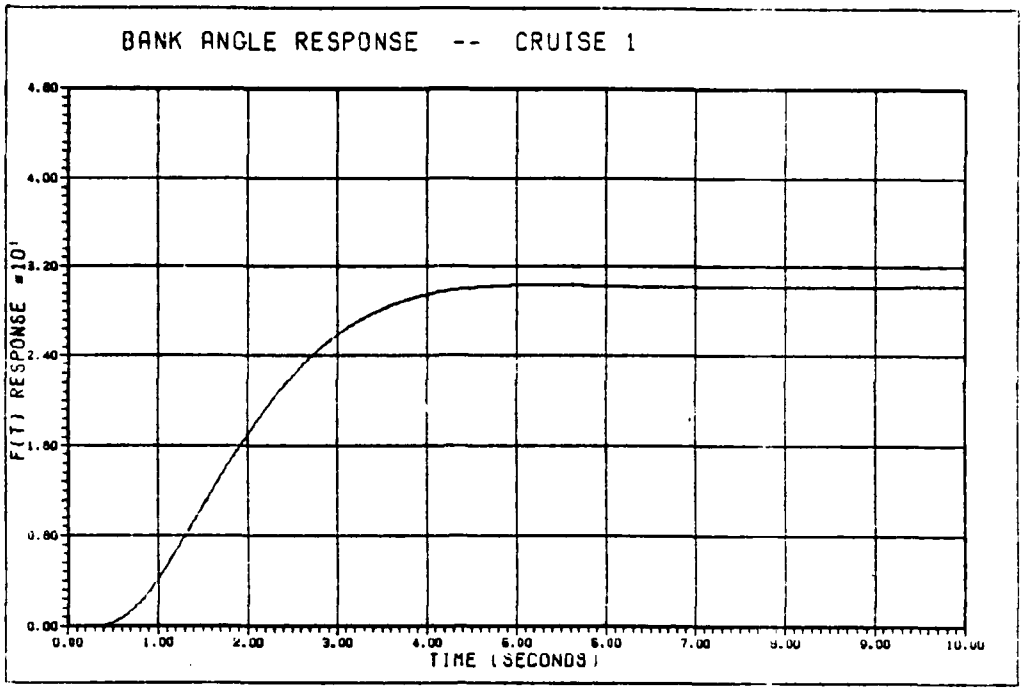

Fig VI-1 Bank Angle Response - Cruise 1 - Design 1

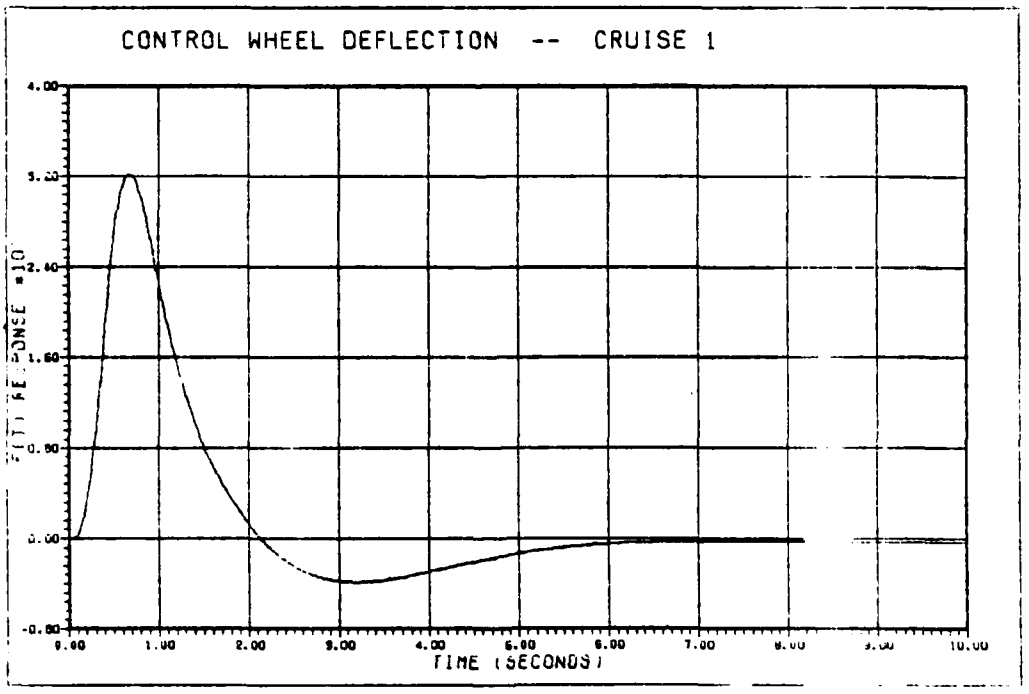

Fig VI-2 Control Wheel Deflection - Cruise 1 - Design 1

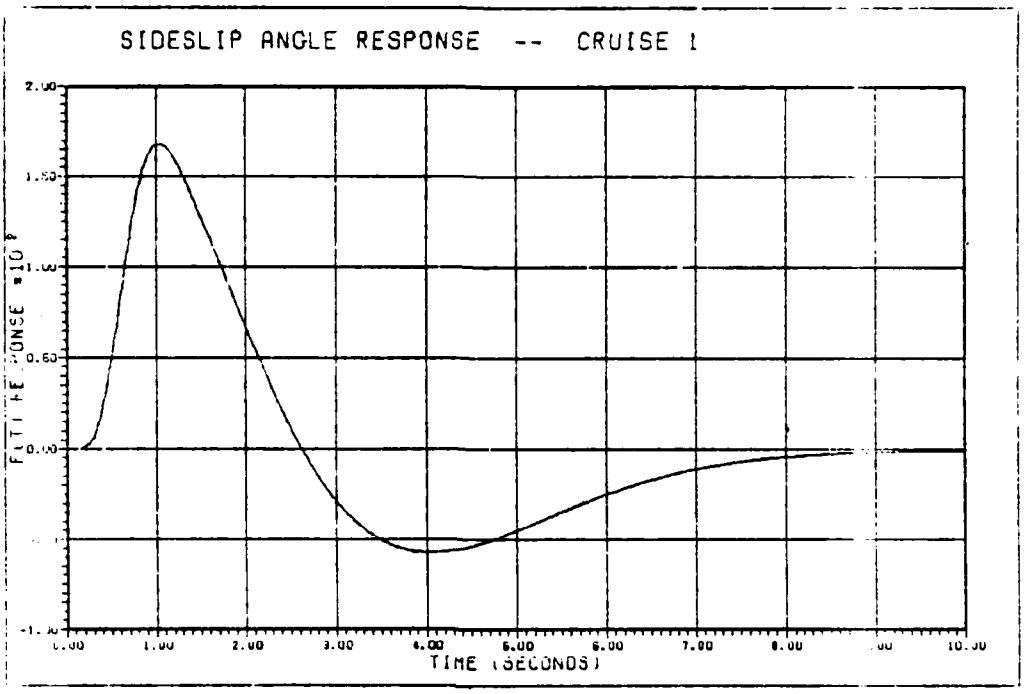

Fig VI-3 Sideslip Angle Response - Cruise 1 - Design 1

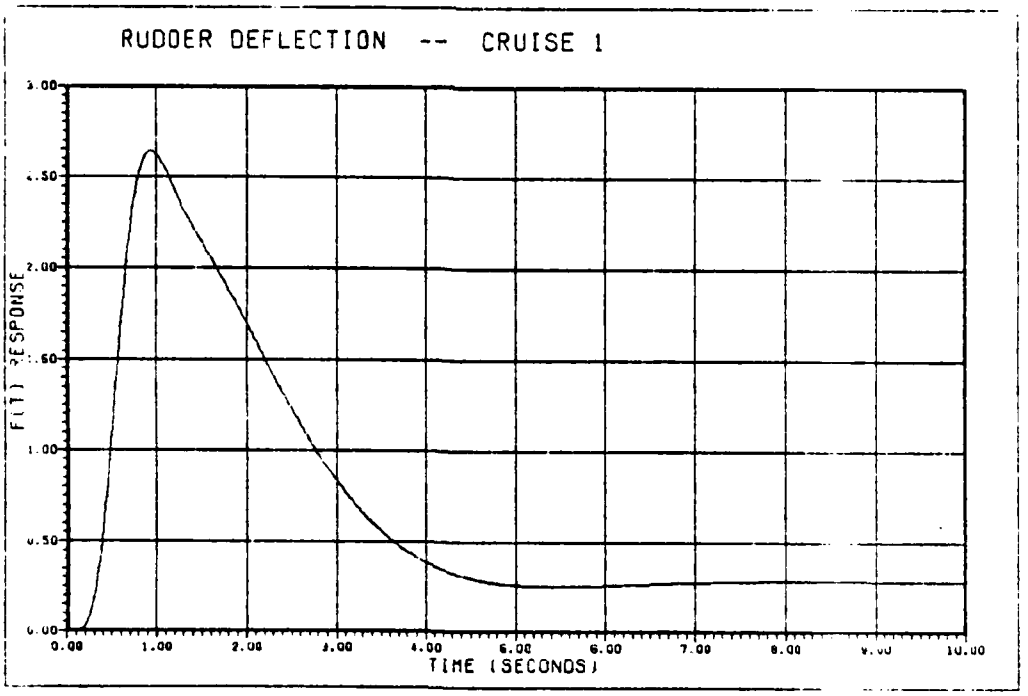

Fig VI-4 Rudder Deflection - Cruise 1 - Design 1

Figs VI-5 through VI-8 are the simulation results for the medium altitude, moderate airspeed flight condition, Cruise 2, to the same thirty degree of bank command input. Although the controller is unchanged, the responses are, again, acceptable.

Fig VI-5 is the bank angle response. The desired first-order response is again achieved but the settling time is about six seconds. Fig VI-6 is the control wheel deflection during the maneuver. Its response is very similar to that of Cruise 1. Fig VI-7 is the sideslip angle response. The peak value is on the order of 0.01 degrees which is even less than that of Cruise 1. Fig VI-8 is the rudder deflection during the maneuver.

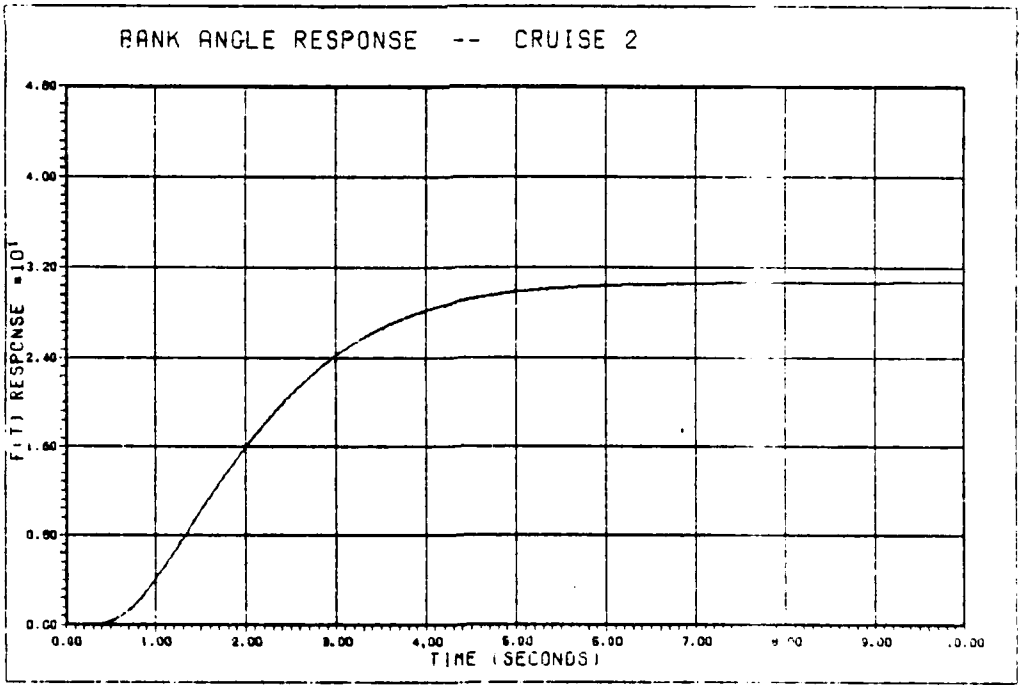

Fig VI-5 Bank Angle Response - Cruise 2 - Design 1

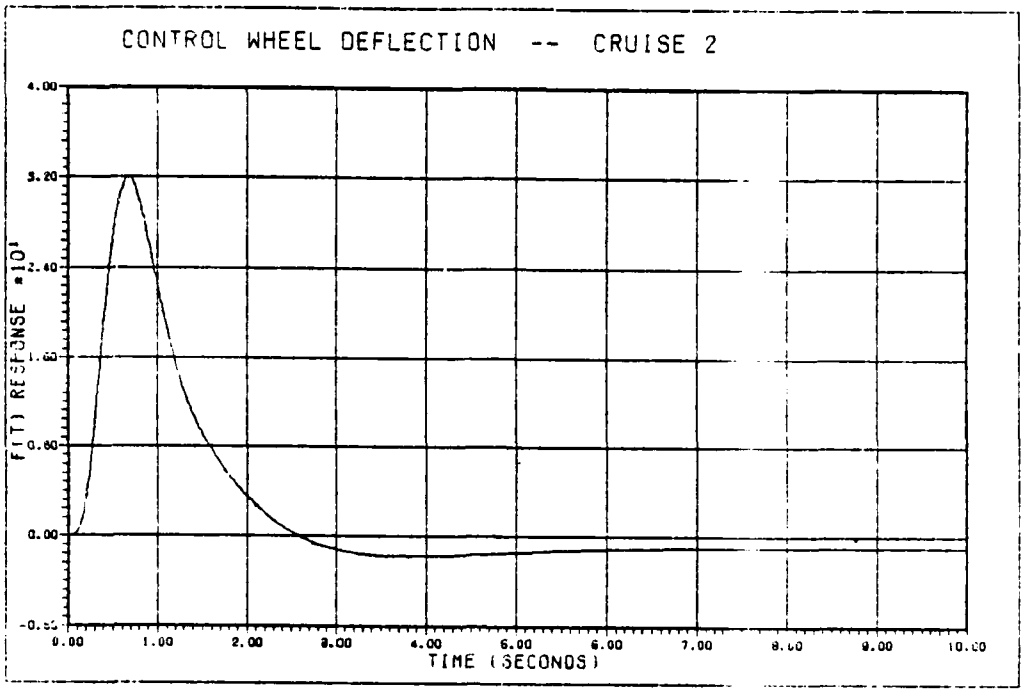

Fig VI-6 Control Wheel Deflection - Cruise 2 - Design 1

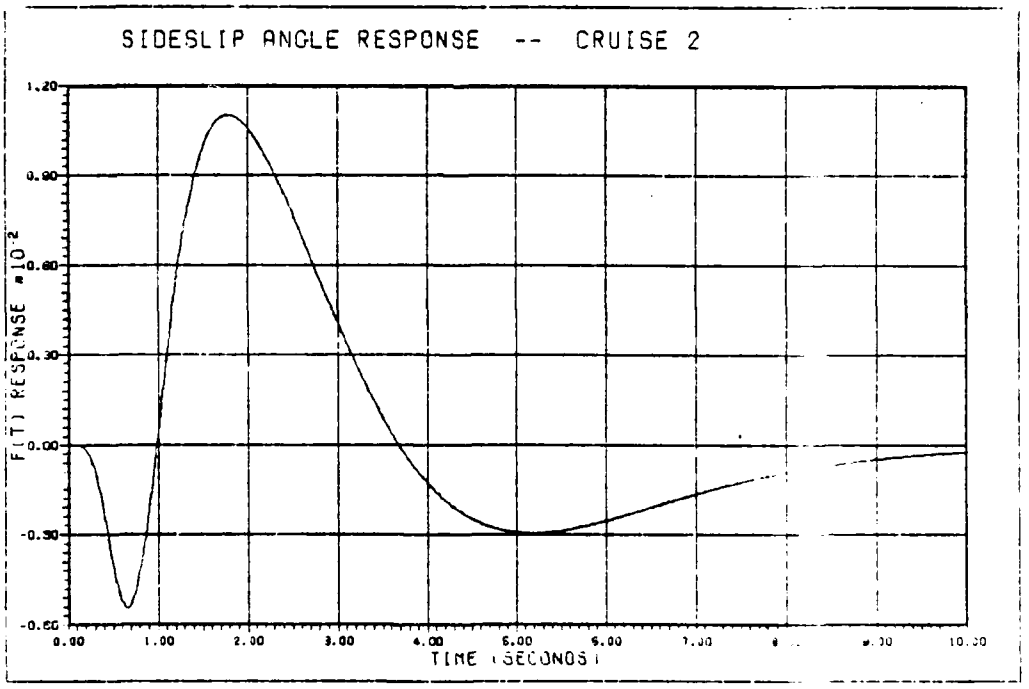

Fig VI-7 Sideslip Angle Response - Cruise 2 - Design 1

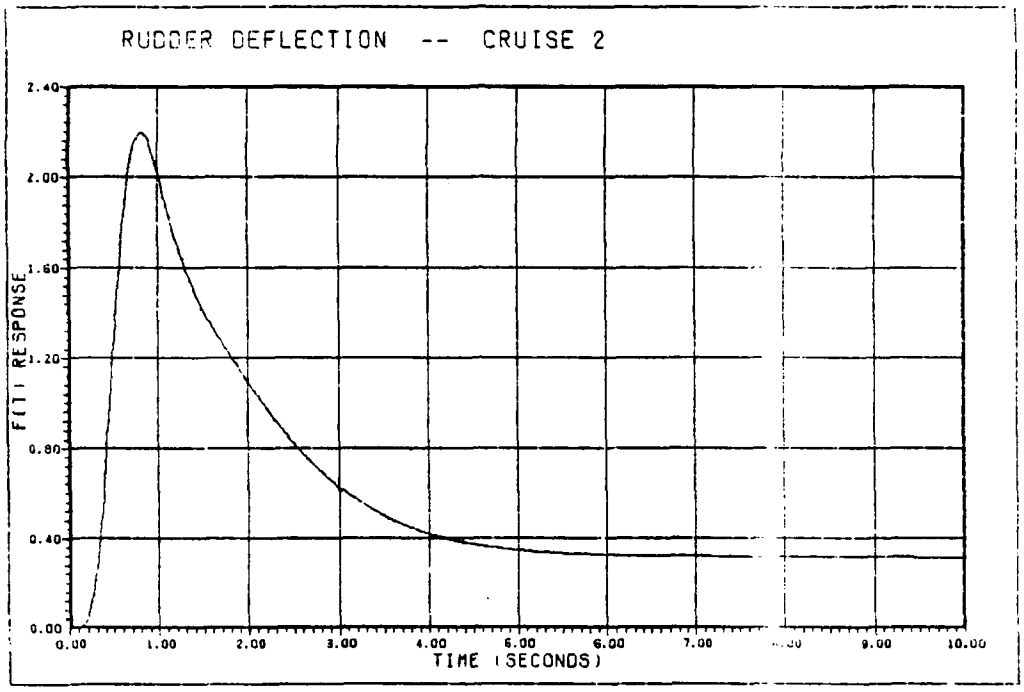

Fig VI-8 Rudder Deflection - Cruise 2 - Design 1

Figs VI-9 through VI-12 are the aircraft responses for the low altitude, low airspeed flight condition in the approach configuration, Powered Approach. As expected, the aircraft response is degraded somewhat but the performance is still well within the specifications of Chapter V.

Fig VI-9 is the bank angle response. It is still first-order but the settling time is about seven seconds. Fig VI-10 is the control wheel deflection during the maneuver. Fig VI-11 is the sideslip angle response. The peak value is about 0.15 degrees, which is about a factor of ten worse than that of Cruise 1, but still well within specifications. Fig VI-12 is the rudder deflection during the maneuver. Notice that the response is much different than that of either Cruise 1 or 2. This is due to the change in spoiler operation in this configuration.

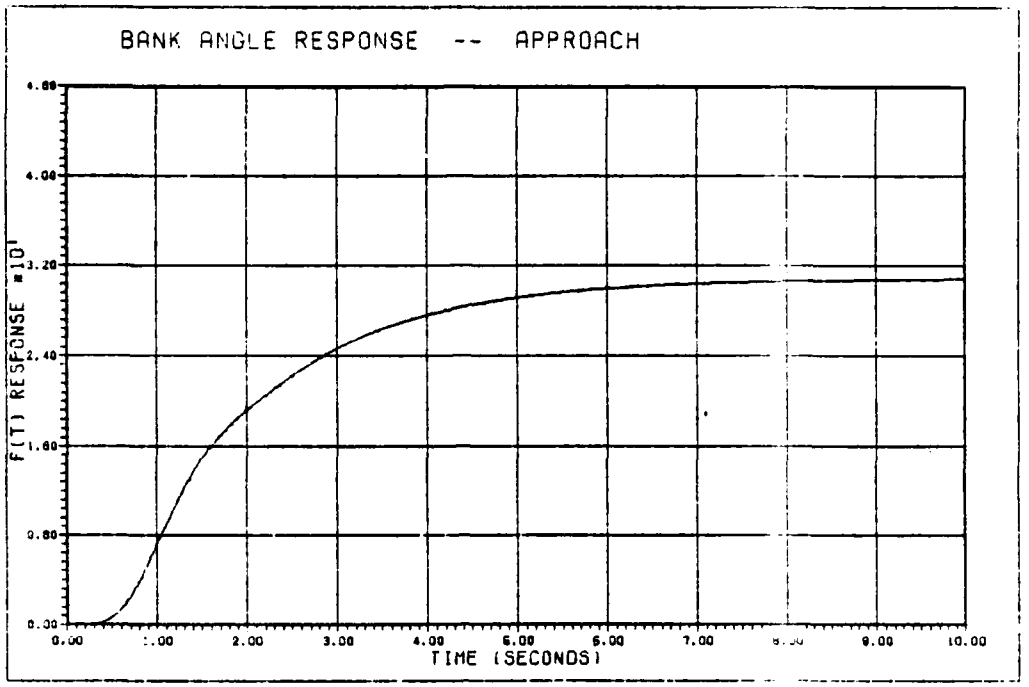

Fig VI-9 Bank Angle Response - Powered Approach - Design 1

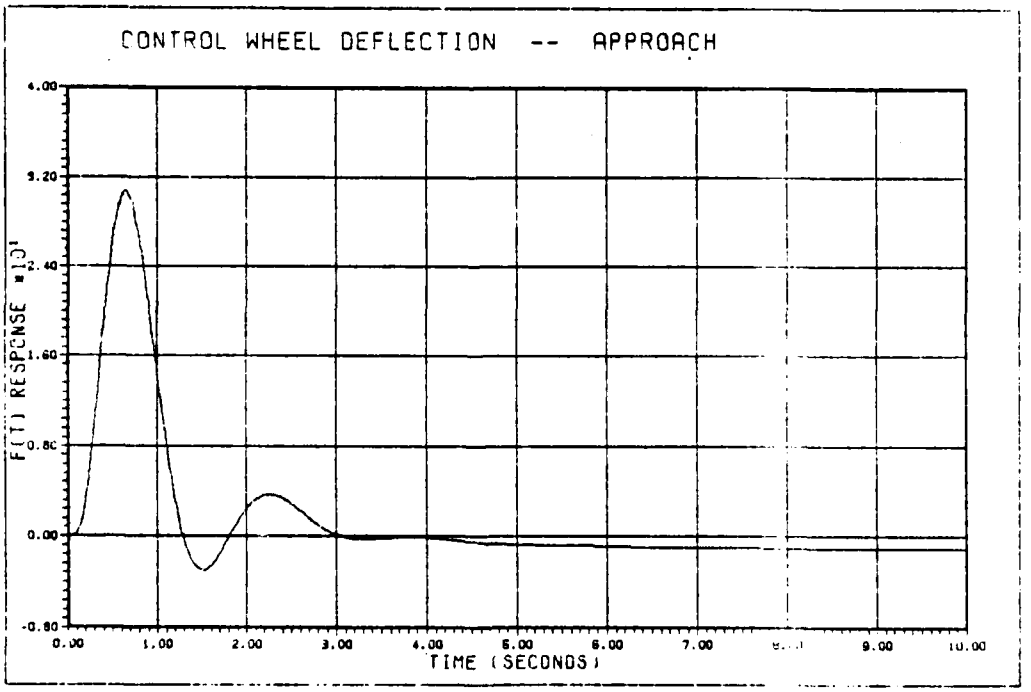

Fig VI-10 Control Wheel Deflection - Powered Approach - Design 1

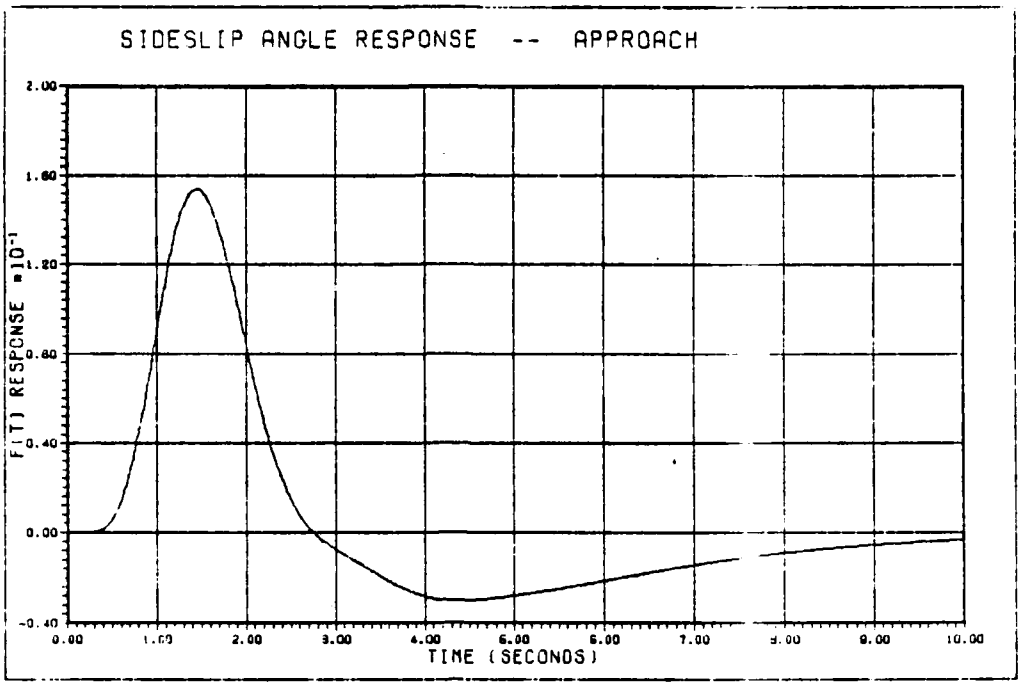

Fig VI-11 Sideslip Angle Response - Powered Approach - Design 1

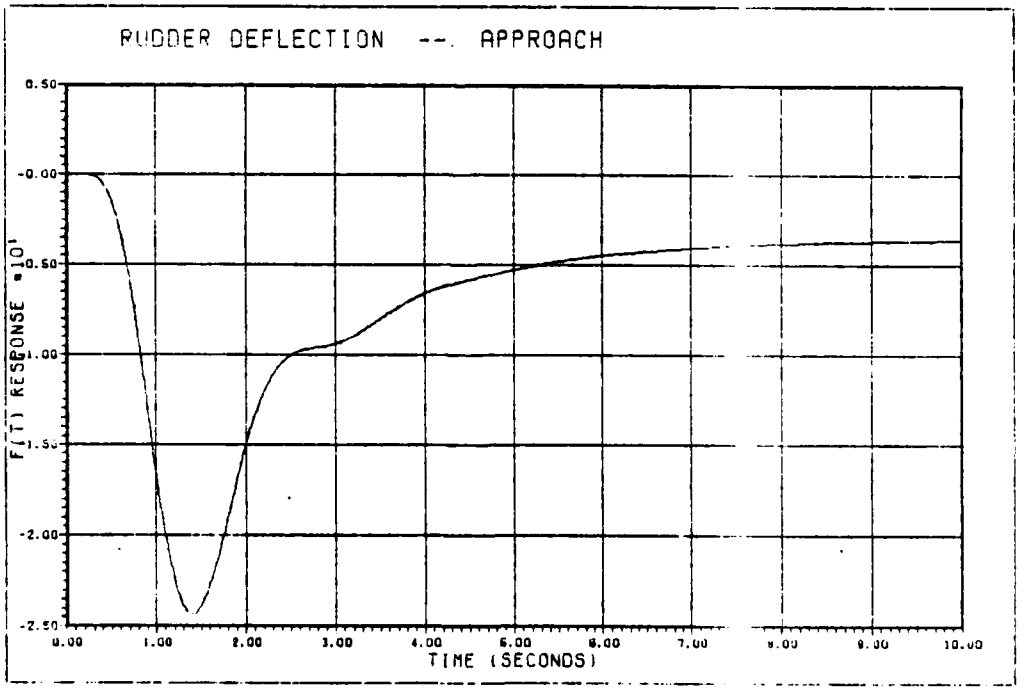

Fig VI-12 Rudder Deflection - Powered Approach - Design 1

The three flight conditions are chosen to represent a major portion of the C-135 flight envelope and are limited by the availability of flight data. These simulation show that the controller produces acceptable aircraft responses at all three flight conditions. It follows logically that the aircraft performance at any flight condition between these extremes would also be acceptable.

Design Two

Figs VI-13 and VI-14 are the results of simulations for the high altitude, high airspeed condition, Cruise 1. Fig VI-13 is the bank angle response to a thirty degree bank angle step command. This response is virtually unchanged from that of Design One. Fig VI-14 is the sideslip angle response to the same command. The maximum value specification is met but the settling time specification is not.

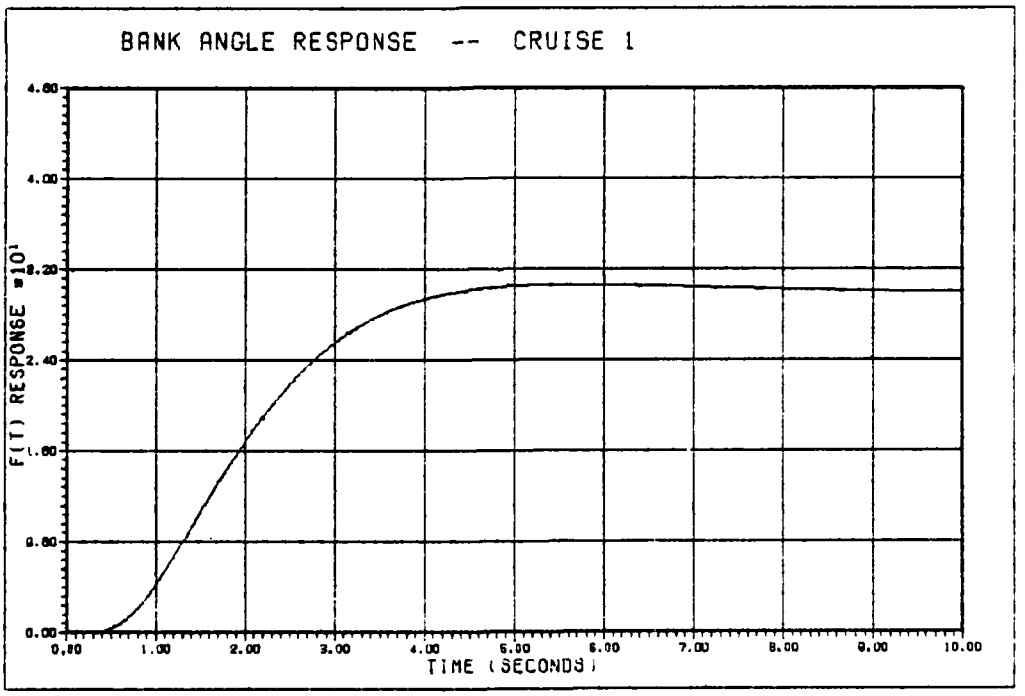

Fig VI-13 Bank Angle Response - Cruise 1 - Design 2

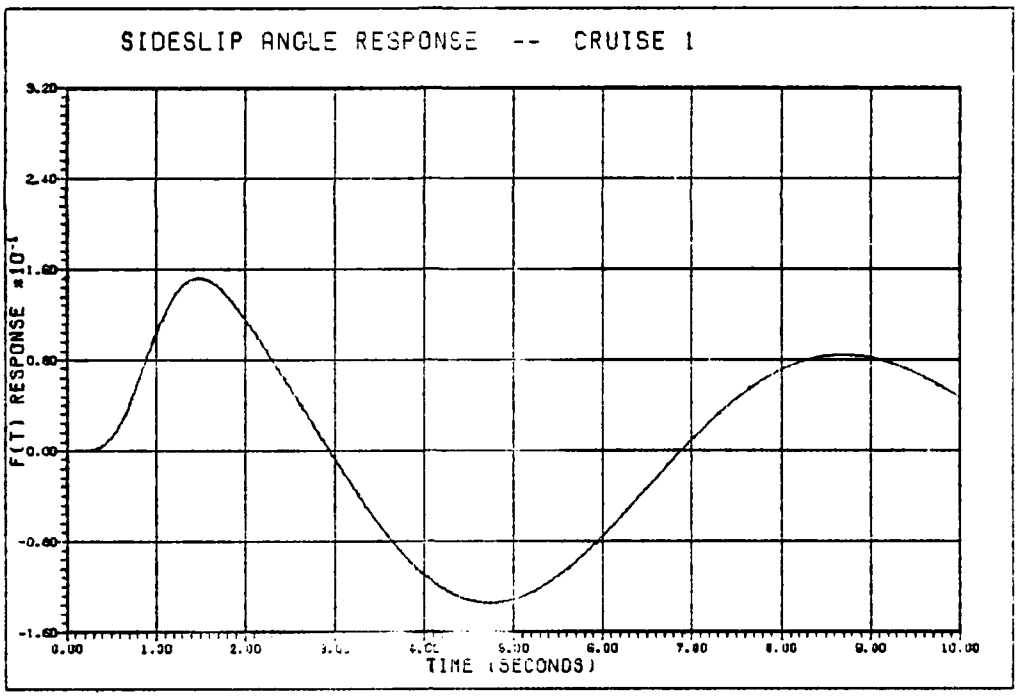

Fig VI-14 Sideslip Angle Response - Cruise 1 - Design 2

Figs VI-15 and VI-16 are the simulation results for the medium altitude, moderate airspeed flight condition, Cruise 2. Fig VI-15 is the bank angle response, which is nearly identical to the response of Design 1 and still well within design specifications. Fig VI-16 is the sideslip angle response. Again, the peak value specification is met, but the settling time is far too long.

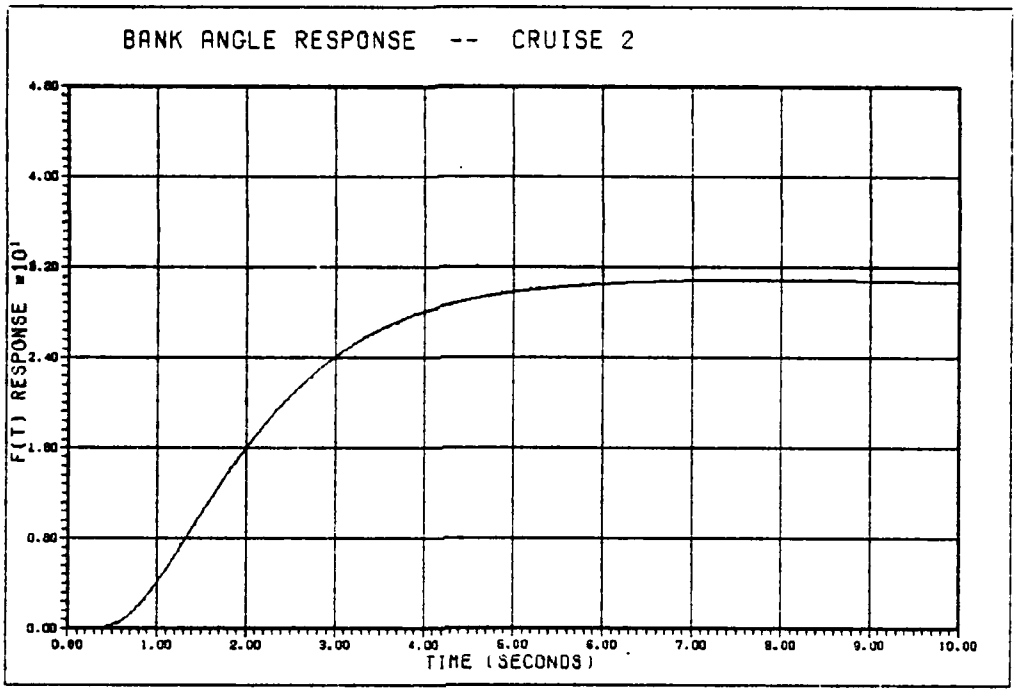

Fig VI-15 Bank Angle Response - Cruise 2 - Design 2

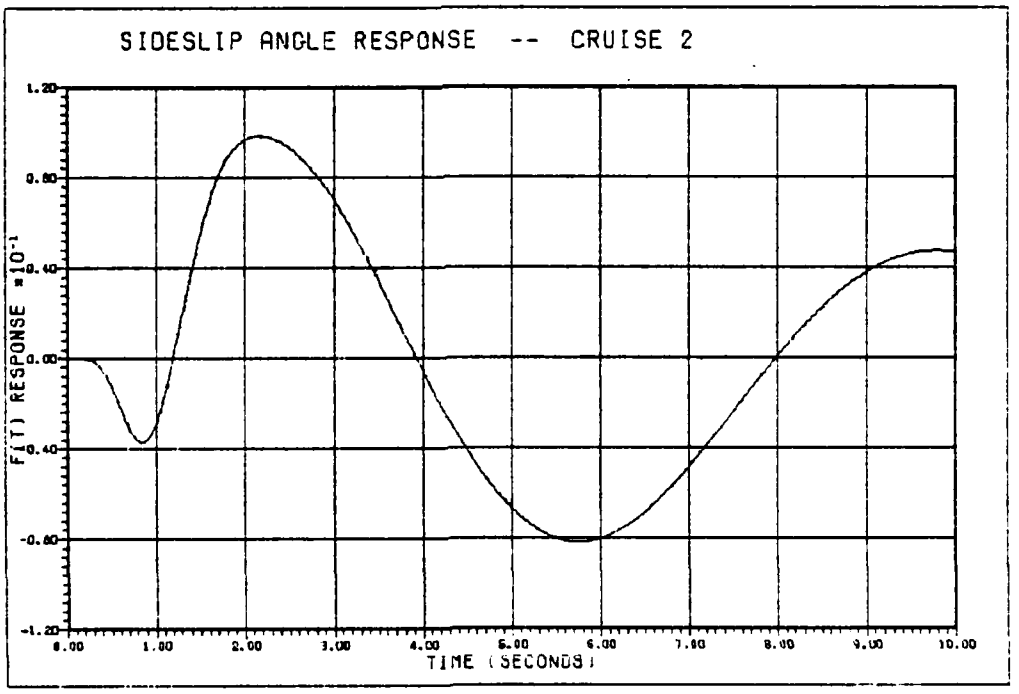

Fig VI-16 Sideslip Angle Response - Cruise 2 - Design 2

Summary

This chapter presents the results of simulations for both the controllers designed in this thesis. The first controller, designed in full compliance with Dr. Horowitz' technique, meets the specifications over the entire range of uncertainty considered. The second design, which is the result of an intentional violation of a dominant boundary, produces results which are within the peak value specifications but which violate the settling time requirements.

VII. Conclusions and Recommendations

Thesis Summary

This thesis is intended to describe and demonstrate the use of Dr. Horowitz' Quantitative Feedback technique to design a lateral controller for a large transport aircraft, specifically the C-135. The first controller presented easily meets all the design specifications over the entire range of uncertainty considered. The fact that the maximum peak sideslip angle is more than ten times less than that allowed by the specifications is significant and is dealt with in the discussion section of this chapter. In addition to conclusions and recommendations, this chapter presents a brief comparison of this design to that of a concurrently produced thesis concerning the use of Dr. Brian Porter's method to design a controller for the C-135 aircraft.

Chapter I presents an introduction to the C-135 lateral flight control problem. Chapters II and III present an overview of Quantitative Feedbeck Synthesis theory. The single input - single output problem is described in Chapter II and the extension to the multiple input - multiple output problem is presented in Chapter III. Chapter IV describes the aircraft model used in the design. The actual design of the controller is presented in Chapter V. The simulation results for both the primary design and an alternate design are shown in Chapter VI.

Appendices to this thesis contain examples of loop transmission shaping (Appendix A) which are provided courtesy of Dr. Horowitz, response models generated during the design (Appendix B), and the actual transfer functions of the effective plants and of the compensated system (Appendix C).

Discussion

The specifications on which both designs are based allow a peak value of 2.0 degrees of sideslip in response to a 30 degree bank command. The worst sideslip response, produced by the Power Approach flight condition, reaches a peak value of only about 0.15 degrees. This is only about 7.5% of the allowable value. One's initial reaction to learning that the design "beats" the specifications by so much might be delight, but it is an indication of serious overdesign and a waste of compensation. Although the problem is not solved here, this section deals with the possible causes and provides a suggested approach to reduce the overdesign.

The first and most obvious place to look for the overdesign is in the sideslip loop. It is this loop which controls the sideslip angle and as noted previously the compensator in the sideslip loop has a rather large bandwidth. Inspection of the bound derivation and actual loop design reveals little overdesign. The combination of low frequency bounds and stability considerations dictate a loop transmission with a bandwidth very close to that of Design 1. Some bandwidth (and therefore some compensation) reduction could be achieved but not enough to account for the magnitude of the overcompensation.

A comparison between the response model used in the design of the sideslip loop and the sideslip responses from the simulations shows that the aircraft reacts much more slowly than assumed during the modeling process. The resulting design appears to provide compensation at much higher frequency than necessary. In other words, the response far exceeds the design specifications because the response model demanded a compensator with a much larger bandwidth than needed to control the

aircraft.

Although, time does not permit a thourough investigation here, the bandwidth of the sideslip compensator could be reduced greatly by re-shaping the sideslip loop transmission based on a slower response model.

Comparison to Porter Design

Capt William Locken, GE-83D, has written a thesis concerning flight control laws for the C-135 using the method of Professor Brian Porter (Ref 13). This section is intended as a qualitative comparison between the Porter technique and the Horowitz technique. By necessity, much of this section is personal opinion on the part of the author.

The primary difference between the two methods is that the Horowitz approach treats plant uncertainty (robustness) and performance specifications as given information on which the design is based, while the Porter approach involves testing for robustness and conformance with specifications after a proposed design is completed.

A Porter design can be completed much more quickly than a Horowitz design, if performance tolerances are met in the first few iterations. It is possible, however, that a Porter design could take considerably longer to complete if the specifications are difficult or impossible to meet. The Horowitz approach provides insight into the design problem and difficult or impossible specifications can be easily identified, giving the designer the information needed to modify the tolerances or abandon the problem if it is hopeless.

The results of simulations for the designs of this thesis and Capt Locken's thesis are very similar, although command inputs were not identical. Both design methods provided the means for successfully

compensating the aircraft.

The final comment in the comparison of the two methods concerns compensation bandwidth. The Porter method relies on straight gains in the feedback loops to achieve desired compensation. Compensation bandwidth is, therefore, unknown. In the Horowitz approach, the bandwidth of the compensator elements is a prime consideration during the design process.

Conclusions

This thesis concludes that Professor Horowitz' quantitative feedback technique is an effective tool for compensating large aircraft. The aircraft can be controlled to specifications over the entire range of uncertainty considered.

The sideslip response model used overestimates the speed with which the aircraft can respond to a bank command. Therefore, the bandwidth of the sideslip loop compensator is higher than necessary. This results in sideslip responses which far exceed the specifications.

Finally, this thesis concludes that Professor Horowitz' method does provide insight into the overall compensation problem throughout the design process. An example of this is the ease in analysing the reasons for the overdesign in the sideslip loop.

Recommendations

Quantitative Feedback and its application to flight control problems should be further investigated. A more complete aircraft model should be developed to include bending modes and coupling between the lateral and longitudinal modes.

Presently, most of the analysis must be done graphically, by hand. A computer-aided-design package could be developed to greatly enhance the speed and accuracy of controller design. Ideally, this package would incorporate a split-screen representation of Bode, Nichols, and time response plots which change as the user changes parameters in the transfer function of the model or compensator. Computer-aided development of frequency domain bounds based on response models and defined range of uncertainty would also be useful.

Bibliography

1. Ashworth, M. J. Feedback Design of Systems with Significant Uncertainty. Chinchester: Research Studies Press, 1982.

2. Blakelock, John H. Automatic Control of Aircraft and Missles. New York: John Wiley and Sons, Inc., 1965.

3. D'Azzo, John J. and Constantine H. Houpis. Linear Control System Analysis and Design, Conventional and Modern (Second edition). New York: McGraw-Hill Book Company, 1981.

4. Etkin, Bernard. Dynamics of Atmospheric Flight. New York: John Wiley and Sons, Inc., 1972.

5. Gamble, Lynn L. and William L. Smith. Improved Dutch Roll Stability Augmentation System for a Modified C-135B Aircraft. MS thesis. Wright-Patterson AFB, Ohio: School of Engineering, Air Force Institute of Technology, June 1970.

6. Horowitz, Isaac M. Synthesis of Feedback Systems. New York: Academic Press, 1963.

7. Horowitz, Isaac, and Marcel Sidi. "Synthesis of Feedback Systems with Large Plant Ignorance for Prescribed Time-Domain Tolerances," International Journal of Control, 16 (2): 287-309 (1972).

8. Horowitz, Isaac. "Quantitative Synthesis of Uncertain Multiple Input-Output Feedback System," International Journal of Control, 30 (1): 81-106 (1979).

9. Horowitz, Isaac et al. Research in Advanced Flight Control Design. AFFDL-TR-79-3120. Department of Applied Mathematics, The Weizmann Institute of Science, Rehovot, Israel., January 1980.

10. Horowitz, Isaac, and Clayton Loecher. "Design of a 3x3 Multivariable Feedback System with Large Plant Uncertainty," International Journal of Control, 33 (4): 677-699 (1981).

11. Horowitz, Isaac. "Improved Design Technique for Uncertain Multiple-Input-Multiple-Output Feedback Systems," International Journal of Control, 36 (6): 977-988 (1982).

12. Horowitz, Isaac, and T. Kopelman. Multivariable Flight Control Design with Uncertain Parameters. Department of Applied Mathematics, The Weizmann Institute of Science, Rehovot, Israel. Final Report, September 1982.

13. Locken, William H. Digital Multivariable Control Laws for the C-135A. MS thesis. Wright-Patterson AFB, Ohio: School of Engineering, Air Force Institute of Technology, June 1982.

AD-A138 011 MULTIPLE INPUT - MULTIPLE OUTPUT FLIGHT CONTROL DESIGN WITH HIGHLY UNCERT..(U) AIR FORCE INST OF TECH WRIGHT-PATTERSON AFB OH SCHOOL OF ENGI.. R W BETZOLD 2/2

UNCLASSIFIED DEC 83 AFIT/GE/EE/83D-11 F/G 1/2 NL

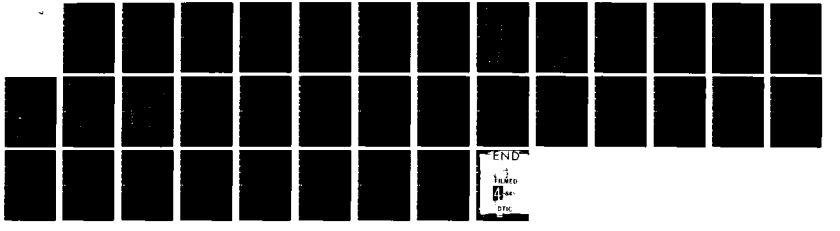

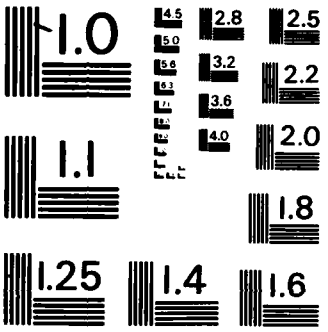

MICROCOPY RESOLUTION TEST CHART
NATIONAL BUREAU OF STANDARDS - 1963 - A

APPENDIX A

EXAMPLES OF LOOP SHAPING

APPENDIX A

Examples of Loop Shaping

Introduction

The folowing loop shaping examples are provided, courtesy of Dr. Horowitz. All information is given and Nichols plots of the shaped loop transmissions are provided.

Example: Shaping of a nominal loop transmission $L_0(j\omega)$ to satisfy boundaries $B(\omega)$ on Nichols Chart.

Previous notes have described how tolerances on the closed-loop system frequency response are readily translated into bounds on a nominal loop transmission function $L_0(j\omega)$. In Fig. 1, for example, $L_0(j2)$ must be on or above the curve labelled B(2), etc. B_h is the "universal high-frequency boundary" applicable, in this example, to $\omega \geq \omega_h = 40$, i.e. $L_0(j\omega)$ (for $\omega \geq 40$) must be contained in the closed curve B_h in Fig. 1. Additional specification is $e_L = 4$, where e_L is excess of poles over zeros of $L_0(s)$. Also, L_0 is to be Type 1 (one pole at the origin). We proceed to describe a reasonable procedure for choosing a rational function $L_0(s)$ which satisfies the above specifications.

In our first step, we try to find the $B(\omega)$ which "dominates" $L_0(j\omega)$. E.g. suppose $L_{01}(j4) = 0db \angle -135°$ (point A in Fig. 1). But at $\omega = 1$, $|L_0(j)|$ needed is $\approx 27db$. In order to decrease $|L_0|$ from 27db to about 0db in 2 octaves ($4/1 = 2^2$), the slope of $|L_0(j\omega)|$ would have to be, on the average, about -14db/octave, involving $\angle L_0 < -180°$. We assume "absolute" stability is required here for $L_0(j\omega)$ with a margin of 40°, not just at crossover ("crossover" is defined as the frequency at which $|L_0(j\omega)| = 1$). Hence B(1) dominates $L_0(j\omega)$, at least more than B(4). In the same way we see that B(1) dominates over all other $B(\omega)$ in Fig. 1.

The $B(\omega)$ for $\omega < 1$ are not shown in Fig. 1. We shall assume that for $\omega < 1$, a slope of -6 db/octave (with 27db at $\omega = 1$, i.e. 33 db at $\omega = .5$, 39db at $\omega = .25$ etc.), suffices. We can tolerate $\approx -140°$ for $\omega \geq 1$, so we choose a lag corner frequency (symbol lacf) at $\omega = 1$ (i.e. pole at -1), and set $|L_0(j\omega)|$ (asymptotic) at 30 db (to allow for the -3db correction). Thus our L_0 is so far: $L_{01} = 31.6/s(s+1)$, whose phase $\angle L_{01}(j\omega)$ is sketched in Fig. 2.

$\angle L_{01}(j\omega)$ violates the -140° bound at $\omega>1.2$, so a lead corner frequency (symbol lecf) is needed. Where should it be located? At $\omega=5$, $\angle L_{01}(j5)=-169°$ (see Fig. 2), so 29° lead is needed; but we know that later there will be a second lacf, so allow say additional 15° for it giving 15+29=45° lead required at $\omega=5$; which is achieved by a lecf at $\omega=5$ i.e. a zero at -5. The resulting $L_{02}(s)=\frac{31.6(1+\frac{s}{5})}{s(1+s)}$, whose phase $\angle L_{02}(j\omega)$ is sketched in Fig. 2.

In the Nichols Chart (N.C.) we are ($\approx\omega=10$ or so) in the region where the maximum phase lag allowed is 135° (i.e. $\angle L_0(j\omega)$ must be $\gtrsim -135°$). Consider $\omega=10$, with present $\angle L_{02}(j\omega) = -112°$, so 135°-112°=23° more lag is allowed. But this lacf will be followed by a lecf, so allow say 10° for it, giving 23°+10°=33° more lag allowable. This locates the lacf at 15.4 (tan33°=.65, and 10/.65=15.4), so we set the lacf at $\omega=15$ (i.e. pole at -15), giving $L_{03}(s)=\frac{31.6(1+.2s)}{s(1+s)(1+\frac{s}{15})}$. $\angle L_{03}(j\omega)$ is sketched in Fig. 2.

Looking ahead at $\omega=40$, $|L_{03}(j40)| \approx -20$db, so soon $L_0(j\omega)$ can make its asymptotic left turn under the B_h boundary. Our plan is to add two more lecfs, and finally two complex pole pairs, in order to have an excess e_L of poles over zeros of 4. We try one lecf at $\omega=40$, giving $L_{04}(s)=\frac{31.6(1+.2s)\ (1+\frac{s}{40})}{s(1+s)\ (1+\frac{s}{15})}$. $\angle L_{04}(j\omega)$ is sketched in Fig. 2.

We're ready now for the last lecf, in order to achieve (an asymptotic) horizontal segment for $|L_0(j\omega)|$, before the final -24db/octave slope. (We follow Bode in this respect, a good master to follow.) Where should this horizontal segment be located? The bottom of B_h (see Fig. 1) is at -22.5db. Allow 2db margin, 3db correction due to the last lecf, 1.5db for the effect of the lecf at $\omega=40$, giving a total of -(22.5+2+3+1.5)=-29db. We'll use a damping factor of $\zeta=.6$ for the 2 complex pole pairs, so no

correction need be allowed for them. Thus the final break for $|L_0(j\omega)|$ asymptotic is to be at -29db, which $|L_{04}(j\omega)|$ achieves at ω=60. Hence, the last lecf is at ω=60. The resulting phase due to L_{04} and the lecf at ω=60, is -66°. We could have -180° at this point, but we'll allow an additional 15° margin (a matter of taste; it depends on the problem -- presence of higher order modes, etc). This means 100° phase lag is permitted, 50° due to each complex pole pair (180-66-15≈100). For ζ=.6, this locates them at 100. Thus $L_0(s) = \dfrac{31.6(1+.2s)(1+\frac{s}{40})(1+\frac{s}{60})}{s(1+s)(1+\frac{s}{15})[1+\frac{(1.2)}{100}s+\frac{s^2}{10}4]^2}$.

Discussion

$L_0(j\omega)$ is sketched in Fig. 1. A well-designed, i.e. "economical" $L_0(j\omega)$ is close to its boundary $B(\omega)$ at each ω. The vertical line -140° is the dominating $B(\omega)$ for $\omega<5$ and the right side of B_h (line -135°) is the boundary effectively for $5\leq\omega\leq30$; so our $L_0(j\omega)$ is pretty good in this respect since it is pretty close to these boundaries. There is tradeoff between complexity of $L_0(s)$ (number of its poles and zeros) and its final cut-off frequency, now at ω=100. There is some phase to spare between $L_0(j\omega)$ and the boundaries. so use of more poles and zeros in $L_0(s)$ would permit this cut-off frequency to be reduced a bit below 100, but not by much. On the other hand, if we want to reduce the number of poles and zeros of $L_0(s)$, we must pay the price in a larger cut-off frequency. We could economize significantly, of course, by allowing more phase lag in the low frequency range. If -180° was permitted at ω=1, we could decrease $|L_0(j\omega)|$ at a rate of 12db/octave; so with $|L_0|$= 25db at ω=1, it would be 13db at ω=2 (instead of the present 18db). Even with no more saving, this 5db difference, would allow a cut-off frequency at about 70 instead of 100.

Also, Fig. 1 reveals (immediately, without any shaping of L_0 required) that reduction (i.e. easing) of the specifications at ω=1 to about 21db (instead of ≈26db), would have the same effect as the above. One can check how badly the specifications are compromised by such easing. The design technique is thus highly "transparent" in revealing the trade-offs between performance tolerances, complexity of the compensation, stability margins, and the "cost of feedback" in bandwidth.

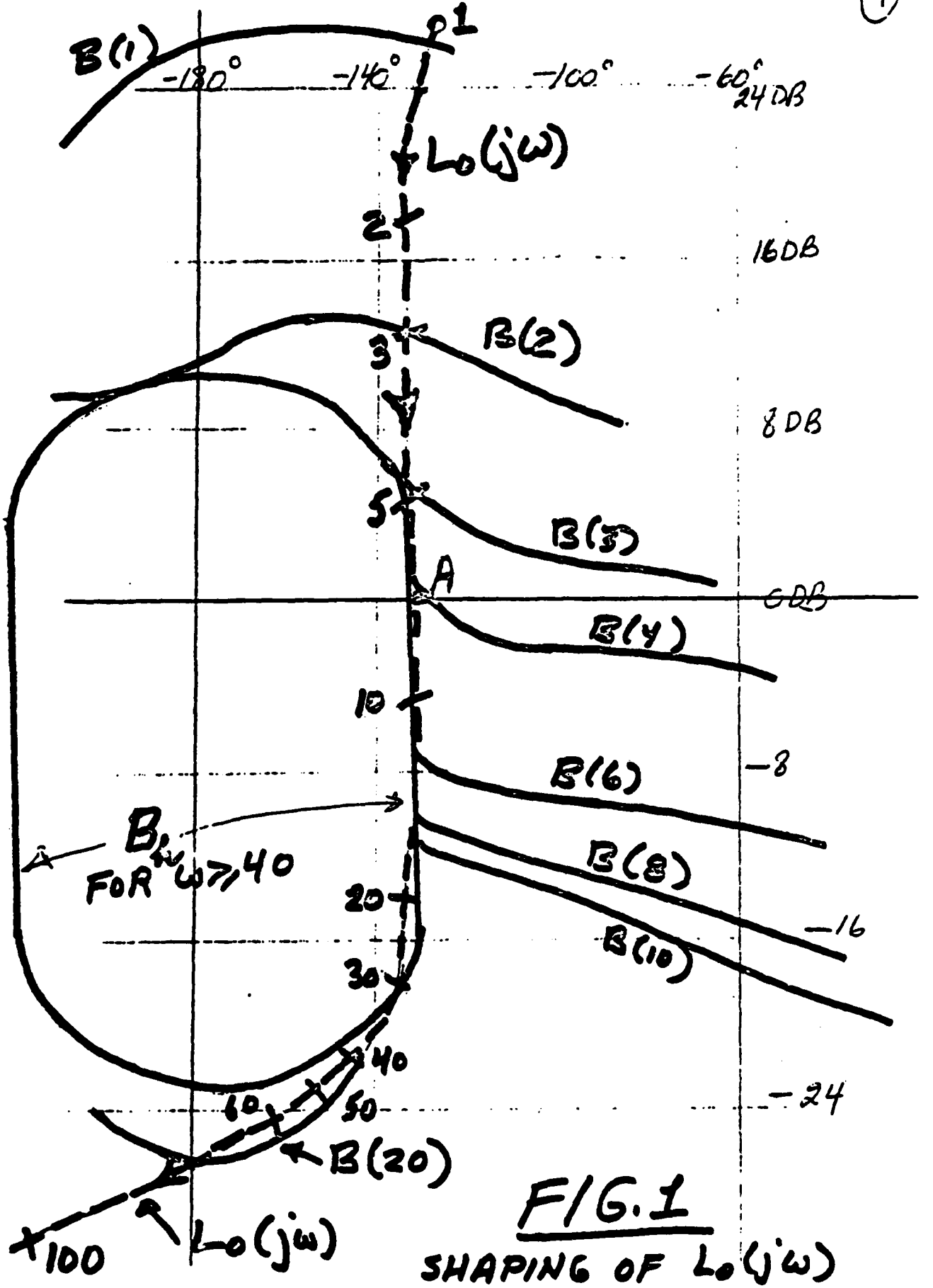

FIG. 1

SHAPING OF $L_o(j\omega)$ ON NICHOLS CHART.

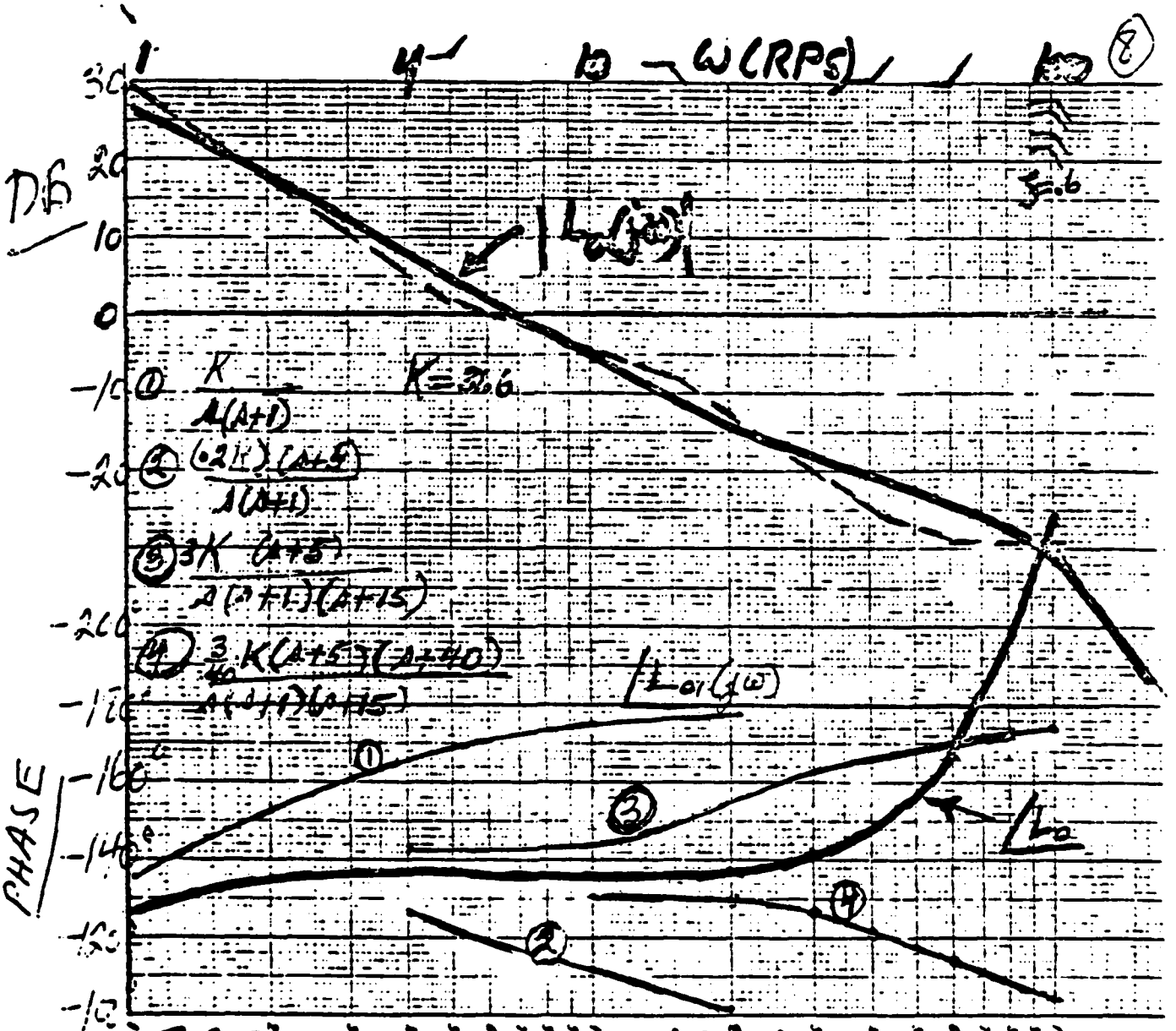

FIG. 2 SHAPING OF $L(j\omega)$ ON BODE PLOT.

DESIGN EXAMPLE: Uncertain Plant $P=\frac{k}{s(s+p)}$

k: [10,80], p: [-2,2].
[10,320] [-4,4]

Note: For part of range of p, plant is unstable.

Note: for $\omega \to 0$, plant template has infinite amplitude

Specifications on $|T(j\omega)|$. (see Fig. A)

ω	0	.5	1	2	5	10
MAX(DB)	0	1.3	1	-6	-17	-33
MIN(DB)	0	-2	-7	-19	-35	-65
$(\Delta\|T\|)$MAX	0	3.3	8	13	18	32

EXCESS e_L OF POLES OVER ZEROS OF L, IS 3.

ALSO $\left|\frac{L}{1+L}\right| \leq 3$DB, FOR ALL ω&P.

N.B. At high ω, $(\Delta|T|)$MAX MUST BE > $|\Delta P|$MAX. OK.

Step 1 Calculation and Construction of Plant Templates $\{P(j\omega)\}$=

The templates are shown in Fig. B_1. It suffices to calculate (at a fixed ω) several values of $1/j\omega(j\omega+p)$, i.e. at different p values. This gives the bottom curve of the template. Then extend vertically by 18db(80/10=8; 20log8=18).

Step 2 Use the procedure described in the notes (p.17 etc) to find bounds on $L_0(j\omega)$ in order to satisfy the specifications on $|T(j\omega)|$. A nominal plant must be chosen; p=2, k=10was chosen as nominal and marked heavily in Fig. B_2. (It helps to have the templates on transparent paper or plastic.) Already at ω=1, the bound on $L_0(j)$, denoted by B(1) is determined by $|L/(1+L)| \leq 3$DB, rather than by the constraints on $|T(j\omega)|$. And this is so for $\omega>1$ also, which is not typical for stable plants but more likely for plants which can be open-loop unstable for part of the parameter range.

Shaping of $L_0(j\omega)$

The boundary at $\omega=2$ dominates, i.e. determines the level of $|L_0|$ at $\omega=2$ to be $\approx$10db. The boundary at $\omega=5$ determines the phase there to be $\approx$-85°or so. This necessitates a lead corner frequency at some $\omega<5$. This was chosen to be at 1 and lags introduced thereafter such that at $\omega=5$ the phase > -85°; they were chosen at 5 and 8 (see Figs. B_2,C). A lecf is then needed to be followed by a complex pole pair with $\zeta=0.6$. The corner below the high-frequency bound can be turned when $|L|$ is $\approx$ -25db. If we try a lecf at 40, then phase requirements at $\omega=20$ force the final cut-off frequency to be well beyond the ω value at which $|L_0|$ =-25db. A lecf at $\omega=25$ gives compatibility of phase needs at $\omega=20$ and turning the corner when $|L_0|$ permits it. This gives 100 as the frequency at which the final complex pole pair can be inserted. This gives $L_0(s)=\dfrac{4(1+s)(1+\frac{s}{25})}{s(1+.2s)(1+\frac{s}{8})[1+\frac{1.2s}{100}+(\frac{s}{100})^2]}$

$=GP.=\dfrac{G(s)}{s(s+2)}$, giving G(s), -- see Figs. B_2, C.

Finding F(s)

The proper G guarantees that $\Delta|T|$ does not exceed those allowed. The next step is to find the range of $|L(j\omega)/(1+L(j\omega)|$. Place the template of the plant at $\omega=5$ (for example) on the point $L_0(j5)$ in the Nichols Chart, i.e. on 5db /-82° and it is seen that $|L/(1+L)|$ max$\approx$ 2.4db, min -1.7db. But the specifications require $|T|=|FL/(1+L)|\in[-35, -17]$ db. Therefore, it is required that: $-33.3db<|F|<-19.4db$. In this way we obtain the bounds on $|F(j\omega)|$ shown in Fig. D. It is easy to find an F(s) which satisfies these bounds, e.g. $F(s)=\dfrac{1}{(s+1)(1+\frac{s}{1.5})(1+\frac{s}{10})}$.

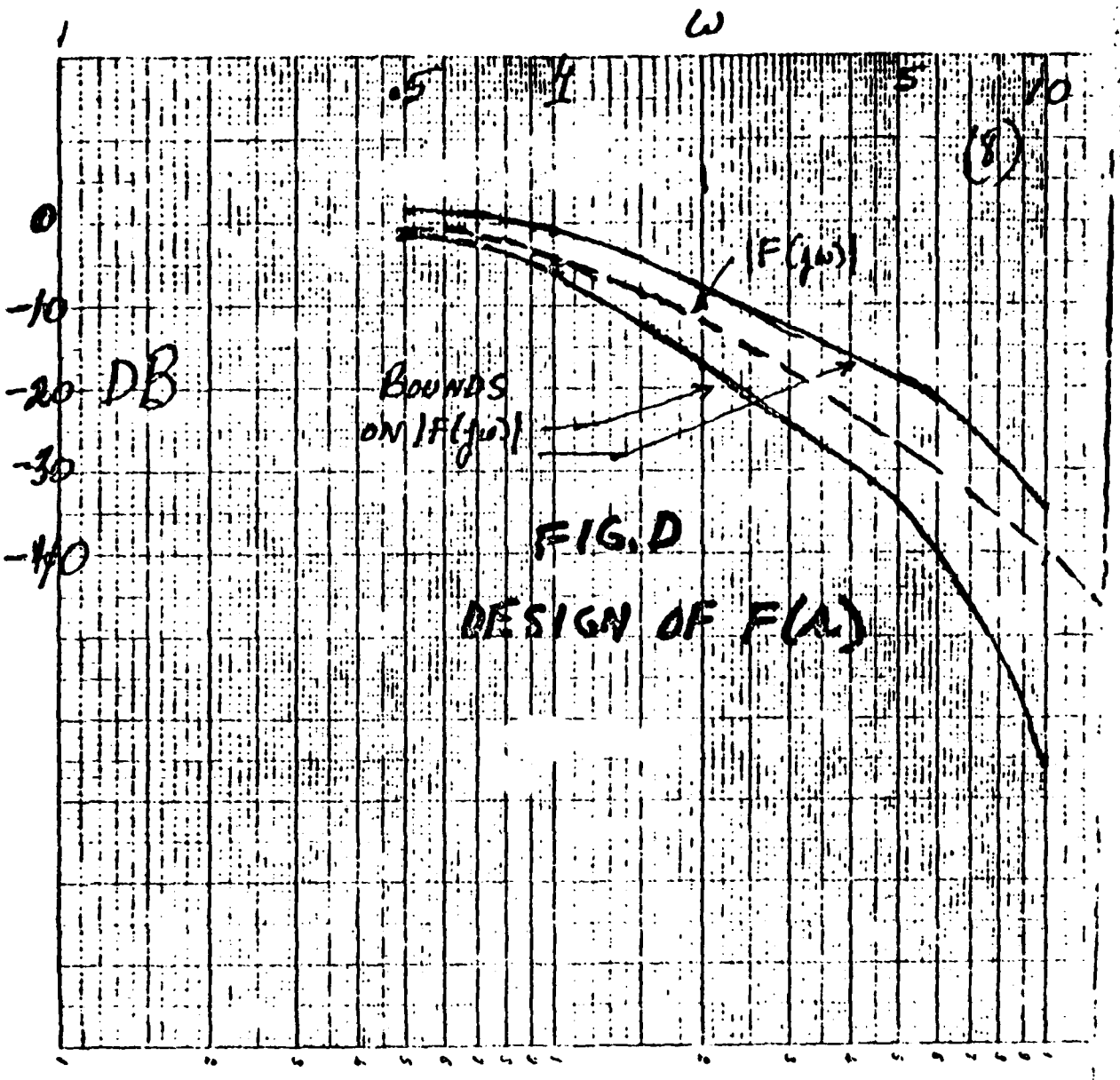

FIG. D

DESIGN OF F(s)

PLANT TEMPLATES- (NICHOLS CHART)

$P = \frac{k}{s(s+p)}$

FIG. B_1

k : 10 to 80

p : -2 to $+2$

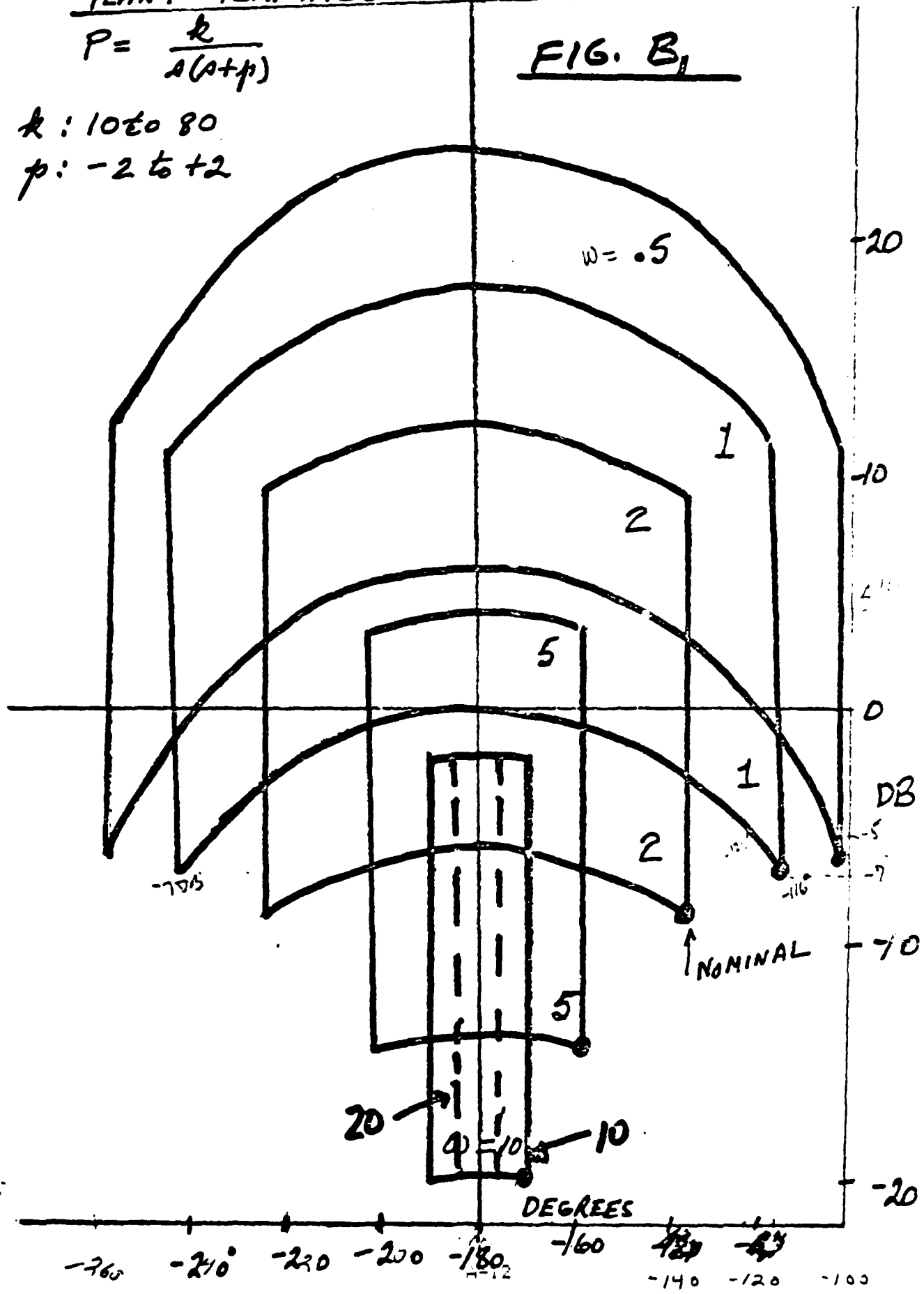

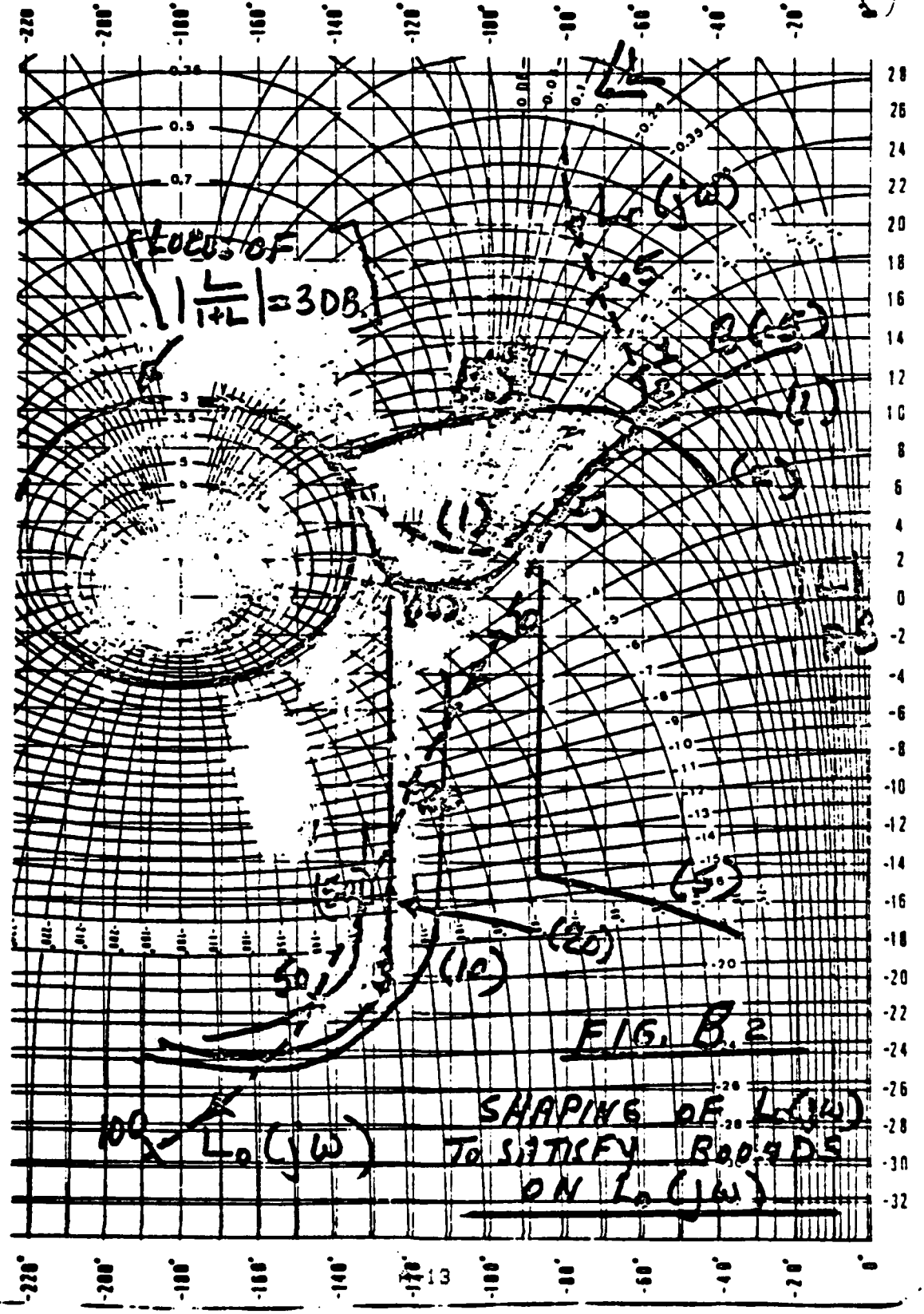

FIG. B.2

SHAPING OF $L_o(j\omega)$ TO SATISFY BODE'S ON $L_o(j\omega)$

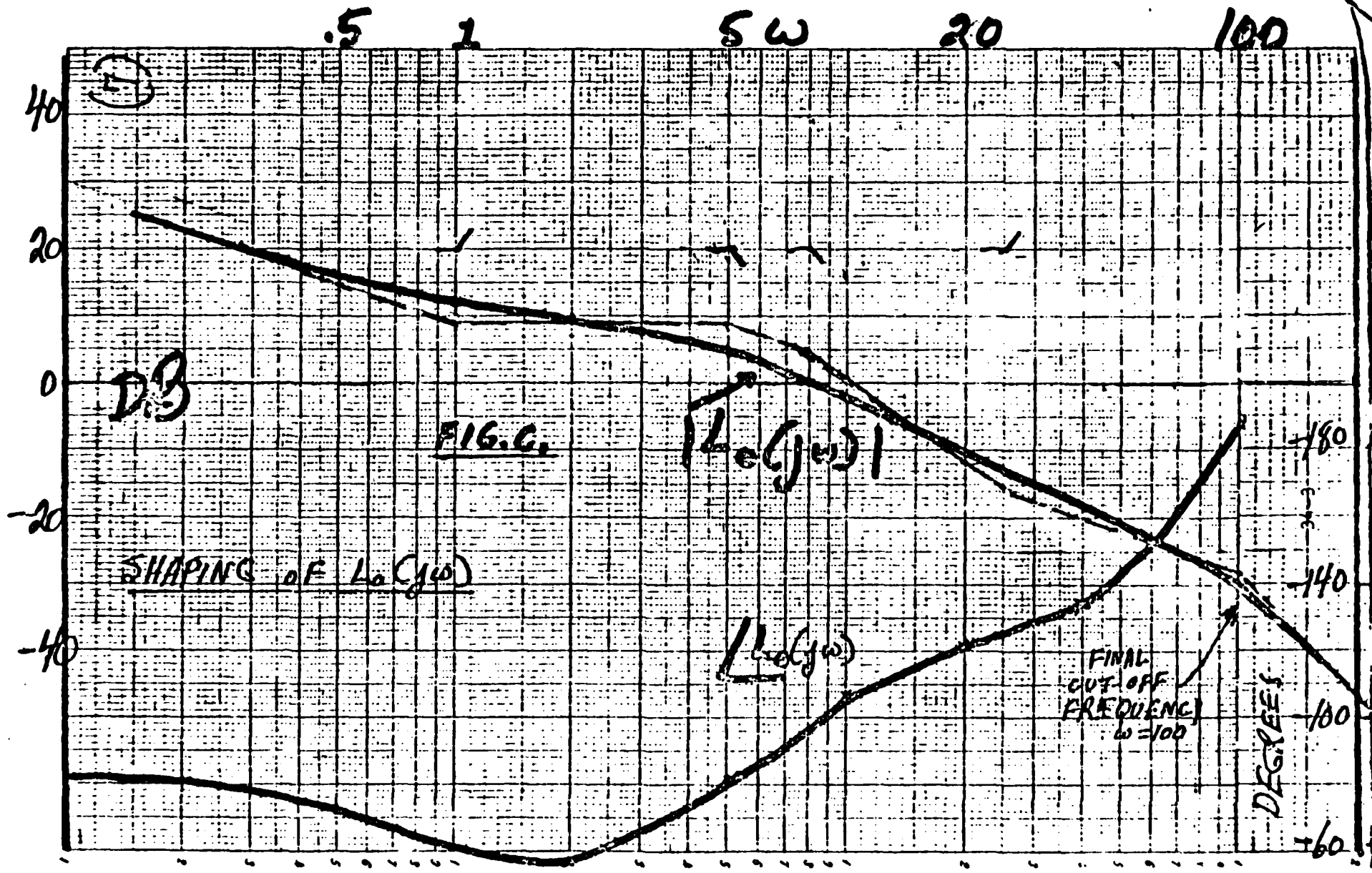
.5
1
5
ω
20
100
40
20
0
-20
-40
DB
FIG. 6.
$|L_o(j\omega)|$
SHAPING OF $L_o(j\omega)$
$L_o(j\omega)$
FINAL CUT-OFF FREQUENCY ω = 100
-180
-140
-100
-60
DEGREES

NO. 3115. 30 DIVISIONS PER INCH (150 DIVISIONS) BY 3 3-INCH CYCLES RATIO RULING. CODES BOOK COMPAN

(4)

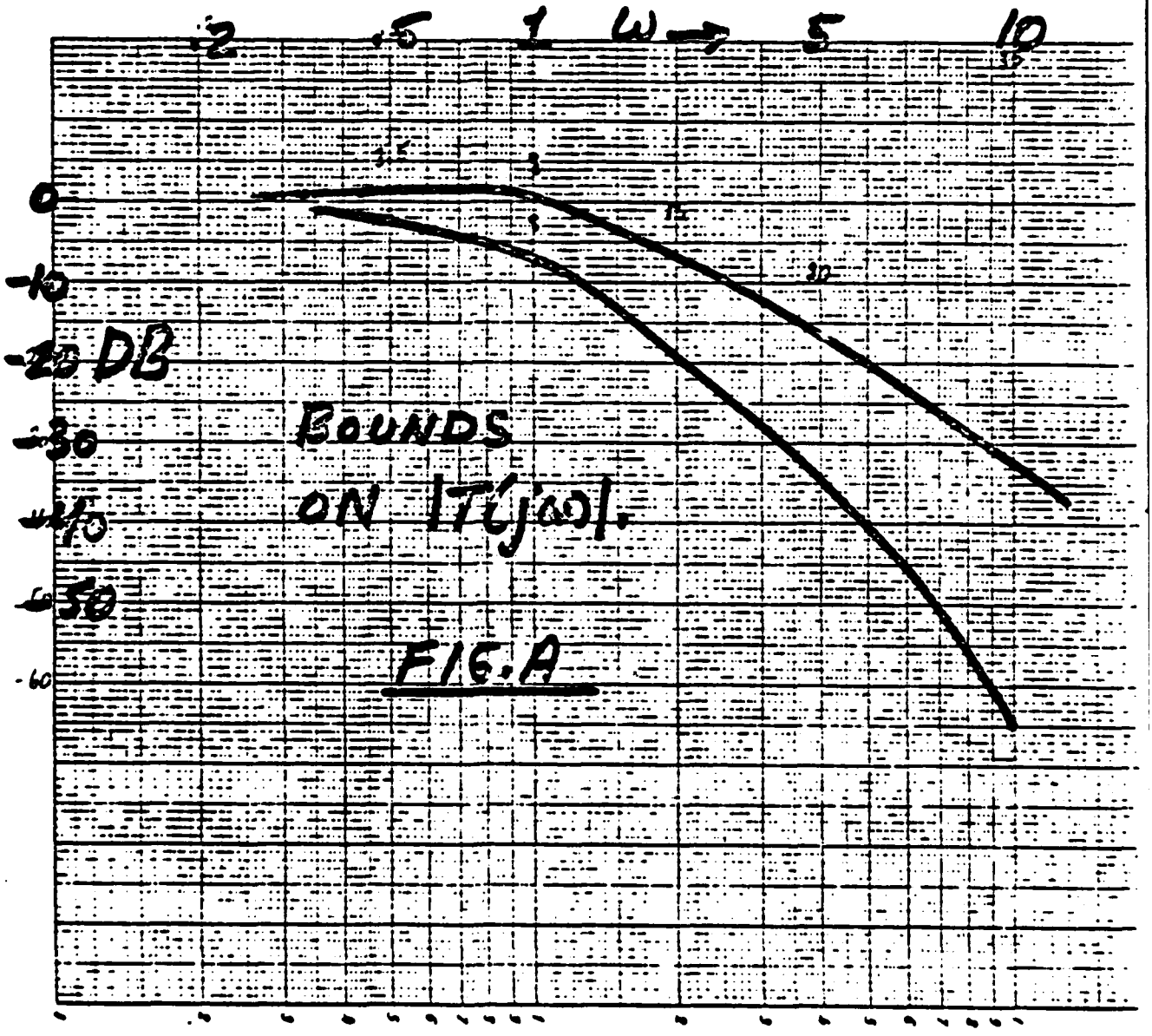

FIG. A

APPENDIX B

RESPONSE MODELS

APPENDIX B

Response Models

Introduction

This appendix contains the output from the computer-aided-design program, TOTAL, of the response modeling process. Included are the transfer functions, the time responses, and the frequency responses for the bank angle and the sideslip angle models.

CLOSED-LOOP TRANSFER FUNCTION
BANK ANGLE UPPER BOUND (B11)

CLK= (CLNK/CLDK)= 5.000

CLTF(S) NUMERATOR

I	CLNPOLY(I)	CLZERO(I)
1	(5.000)	CLNK= 5.000

CLTF(S) DENOMINATOR

I	CLDPOLY(I)	CLPOLE(I)
1	(1.000)S** 2	(-.5000) + J(0.)
2	(10.50)S** 1	(-10.00) + J(0.)
3	(5.000)	CLDK= 1.000

OPTION >37
CONTINUOUS TIME RESPONSE FOR CLTF(S)
WITH STEP INPUT OF STRENGTH = 30.

RISE TIME: TR= 4.39982
DUPLICATION TIME: TD= VERY LARGE
PEAK TIME: TP= VERY LARGE
SETTLING TIME: TS= 7.92663
PEAK VALUE: MP= 30.0000
FINAL VALUE: FV= 30.0000

OPTION >31
CONTINUOUS TIME RESPONSE FOR CLTF(S)
WITH STEP INPUT OF STRENGTH = 30.

ENTER INITIAL TIME, FINAL TIME, DELTA TIME >0,15,1

0.	0.
1.0000000	10.846472
2.0000000	18.382754
3.0000000	22.953784
4.0000000	25.726254
5.0000000	27.407842
6.0000000	28.427777
7.0000000	29.046398
8.0000000	29.421611
9.0000000	29.649190
10.000000	29.787223
11.000000	29.870944
12.000000	29.921724
13.000000	29.952523
14.000000	29.971204
15.000000	29.982534

```
OPTION )32
 CONTINUOUS TIME RESPONSE FOR CLTF(S) WITH STEP INPUT OF STRENGTH = 30.
REGION OF CALCULATION:  T=   0.          TO    T=    10.00
                      F(T)=   0.          TO F(T)=    30.00
0
*++++++++++++++++++++++++++++++++++++++++++++++++++++++++++++++++F(T)
+  *       -          -          -          -          -          .
+         * -          -          -          -          -          .
+           -  *       -          -          -          -          .
+           -        * -          -          -          -          .
+-------------------*----------------------------------------------.
+           -          -    *     -          -          -          .
+           -          -         *-          -          -          .
+           -          -           - *       -          -          .
+           -          -           -   *     -          -          .
+-------------------------------------*--------------------------.
+           -          -          -          *-         -          .
+           -          -          -           -*        -          .
+           -          -          -           -  *      -          .
+           -          -          -           -   *     -          .
+-------------------------------------------------*------------------.
+           -          -          -          -       *  -          .
+           -          -          -          -        * -          .
+           -          -          -          -          *          .
+           -          -          -          -          -*         .
+-------------------------------------------------------*----------.
+           -          -          -          -          - *        .
+           -          -          -          -          -  *       .
+           -          -          -          -          -   *      .
+           -          -          -          -          -   *      .
+-------------------------------------------------------------*----.
+           -          -          -          -          -     *    .
+           -          -          -          -          -      *   .
+           -          -          -          -          -      *   .
+           -          -          -          -          -       *  .
+-------------------------------------------------------------------*.
+           -          -          -          -          -       *  .
+           -          -          -          -          -       *  .
+           -          -          -          -          -        * .
+           -          -          -          -          -        * .
+-------------------------------------------------------------------*.
+           -          -          -          -          -        * .
+           -          -          -          -          -        * .
+           -          -          -          -          -        * .
+           -          -          -          -          -        * .
+-------------------------------------------------------------------*.
+           -          -          -          -          -        * .
T++++++++++++++++++++++++++++++++++++++++++++++++++++++++++++++++++++
```

```
CLOSED-LOOP FREQUENCY RESPONSE USING OPTION 54
     MAGNITUDE (***) AXIS RANGE:    -70.0     TO      50.0     DECIBELS
  FREQUENCY (RAD/SEC)
  .100E+00 +++++++++++++++++++++++++++++++++++++++++++++++++++++++++++++++++++++++
  .112     +          .         -         -    *    -         -          +
  .126     +          -         -         -    *    -         -          +
  .141     +          -         -         -    *    -         -          +
  .158     +          -         -         -    *    -         -          +
  .178     +          -         -         -    *    -         -          +
  .200     +----------------------------------*----------------------------+
  .224     +          -         -         -    *    -         -          +
  .251     +          -         -         -    *    -         -          +
  .282     +          -         -         -   *     -         -          +
  .316     +          -         -         -   *     -         -          +
  .355     +----------------------------------*----------------------------+
  .398     +          -         -         -   *     -         -          +
  .447     +          -         -         -   *     -         -          +
  .501     +          -         -         -  *      -         -          +
  .562     +----------------------------------*----------------------------+
  .631     +          -         -         -  *      -         -          +
  .708     +          -         -         -  *      -         -          +
  .794     +----------------------------------*----------------------------+
  .891     +          -         -         - *       -         -          +
  1.00     +----------------------------------*----------------------------+
  1.12     +          -         -         -*        -         -          +
  1.26     +          -         -         -*        -         -          +
  1.41     +          -         -         *         -         -          +
  1.58     +          -         -         *         -         -          +
  1.78     +          -         -        *-         -         -          +
  2.00     +----------------------------------*----------------------------+
  2.24     +          -         -       * -         -         -          +
  2.51     +          -         -       * -         -         -          +
  2.82     +          -         -      *  -         -         -          +
  3.16     +          -         -      *  -         -         -          +
  3.55     +---------------------------*----------------------------------+
  3.98     +          -         -     *   -         -         -          +
  4.47     +          -         -    *    -         -         -          +
  5.01     +          -         -   *     -         -         -          +
  5.62     +---------------------*----------------------------------------+
  6.31     +          -         -  *      -         -         -          +
  7.08     +          -         -  *      -         -         -          +
  7.94     +---------------------*----------------------------------------+
  8.91     +          -        -*         -         -         -          +
  10.0     +---------------------*----------------------------------------+
  11.2     +          -         *         -         -         -          +
  12.6     +          -        *-         -         -         -          +
  14.1     +          -       * -         -         -         -          +
  15.8     +          -      *  -         -         -         -          +
  17.8     +          -     *   -         -         -         -          +
  20.0     +----------------*-----------------------------------------------+
  22.4     +          -   *     -         -         -         -          +
  25.1     +          -  *      -         -         -         -          +
  28.2     +++++++++++++*++++++++++++++++++++++++++++++++++++++++++++++++++++++
```

CLOSED-LOOP TRANSFER FUNCTION
BANK ANGLE LOWER BOUND (A11)

CLK= (CLNK/CLDK)= 5.000

CLTF(S) NUMERATOR

I	CLNPOLY(I)	CLZERO(I)
1	(5.000)	CLNK= 5.000

CLTF(S) DENOMINATOR

I	CLDPOLY(I)	CLPOLE(I)
1	(1.000)S** 3	(-.5000) + J(0.)
2	(11.50)S** 2	(-1.000) + J(0.)
3	(15.50)S** 1	(-10.00) + J(0.)
4	(5.000)	CLDK= 1.000

OPTION)37
CONTINUOUS TIME RESPONSE FOR CLTF(S)
WITH STEP INPUT OF STRENGTH = 30.

RISE TIME: TR= 5.18511
DUPLICATION TIME: TD= VERY LARGE
PEAK TIME: TP= VERY LARGE
SETTLING TIME: TS= 9.30283
PEAK VALUE: MP= 30.0000
FINAL VALUE: FV= 30.0000

OPTION)31
CONTINUOUS TIME RESPONSE FOR CLTF(S)
WITH STEP INPUT OF STRENGTH = 30.

ENTER INITIAL TIME, FINAL TIME, DELTA TIME)0,15,1

0.	0.
1.000000	3.9554405
2.0000000	11.276685
3.0000000	17.567138
4.0000000	22.063030
5.0000000	25.040283
6.0000000	26.938179
7.0000000	28.123193
8.0000000	28.854405
9.0000000	29.302493
10.000000	29.575959
11.000000	29.742445
12.000000	29.843652
13.000000	29.905121
14.000000	29.942435
15.000000	29.965079

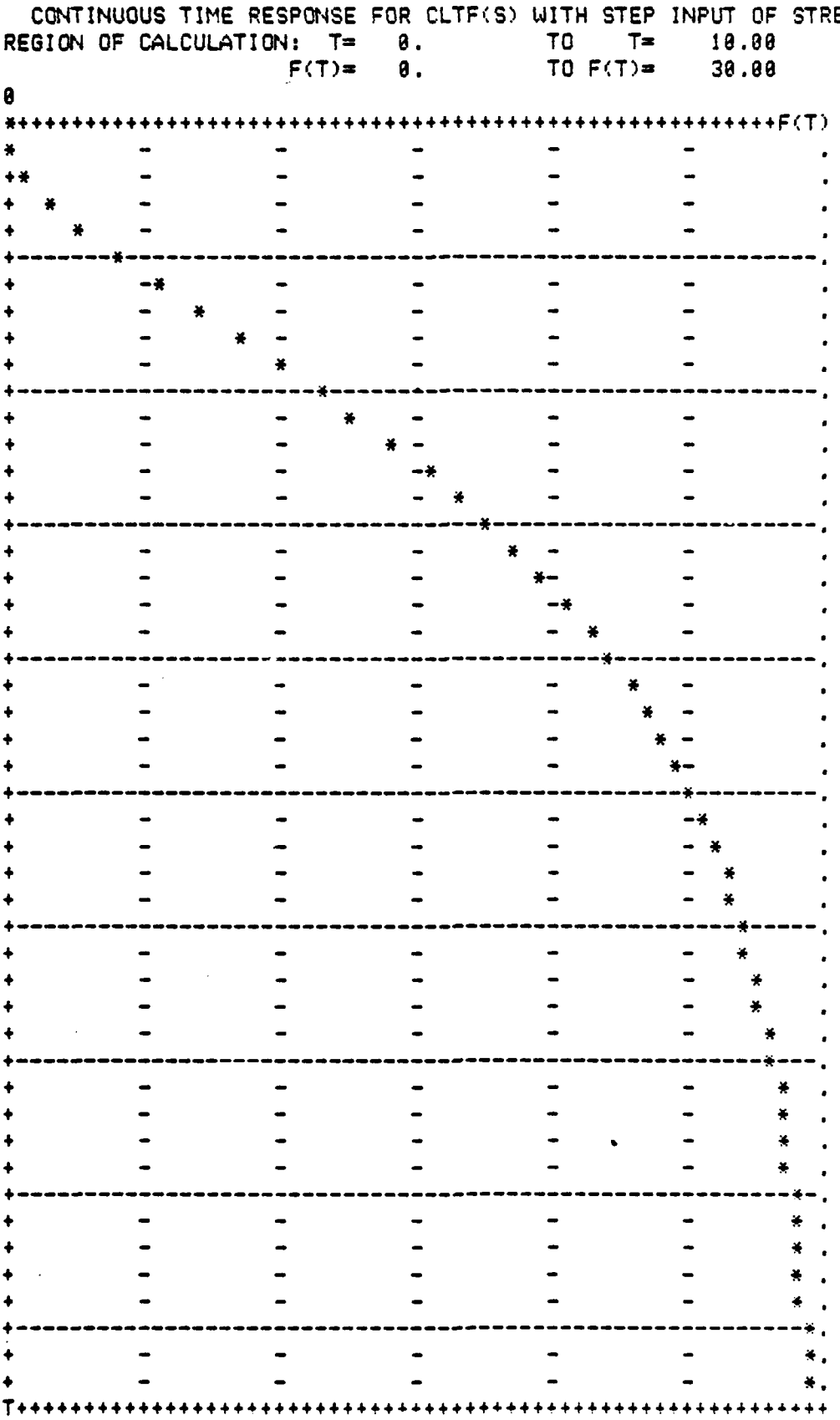
CONTINUOUS TIME RESPONSE FOR CLTF(S) WITH STEP INPUT OF STRENGTH = 30.
REGION OF CALCULATION: T= 0. TO T= 10.00
F(T)= 0. TO F(T)= 30.00
0
F(T)
T

CLOSED-LOOP FREQUENCY RESPONSE USING OPTION 54

MAGNITUDE (***) AXIS RANGE: -110. TO 10.0 DECIBELS

FREQUENCY (RAD/SEC)

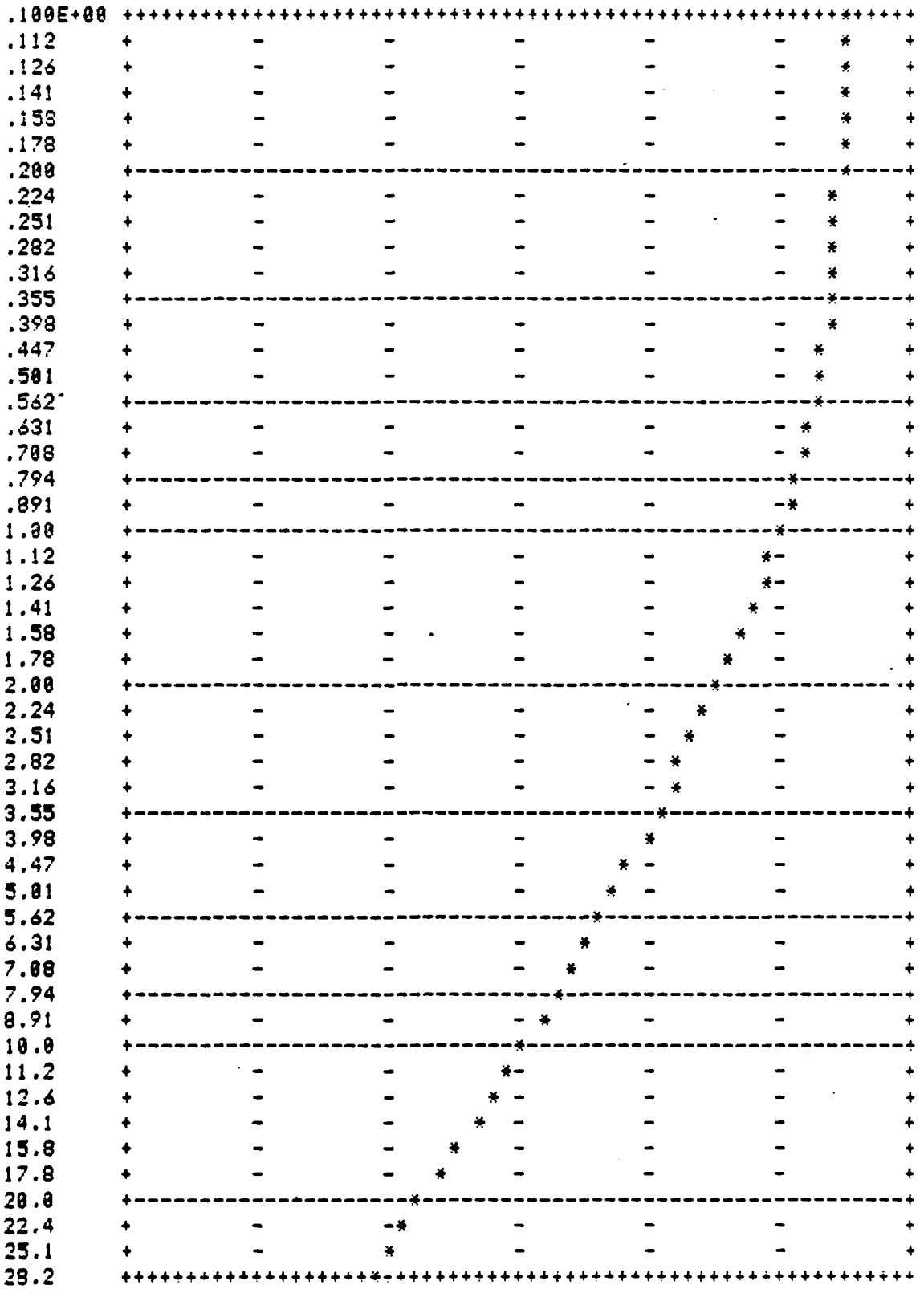

CLOSED-LOOP TRANSFER FUNCTION
SIDESLIP ANGLE UPPER BOUND (B21)

CLK= (CLNK/CLDK)= 2.000

CLTF(S) NUMERATOR

I	CLNPOLY(I)		CLZERO(I)
1	(2.000)S** 2	(0.) + J(0.)	
2	(1.400)S** 1	(-.7000) + J(0.)	
3	(0.)	CLNK= 2.000	

CLTF(S) DENOMINATOR

I	CLDPOLY(I)		CLPOLE(I)
1	(1.000)S** 3	(-1.000) + J(0.)	
2	(24.00)S** 2	(-3.000) + J(0.)	
3	(83.00)S** 1	(-20.00) + J(0.)	
4	(60.00)	CLDK= 1.000	

OPTION >37
CONTINUOUS TIME RESPONSE FOR CLTF(S)
WITH STEP INPUT OF STRENGTH = 30.

RISE TIME: TR= UNDEFINED
DUPLICATION TIME: TD= UNDEFINED
PEAK TIME: TP= .107202
SETTLING TIME: TS= VERY LARGE
PEAK VALUE: MP= 2.09694
FINAL VALUE: FV= 0.

OPTION >31
CONTINUOUS TIME RESPONSE FOR CLTF(S)
WITH STEP INPUT OF STRENGTH = 30.

ENTER INITIAL TIME, FINAL TIME, DELTA TIME >0,15,1

0.	0.
1.0000000	.27818235E-01
2.0000000	-.54045369E-01
3.0000000	-.23082450E-01
4.0000000	-.86508907E-02
5.0000000	-.31904175E-02
6.0000000	-.11740840E-02
7.0000000	-.43194101E-03
8.0000000	-.15890320E-03
9.0000000	-.58457268E-04
10.000000	-.21505230E-04
11.000000	-.79113319E-05
12.000000	-.29104164E-05
13.000000	-.10706824E-05
14.000000	-.39388202E-06
15.000000	-.14490110E-06

CONTINUOUS TIME RESPONSE FOR CLTF(S) WITH STEP INPUT OF STRENGTH = 30.
REGION OF CALCULATION: T= 0. TO T= 10.00
F(T)= -.4000 TO F(T)= 2.000

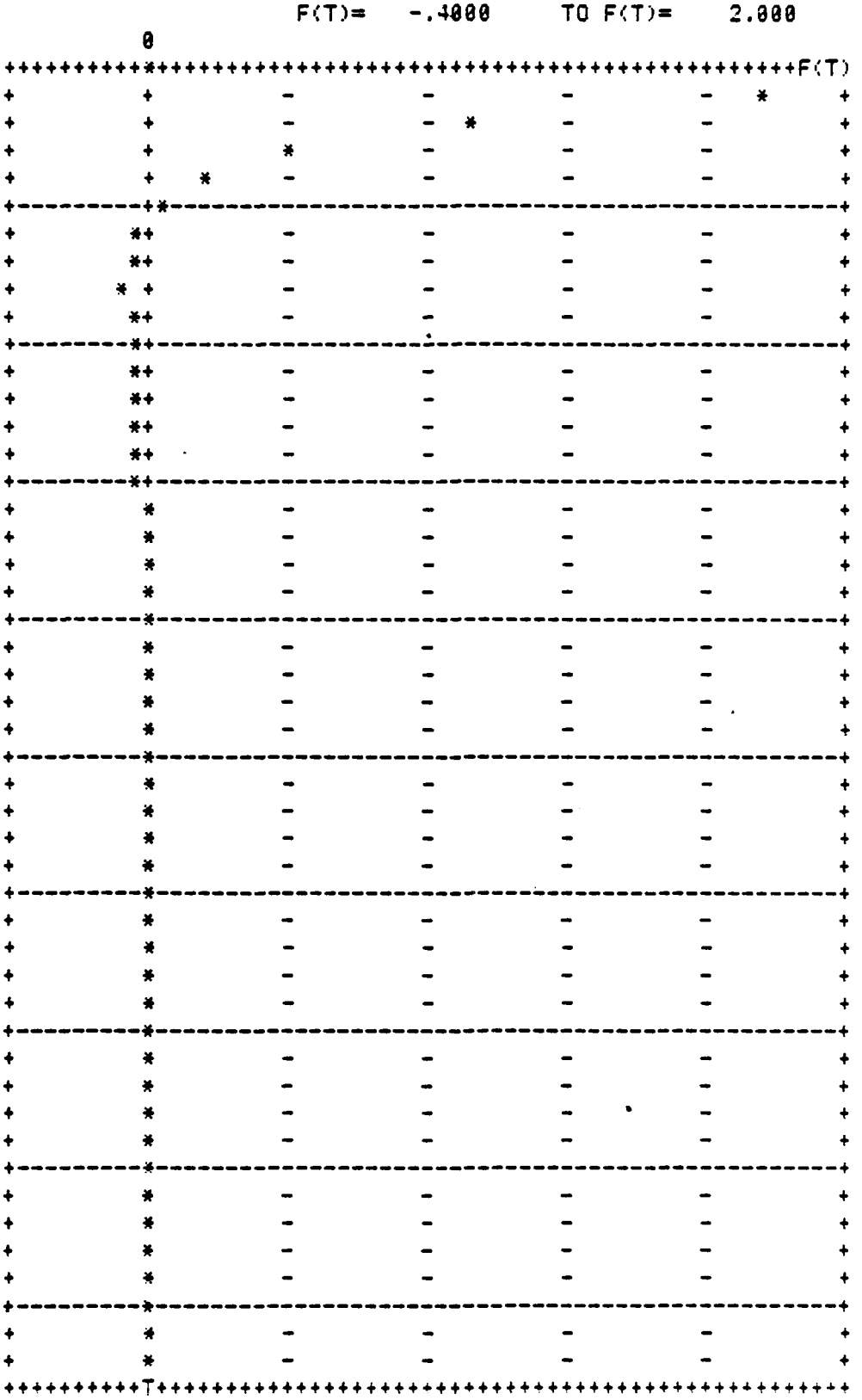

CLOSED-LOOP FREQUENCY RESPONSE USING OPTION 54

MAGNITUDE (***) AXIS RANGE: -60.0 TO 0. DECIBELS

FREQUENCY (RAD/SEC)

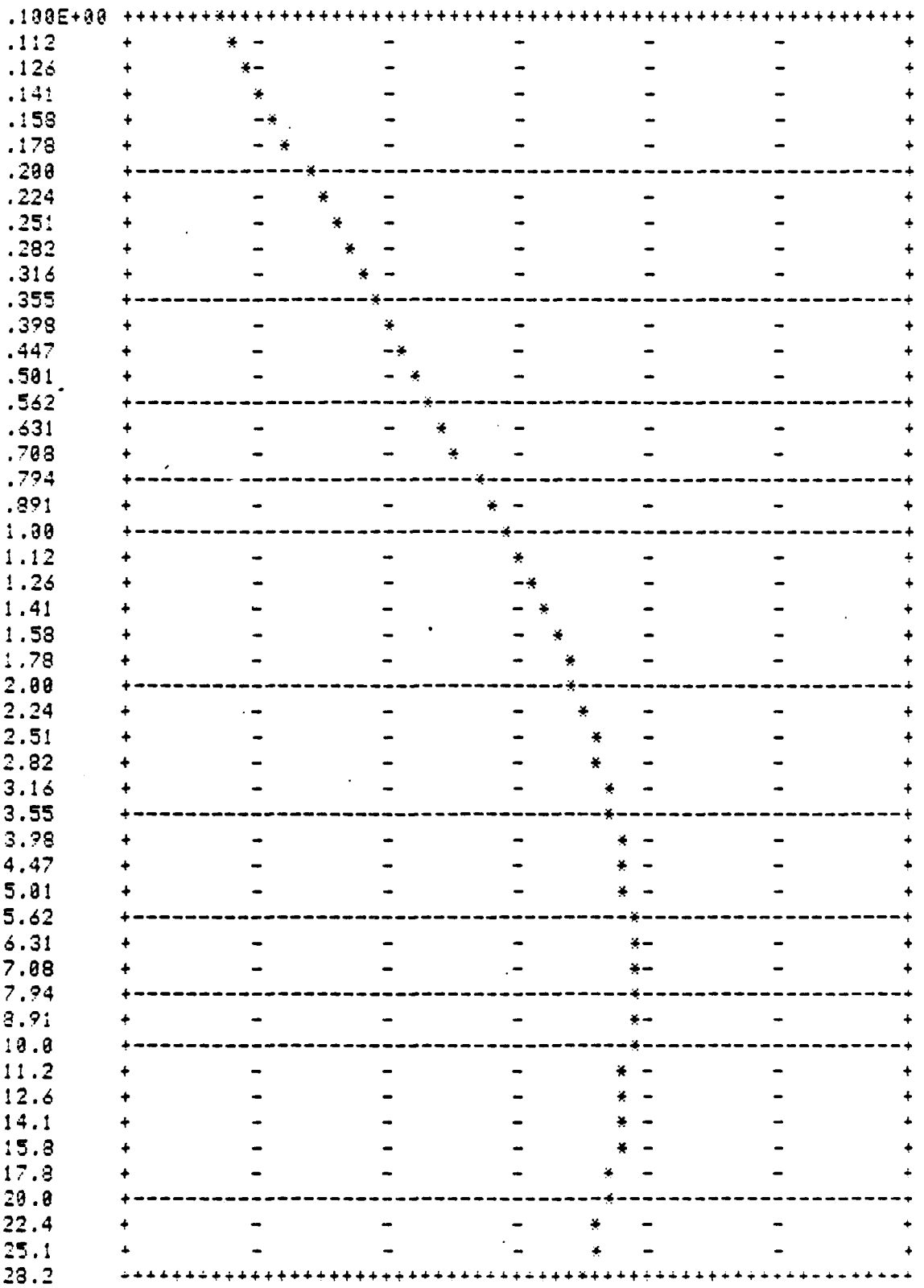

APPENDIX C

TRANSFER FUNCTIONS

APPENDIX C

Transfer Functions

Introduction

This appendix contains the transfer functions of the effective plants used in the design of the bank angle loop and the transfer functions of the compensated system used during the simulations of the design.

Effective q's

Cruise 1

$$q_{11}^* = \frac{0.7278\ (s + 22.35)\ (s + 15.66)}{(s + 0.5295)\ (s + 23.27)\ (s + 16.52)\ (s - 0.01572)} \quad \text{(C-1)}$$

Cruise 2

$$q_{11}^* = \frac{0.7088\ (s + 0.8731)\ (s + 30.3)}{(s + 0.785 \pm j\ 0.041)\ (s + 28.71)\ (s - 0.032)} \quad \text{(C-2)}$$

Power Approach

$$q_{11}^* = \frac{1.434\ (s + 0.006)\ (s + 1.37)\ (s + 4.12)}{s\ (s + 1.28 \pm j\ 0.23)\ (s + 3.42)\ (s - 0.04)} \quad \text{(C-3)}$$

Simulation Transfer Functions

Cruise 1

Denominator

$$(s+0.8\pm j0.3)(s+1.2)(s+0.95)(s+0.7)(s+3.7\pm j4.3)(s+5.3\pm j7.7)$$
$$\times\ (s+8.4\pm j5)(s+23.3)(s+16.5)(s+96.6\pm j119.5)(s+125\pm j176) \quad \text{(C-4)}$$

Numerators

Bank Angle Response

$$2699\ (s+1.2)(s+1)(s+0.86)(s+8.7\pm j5)(s+22.4)(s+15.7) \times (s+96.7\pm j119.6)(s+125\pm j176) \quad \text{(C-5)}$$

Control Wheel Deflection

$$3708\ (s+1)(s+1.2)(s+0.87)(s+0.52)(s-0.016)(s+9.3\pm j5.2) \times (s+22.3)(s+14.5)(s+96.8\pm j119.5)(s+125\pm j176) \quad \text{(C-6)}$$

Sideslip Response

$$85.9\ s(s+1)(s+0.06)(s+2)(s+2.4)(s+20)(s+114\pm j152)^2 \times (s+23.3) \quad \text{(C-7)}$$

Rudder Deflection

$$-5.9\times10^{13}\ (s+1)^3(s+0.06)(s+2.4)(s+5)(s+22.4) \quad \text{(C-8)}$$

Cruise 2

Denominator

$$(s+0.9)(s+0.7)(s+1.1)(s+0.96\pm j0.65)(s+3.6\pm j4.3) \times (s+5.4\pm j7.7)(s+6.5)(s+14.1\pm j14.7)(s+30.3) \times (s+95.5\pm j115)(s+125.3\pm j177.7) \quad \text{(C-9)}$$

Numerators

Bank Angle Response

$$2630\ (s+0.9)(s+1)(s+1.15)(s+6.4)(s+14\pm j15.3)(s+30.3) \times (s+95.7\pm j115.2)(s+125.3\pm j177.7) \quad \text{(C-10)}$$

Control Wheel Deflection

$$3708\,(s+1)(s+.09)(s+0.7)(s-0.03)(s+1.12)(s+6.5)$$
$$\times\ (s+14\pm j14.7)(s+30.3)(s+95.5\pm j115)(s+125.3\pm j177.7) \qquad \text{(C-11)}$$

Sideslip Response

$$-151.6\,s(s+0.095)(s-1.6)(s+1)(s+2)(s+30.3)(s+20)$$
$$\times\ (s+114\pm j152)(s+114\pm j152) \qquad \text{(C-12)}$$

Rudder Deflection

$$1.04\times10^{14}\,(s+0.095)(s+1)^3(s-1.6)(s+5)(s+30.3) \qquad \text{(C-13)}$$

Power Approach

Denominator

$$(s+0.8\pm j0.05)(s+0.7)(s+0.006)(s+1.3)(s+2.8\pm j2.5)$$
$$\times\ (s+1.5\pm j3.7)(s+4.3\pm j0.02)(s+5.6\pm j8.1)(s+49.1)$$
$$\times\ (s+82.6\pm j107.6)(s+128.5\pm j181.6) \qquad \text{(C-14)}$$

Numerators

Bank Angle Response

$$5318\,(s+1)(s+0.8)(s+1.4)(s+0.006)(s+2.5\pm j2.2)$$
$$\times\ (s+4.1)(s+49.5)(s+82.6\pm j107.6)(s+128.5\pm j181.6) \qquad \text{(C-15)}$$

Control Wheel Deflection

$$3708\,s(s+1.1)(s+1)(s+0.8)(s+1.6)(s-0.04)(s+2.3\pm j2.3)$$
$$\times\ (s+4.1)(s+49.1)(s+82.6\pm j107.6)(s+128.5\pm j181.6) \qquad \text{(C-16)}$$

Sideslip Response

$$-16.9\,s^2(s+0.09)(s+1)(s+2)(s+4.1)(s+20)(s-68)$$
$$\times\ (s+114\pm j152)(s+114\pm j152) \qquad \text{(C-17)}$$

Rudder Deflection

$$1.16\times10^{13}\ s(s+1)^3(s+0.09)(s+4.1)(s+5)(s-68) \qquad \text{(C-18)}$$

VITA

Robert W. Betzold was born in Tuscola, Illinois on 6 February 1952. After graduation from Tuscola Community High School he attended the U.S. Air Force Academy, Colorado Springs, Colorado, from June 1970 to June 1974. He received his Bachelor of Science Degree in Electrical Engineering from USAFA.

After completing Undergraduate Pilot Training at Moody AFB, Valdosta, Georgia in August 1975 he was assigned to the 50th Tactical Airlift Squadron, Little Rock AFB, Arkansas. In 1977 he was assigned to the 21st Tactical Airlift Squadron, Clark AB, Republic of the Philippines. He currently has a Senior Pilot rating with approximately 3000 hours flying experience in the U.S., European, and Pacific theaters.

He entered the Graduate Electrical Engineering program at the School of Engineering, Air Force Institute of Technology in June 1982. His next assignment is with the Air Force Weapons Laboratory, Kirtland AFB, New Mexico.

Permanent Home Address: 516 Allen Ave
Franklin, Tn.
37064

UNCLASSIFIED

SECURITY CLASSIFICATION OF THIS PAGE

REPORT DOCUMENTATION PAGE

1a. REPORT SECURITY CLASSIFICATION UNCLASSIFIED	1b. RESTRICTIVE MARKINGS
2a. SECURITY CLASSIFICATION AUTHORITY	3. DISTRIBUTION/AVAILABILITY OF REPORT Approved for public release; Distribution unlimited
2b. DECLASSIFICATION/DOWNGRADING SCHEDULE	
4. PERFORMING ORGANIZATION REPORT NUMBER(S) AFIT/GE/EE/83D-11	5. MONITORING ORGANIZATION REPORT NUMBER(S)
6a. NAME OF PERFORMING ORGANIZATION AF Institute of Technology School of Engineering 6b. OFFICE SYMBOL (If applicable) AFIT/EN	7a. NAME OF MONITORING ORGANIZATION AFWAL/Flight Dynamics Laboratory Flight Control Division (FIC)
6c. ADDRESS (City, State and ZIP Code) Wright-Patterson AFB Ohio 45433	7b. ADDRESS (City, State and ZIP Code) Wright-Patterson AFB Ohio 45433
8a. NAME OF FUNDING/SPONSORING ORGANIZATION 8b. OFFICE SYMBOL (If applicable) AFWAL/FIG	9. PROCUREMENT INSTRUMENT IDENTIFICATION NUMBER
8c. ADDRESS (City, State and ZIP Code)	10. SOURCE OF FUNDING NOS. PROGRAM ELEMENT NO. / PROJECT NO. / TASK NO. / WORK UNIT NO.
11. TITLE (Include Security Classification) See 19	
12. PERSONAL AUTHOR(S) Betzold, Robert William, Capt, USAF	
13a. TYPE OF REPORT MS Thesis 13b. TIME COVERED FROM _____ TO _____	14. DATE OF REPORT (Yr., Mo., Day) 1983 December 15. PAGE COUNT 116
16. SUPPLEMENTARY NOTATION	
17. COSATI CODES FIELD / GROUP / SUB. GR.	18. SUBJECT TERMS (Continue on reverse if necessary and identify by block number) Multiple Input - Multiple Output, Multivariable Control, Flight Control, Lateral Controllers, Uncertain Plants, Robustness, Quantitative Feedback, C-135

19. ABSTRACT (Continue on reverse if necessary and identify by block number)

Title- Multiple Input - Multiple Output Flight Control Design With Highly Uncertain Parameters; Application to the C-135 Aircraft (UNCLASSIFIED)

Approved for public release: IAW AFR 190-17.
Lynn Wolaver 7 Feb 84
LYNN E. WOLAVER
Dean for Research and Professional Development
Air Force Institute of Technology (AIC)
Wright-Patterson AFB OH 45433

Abstract-

This thesis demonstrates the design of a lateral flight controller for the C-135 aircraft using the frequency response approach of Professor Izaac Horowitz, University of Colorado, Boulder, Colorado. A single controller is designed for the entire flight envelope of the aircraft, from high speed, high altitude cruise to a low altitude approach condition.

A three degree-of-freedom lateral model is reduced to a two degree-of-freedom model.

20. DISTRIBUTION/AVAILABILITY OF ABSTRACT UNCLASSIFIED/UNLIMITED ☐ SAME AS RPT. ☒ DTIC USERS ☐	21. ABSTRACT SECURITY CLASSIFICATION UNCLASSIFIED
22a. NAME OF RESPONSIBLE INDIVIDUAL Houpis, Constantine H. PHD.	22b. TELEPHONE NUMBER (Include Area Code) 513-255-3576 22c. OFFICE SYMBOL AFIT/EN

DD FORM 1473, 83 APR EDITION OF 1 JAN 73 IS OBSOLETE.

UNCLASSIFIED

SECURITY CLASSIFICATION OF THIS PAGE

The equations of motion assume a linearized aircraft model operating around equilibrium flight conditions allowing only small perturbations from equilibrium.

Robustness of the design is guaranteed, since the variation in flight parameters is considered throughout the entire design process. Robustness is demonstrated by simulating the compensated aircraft at the extremes of the flight envelope considered.

This thesis concludes that the approach of Professor Horowitz is useful for the design of flight controllers for the C-135 aircraft. Some software development to aid in the design process is recommended.


FILME
4-84